



U.S. Department
of Transportation

**Federal Highway
Administration**

Publication No. FHWA-RD-88-074
July 1989

Rehabilitation of Concrete Pavements

Volume IV: Appendixes

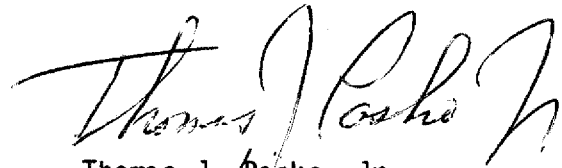
Research, Development, and Technology
Turner-Fairbank Highway Research Center
6300 Georgetown Pike
McLean, Virginia 22101-2296

FOREWORD

This report is one volume of a four-volume set presenting the results of a research study to develop improved evaluation procedures and rehabilitation techniques for concrete pavements. Each report includes the Table of Contents for all four volumes. Eight rehabilitation techniques were selected for detailed investigation by field inspection and analytical study. These eight techniques are diamond grinding, load transfer restoration, edge support, full-depth repair, partial-depth repair, bonded concrete overlays, unbonded concrete overlays, and crack-and-seat with AC overlay. Based on analysis of the field data, a series of distress models were developed to predict the performance of the various rehabilitation techniques under a variety of conditions. These models and other information were then used to develop a comprehensive prototype system for jointed plain, jointed reinforced, and continuously reinforced pavement evaluation and rehabilitation.

This report will be of interest to engineers involved in planning, designing, or performing rehabilitation of concrete pavements.

Sufficient copies of this report are being distributed by FHWA memorandum to provide one copy to each FHWA Region and Division and two copies to each State highway agency. Direct distribution is being made to the division offices. Additional copies for the public are available from the National Technical Information Service (NTIS), U.S. Department of Commerce, 5285 Port Royal Road, Springfield, Virginia 22161.



Thomas J. Pasko, Jr.
Director, Office of Engineering
and Highway Operations
Research and Development

NOTICE

This document is disseminated under the sponsorship of the Department of Transportation in the interest of information exchange. The United States Government assumes no liability for its contents or use thereof. The contents of this report reflect the views of the contractor, who is responsible for the accuracy of the data presented herein. The contents do not necessarily reflect the official policy of the Department of Transportation. This report does not constitute a standard, specification, or regulation.

The United States Government does not endorse products or manufacturers. Trade or manufacturers' names appear herein only because they are considered essential to the object of this document.

1. Report No. FHWA-RD-88-074		2. Government Accession No.		3. Recipient's Catalog No.													
4. Title and Subtitle REHABILITATION OF CONCRETE PAVEMENTS Volume IV - Appendixes			5. Report Date July 1989														
			6. Performing Organization Code														
7. Author(s) Michael J. Reiter, Gerald F. Voigt, Michael I. Darter			8. Performing Organization Report No.														
9. Performing Organization Name and Address Department of Civil Engineering University of Illinois at Urbana-Champaign 208 North Romine Street Urbana, Illinois 61801			10. Work Unit No. (TRAIS) 3C1c-3012														
			11. Contract or Grant No. DEFH-61-85-C-00004														
12. Sponsoring Agency Name and Address Office of Eng. and Hwy. Ops. Res. and Dev. Federal Highway Administration 6300 Georgetown Pike McLean, Virginia 22101-2296			13. Type of Report and Period Covered Final Report November 1984 to April 1989														
			14. Sponsoring Agency Code														
15. Supplementary Notes FHWA contract manager (COTR): Dr. Stephen W. Forster																	
16. Abstract Extensive field, laboratory and analytical studies were conducted into the evaluation and rehabilitation of concrete pavements. Field studies included over 350 rehabilitated pavement sections throughout the U.S., and the construction of two field experiments. A laboratory study was conducted on anchoring dowels in full-depth repairs. Analyses of field and laboratory data identified performance characteristics, improved design and construction procedures, and provided deterioration models for rehabilitated pavements. A concrete pavement advisory system was developed to assist engineers in project level evaluation and rehabilitation. This Volume IV contains a description of the data collection procedures, original pavement and rehabilitation design factors, extent of the database, description of database variables, and documentation of the laboratory dowel anchoring experiment. This volume is the fourth in a series. The others in the series are:																	
<table border="1"> <thead> <tr> <th><u>FHWA NO.</u></th> <th><u>Vol. No.</u></th> <th><u>Title</u></th> </tr> </thead> <tbody> <tr> <td>RD-88-071</td> <td>I</td> <td>Repair Rehabilitation Techniques</td> </tr> <tr> <td>RD-88-072</td> <td>II</td> <td>Overlay Rehabilitation Techniques</td> </tr> <tr> <td>RD-88-073</td> <td>III</td> <td>Conc. Pvt. Eval. and Reh. System</td> </tr> </tbody> </table>						<u>FHWA NO.</u>	<u>Vol. No.</u>	<u>Title</u>	RD-88-071	I	Repair Rehabilitation Techniques	RD-88-072	II	Overlay Rehabilitation Techniques	RD-88-073	III	Conc. Pvt. Eval. and Reh. System
<u>FHWA NO.</u>	<u>Vol. No.</u>	<u>Title</u>															
RD-88-071	I	Repair Rehabilitation Techniques															
RD-88-072	II	Overlay Rehabilitation Techniques															
RD-88-073	III	Conc. Pvt. Eval. and Reh. System															
17. Key Words Concrete pavement, evaluation, rehabilitation, maintenance, full-depth repairs, grinding, load transfer restoration, partial-depth repairs, concrete shoulders, expert system, concrete overlays, crack and seat			18. Distribution Statement No restrictions. This document is available to the public through the National Technical Information Service, Springfield, Virginia 22161														
19. Security Classif. (of this report) Unclassified		20. Security Classif. (of this page) Unclassified		21. No. of Pages 111	22. Price												

SI* (MODERN METRIC) CONVERSION FACTORS

APPROXIMATE CONVERSIONS TO SI UNITS

Symbol	When You Know	Multiply By	To Find	Symbol
--------	---------------	-------------	---------	--------

LENGTH

in	inches	25.4	millimetres	mm
ft	feet	0.305	metres	m
yd	yards	0.914	metres	m
mi	miles	1.61	kilometres	km

AREA

in ²	square inches	645.2	millimetres squared	mm ²
ft ²	square feet	0.093	metres squared	m ²
yd ²	square yards	0.836	metres squared	m ²
ac	acres	0.405	hectares	ha
mi ²	square miles	2.59	kilometres squared	km ²

VOLUME

fl oz	fluid ounces	29.57	millilitres	mL
gal	gallons	3.785	litres	L
ft ³	cubic feet	0.028	metres cubed	m ³
yd ³	cubic yards	0.765	metres cubed	m ³

NOTE: Volumes greater than 1000 L shall be shown in m³.

MASS

oz	ounces	28.35	grams	g
lb	pounds	0.454	kilograms	kg
T	short tons (2000 lb)	0.907	megagrams	Mg

TEMPERATURE (exact)

°F	Fahrenheit temperature	$5(F-32)/9$	Celcius temperature	°C
----	------------------------	-------------	---------------------	----

APPROXIMATE CONVERSIONS FROM SI UNITS

Symbol	When You Know	Multiply By	To Find	Symbol
--------	---------------	-------------	---------	--------

LENGTH

mm	millimetres	0.039	inches	in
m	metres	3.28	feet	ft
m	metres	1.09	yards	yd
km	kilometres	0.621	miles	mi

AREA

mm ²	millimetres squared	0.0016	square inches	in ²
m ²	metres squared	10.764	square feet	ft ²
ha	hectares	2.47	acres	ac
km ²	kilometres squared	0.386	square miles	mi ²

VOLUME

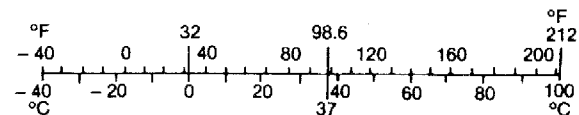
mL	millilitres	0.034	fluid ounces	fl oz
L	litres	0.264	gallons	gal
m ³	metres cubed	35.315	cubic feet	ft ³
m ³	metres cubed	1.308	cubic yards	yd ³

MASS

g	grams	0.035	ounces	oz
kg	kilograms	2.205	pounds	lb
Mg	megagrams	1.102	short tons (2000 lb)	T

TEMPERATURE (exact)

°C	Celcius temperature	$1.8C + 32$	Fahrenheit temperature	°F
----	---------------------	-------------	------------------------	----



* SI is the symbol for the International System of Measurement

(Revised April 1989)

TABLE OF CONTENTS

	PAGE
VOLUME I REPAIR REHABILITATION TECHNIQUES	
CHAPTER 1. INTRODUCTION	1
1.0 STUDY OBJECTIVE	1
1.1 FIELD STUDIES	1
1.1.1 Field Condition Surveys	5
1.1.2 Original Pavement and Rehabilitation Design Factors.	6
1.1.3 Traffic Data	6
1.1.4 Environmental Data	6
1.2 LABORATORY STUDIES	7
1.3 ANALYTICAL STUDIES	7
1.4 EVALUATION AND REHABILITATION SYSTEM	7
CHAPTER 2. DIAMOND GRINDING	8
2.0 RESEARCH APPROACH	8
2.1 DATABASE AND DATA COLLECTION	9
2.2 FIELD PERFORMANCE AND EVALUATION	15
2.2.1 Transverse Cracking	15
2.2.2 Longitudinal Cracking	18
2.2.3 Corner Breaks	18
2.2.4 Joint/Crack Faulting and Pumping	18
2.2.5 "D" Cracking	21
2.2.6 Wearout of Grinding Texture	21
2.3 PERFORMANCE MODEL	21
2.3.1 Model Development	21
2.3.2 Faulting Model	21
2.4 DIAMOND GRINDING -- DESIGN AND CONSTRUCTION GUIDELINES	24
2.4.1 Introduction	24
2.4.2 Concurrent Work	34
2.4.3 Design	35
2.4.4 Construction	37
2.4.5 Preparation of Plans and Specifications	38
2.5 CONCLUSIONS AND RECOMMENDATIONS	39
CHAPTER 3. RESTORATION OF LOAD TRANSFER	41
3.0 RESEARCH APPROACH	41
3.1 DATABASE AND DATA COLLECTION	41
3.1.1 General Project Description	41

	PAGE
3.1.2 Load Transfer Restoration Design Variation	44
3.1.3 Traffic and Climatic Variation	44
3.1.4 Performance Variation	44
3.2 DATA COLLECTION	44
3.3 FIELD PERFORMANCE AND EVALUATION	46
3.3.1 Field Performance	46
3.3.2 Retrofit Dowel Bar Performance	46
3.3.3 Double-vee Shear Device Performance	46
3.3.4 Miniature I-Beam Device Performance	51
3.3.5 Figure-eight Device Performance	51
3.3.6 Performance Summary	56
3.4 PERFORMANCE MODELS	56
3.4.1 Model Development	56
3.4.2 Faulting Model	56
3.5 CURRENT RESEARCH IN LOAD TRANSFER RESTORATION	61
3.6 DESIGN AND CONSTRUCTION GUIDELINES -- RESTORATION OF JOINT LOAD TRANSFER	61
3.6.1 Introduction	61
3.6.2 Concurrent Work	68
3.6.3 Design	69
3.6.4 Construction	73
3.6.5 Preparation of Plans and Specifications	75
3.7 CONCLUSIONS AND RECOMMENDATIONS	75
CHAPTER 4. EDGE SUPPORT	77
4.0 RESEARCH APPROACH	77
4.1 DATABASE AND DATA COLLECTION	77
4.1.1 General Project Description	77
4.1.2 Edge Support Design Variation	80
4.1.3 Traffic and Climatic Variation	80
4.2 DATA COLLECTION	80
4.3 PERFORMANCE MODELS	80
4.4 EDGE SUPPORT CASE STUDIES	83
4.5 DESIGN AND CONSTRUCTION GUIDELINES -- EDGE SUPPORT	98
4.5.1 Introduction	98
4.5.2 Concurrent Work	100
4.5.3 Design	105
4.5.4 Construction	108
4.5.5 Preparation of Plans and Specifications	108

	PAGE
4.6 CONCLUSIONS AND RECOMMENDATIONS	108
CHAPTER 5. FULL-DEPTH REPAIR	113
5.1 INTRODUCTION	113
5.2 DATABASE AND DATA COLLECTION	115
5.2.1 Project Field Database	115
5.2.2 Range of the Database	119
5.2.3 Illinois DOT Experimental Full-Depth Repair Project. (I-70 near St. Elmo)	119
5.3 FIELD PERFORMANCE AND EVALUATION	119
5.3.1 Transverse Joint Faulting	124
5.3.2 Transverse Joint Spalling	140
5.3.3 Transverse Cracking of Full-Depth Repairs	145
5.3.4 Longitudinal Cracking of Full-Depth Repairs	149
5.4 LABORATORY SHEAR TESTING OF DOWELS ANCHORED IN CONCRETE	151
5.4.1 Introduction	151
5.4.2 Experimental Design	151
5.4.3 Preparation of the Test Specimens	153
5.4.4 Description of the Test and Related Equipment	155
5.5 LABORATORY STUDY RESULTS	155
5.5.1 Preliminary Results and Observations	155
5.5.2 Factors Affecting Dowel Deflection and Looseness	159
5.5.3 Dowel Deflection and Looseness Models	161
5.6 DESIGN AND CONSTRUCTION GUIDELINES -- FULL-DEPTH REPAIR	167
5.6.1 Introduction	167
5.6.2 Need for Full-Depth Repair	168
5.6.3 Limitations and Effectiveness	170
5.6.4 Concurrent Work	170
5.6.5 Design	173
5.6.6 Construction	178
5.6.7 Preparation of Plans and Specifications	187
5.7 CONCLUSIONS AND RECOMMENDATIONS	190
5.7.1 Conclusions from Laboratory Experiment	190
5.7.2 Conclusions from Laboratory Data Analysis	192
CHAPTER 6. PARTIAL-DEPTH REPAIR	194
6.0 RESEARCH APPROACH	194
6.1 DATABASE AND DATA COLLECTION	195
6.2 FIELD PERFORMANCE AND EVALUATION	200

	PAGE
6.3 DESIGN AND CONSTRUCTION GUIDELINES	205
6.3.1 Introduction	205
6.3.2 Need for Partial-Depth Repair	205
6.3.3 Effectiveness of Partial-Depth Repair	206
6.3.4 Limitations of Partial-Depth Repair	206
6.3.5 Concurrent Work	206
6.3.6 Partial-Depth Repair Materials	207
6.3.7 Preparation of the Repair Area	208
6.3.8 Repair Placement and Finishing	213
6.3.9 Preparation of Plans and Specifications	214
6.4 CONCLUSIONS AND RECOMMENDATIONS	214
6.4.1 Appropriate Use of Partial-Depth Repairs	215
6.4.2 Construction Techniques and Materials	216
REFERENCES VOLUME I	218

VOLUME II OVERLAY REHABILITATION TECHNIQUES

CHAPTER 1. INTRODUCTION	1
1.0 STUDY OBJECTIVE	1
1.1 FIELD STUDIES	1
1.1.1 Field Condition Surveys	5
1.1.2 Original Pavement and Rehabilitation Design Factors.	6
1.1.3 Traffic Data	6
1.1.4 Environmental Data	6
1.2 LABORATORY STUDIES	7
1.3 ANALYTICAL STUDIES	7
1.4 EVALUATION AND REHABILITATION SYSTEM	7
CHAPTER 2. BONDED PORTLAND CEMENT CONCRETE OVERLAY	8
2.0 RESEARCH APPROACH	8
2.1 DATABASE AND DATA COLLECTION	9
2.2 FIELD PERFORMANCE AND EVALUATION	17
2.2.1 Transverse (Reflective) Cracking	17
2.2.2 Longitudinal (Reflective) Cracking	23
2.2.3 Joint/Crack Faulting And Pumping	23
2.2.4 Secondary Joint Cracking	25
2.2.5 Shrinkage Cracking	27
2.2.6 Overlay Delamination	27
2.2.7 "D" Cracking	35

	PAGE
2.3 PERFORMANCE MODELS	35
2.3.1 Model Development	35
2.3.2 Joint Faulting	37
2.3.3 Reflective Cracking	41
2.3.4 Joint Deterioration	44
2.4 DESIGN AND CONSTRUCTION GUIDELINES -- BONDED CONCRETE OVERLAYS	48
2.4.1 Introduction	48
2.4.2 Concurrent Work	51
2.4.3 Design And Construction	52
2.4.4 Preparation of Plans and Specifications	59
2.5 BONDED OVERLAYS ON CRCP	59
2.6 CONCLUSIONS AND RECOMMENDATIONS	59
CHAPTER 3. UNBONDED PORTLAND CEMENT CONCRETE OVERLAY	62
3.0 RESEARCH APPROACH	62
3.1 DATABASE AND DATA COLLECTION	63
3.2 FIELD PERFORMANCE AND EVALUATION	68
3.2.1 Transverse Cracking	68
3.2.2 Longitudinal Cracking	71
3.2.3 Faulting and Pumping	75
3.3 PERFORMANCE MODELS	77
3.3.1 Joint Faulting	77
3.3.2 Other Distress Models	80
3.4 DESIGN AND CONSTRUCTION GUIDELINES -- UNBONDED CONCRETE OVERLAYS	80
3.4.1 Introduction	80
3.4.2 Concurrent Work	81
3.4.3 Design and Construction	82
3.4.4 Preparation of Plans and Specifications	87
3.5 CONCLUSIONS AND RECOMMENDATIONS	87
CHAPTER 4. CRACK AND SEAT AND ASPHALT CONCRETE OVERLAYS	89
4.0 RESEARCH APPROACH	89
4.1 DATABASE AND DATA COLLECTION	90
4.2 FIELD PERFORMANCE AND EVALUATION	95
4.2.1 Transverse (Reflective) Cracking	95
4.2.2 Serviceability	101
4.2.3 Rutting	101

	PAGE
4.3 PERFORMANCE MODELS	105
4.3.1 Model Development	105
4.3.2 Reflection Cracking	106
4.3.3 Rutting	117
4.4 DESIGN AND CONSTRUCTION GUIDELINES -- CRACK AND SEAT AND ASPHALT CONCRETE OVERLAY	118
4.4.1 Introduction	118
4.4.2 Concurrent Work	121
4.4.3 Design Considerations	121
4.4.4 Construction Considerations	123
4.4.5 Preparation of Plans and Specifications	125
4.5 CONCLUSIONS AND RECOMMENDATIONS	125
APPENDIX A DESCRIPTIONS OF SELECTED PROJECTS	128
BONDED CONCRETE OVERLAYS	128
New York, I-81	129
Wyoming, I-25	130
Louisiana, US 61	132
Iowa, I-80 (Milepost 182)	134
Iowa, County Route C17	135
UNBONDED CONCRETE OVERLAYS	139
Illinois, East-West Tollway (I-5)	139
Georgia, I-85	140
Michigan, US 23	142
Colorado, I-25	144
Pennsylvania, I-367	146
CRACK AND SEAT AND ASPHALT CONCRETE OVERLAYS	148
Illinois, Spring Creek Road	148
Illinois, Rockton Road	149
Illinois, Lincoln Trail Road	150
Illinois, State Route 97	151
Illinois, State Route 101	152
Wisconsin, US Route 14 (Rock County)	153
Wisconsin, US Route 14 (Dane and Rock Counties)	154
REFERENCES VOLUME II	155

**VOLUME III CONCRETE PAVEMENT EVALUATION AND
REHABILITATION SYSTEM**

CHAPTER 1 INTRODUCTION	1
----------------------------------	---

	PAGE
1.1 PROBLEM STATEMENT AND RESEARCH OBJECTIVE	1
1.2 RESEARCH APPROACH	1
1.3 BRIEF DESCRIPTION OF EVALUATION AND REHABILITATION SYSTEM . .	2
CHAPTER 2 KNOWLEDGE-BASED SYSTEM APPROACH TO CONCRETE PAVEMENT EVALUATION AND REHABILITATION	4
2.1 PROBLEM STATEMENT	4
2.2 NATURE OF ENGINEERING PROBLEM-SOLVING	4
2.3 KNOWLEDGE-BASED APPROACH TO ENGINEERING PROBLEM SOLVING . . .	5
2.4 KNOWLEDGE-BASED APPROACH TO PAVEMENT EVALUATION AND REHABILITATION	6
2.4.1 Pavement Evaluation: A Diagnostic Activity	6
2.4.2 Pavement Rehabilitation: A Design Activity	8
2.5 IMPLEMENTATION OF THE SYSTEM	9
2.6 FUTURE OF KNOWLEDGE-BASED SYSTEMS IN ENGINEERING	10
CHAPTER 3 DESCRIPTION OF EVALUATION AND REHABILITATION SYSTEM	11
3.1 INTRODUCTION	11
3.2 PAVEMENT GEOMETRY	11
3.3 STEPS IN EVALUATION/REHABILITATION PROCEDURE	12
3.4 PROJECT DATA COLLECTION	12
3.4.1 Conducting the Project Survey	14
3.4.2 Number and Length of Sample Units	14
3.4.3 Project Survey Data Entry	15
3.5 EXTRAPOLATION OF PROJECT CONDITION	15
3.6 EVALUATION OF PRESENT CONDITION	15
3.6.1 Major Problem Areas	15
3.6.2 Evaluation Decision Trees and Conclusions	16
3.6.3 Critical Distress Levels	17
3.6.4 Candidate Rehabilitation Techniques	17
3.7 PREDICTION OF FUTURE CONDITION WITHOUT REHABILITATION	17

	PAGE
3.8 PHYSICAL TESTING RECOMMENDATIONS	19
3.8.1 Nondestructive Deflection Testing	19
3.8.2 Destructive Testing and Laboratory Testing	19
3.8.3 Skid Testing	20
3.8.4 Roughness Testing	20
3.8.5 Use of Physical Testing Data	20
3.9 SELECTION OF MAIN REHABILITATION APPROACH	20
3.10 DEVELOPMENT OF COMPLETE REHABILITATION STRATEGY	23
3.10.1 Traffic Lane Reconstruction	23
3.10.2 Shoulder Rehabilitation Adjacent to a Reconstructed Lane	24
3.10.3 Traffic Lane Overlay	24
3.10.4 Shoulder Rehabilitation Adjacent to an Overlaid Lane .	25
3.10.5 Traffic Lane Restoration	25
3.10.6 Shoulder Rehabilitation Adjacent to a Restored Lane .	25
3.11 PREDICTION OF REHABILITATION STRATEGY PERFORMANCE	25
3.12 QUANTITY ESTIMATES FOR LIFE-CYCLE COST ANALYSIS	26
CHAPTER 4 JRCP EVALUATION AND REHABILITATION	28
4.1 JRCP PROJECT SURVEY	28
4.2 EXTRAPOLATION OF OVERALL PROJECT CONDITION	28
4.2.1 Average Per Mile Data Items	28
4.2.2 Deteriorated Joints Per Mile	37
4.2.3 Faulting	38
4.2.4 Toggle Values	38
4.3 EVALUATION OF PRESENT CONDITION	39
4.4 PREDICTION OF FUTURE CONDITION	40
4.5 REHABILITATION STRATEGY DEVELOPMENT	40
4.5.1 Restoration Alternative	40
4.5.2 AC Structural Overlay Alternative	53
4.5.3 Unbonded Concrete Overlay Alternative	53
4.6 REHABILITATION ALTERNATIVE SELECTION	53
CHAPTER 5 JPCP EVALUATION AND REHABILITATION	61
5.1 JPCP PROJECT SURVEY	61
5.2 EXTRAPOLATION OF OVERALL PROJECT CONDITION	61
5.2.1 Average Per Mile Data Items	61
5.2.2 Deteriorated Joints Per Mile	74
5.2.3 Faulting	75
5.2.4 Toggle Values	75

	PAGE
5.3 EVALUATION OF PRESENT CONDITION	76
5.4 PREDICTION OF FUTURE CONDITION	81
5.5 REHABILITATION STRATEGY DEVELOPMENT	81
5.5.1 AC Structural Overlay Alternative	81
5.5.2 Crack and Seat and AC Structural Overlay Alternative	81
5.5.3 Bonded Concrete Overlay Alternative	92
5.5.4 Unbonded Concrete Overlay Alternative	92
5.5.5 Reconstruct / Restore Alternative	92
5.6 REHABILITATION ALTERNATIVE SELECTION	102
CHAPTER 6 CRCP EVALUATION AND REHABILITATION	103
6.1 CRCP PROJECT SURVEY	103
6.2 EXTRAPOLATION OF OVERALL PROJECT CONDITION	103
6.2.1 Average Per Mile Data Items	103
6.2.2 Toggle Values	114
6.3 EVALUATION OF PRESENT CONDITION	114
6.4 PREDICTION OF FUTURE CONDITION	115
6.5 REHABILITATION STRATEGY DEVELOPMENT	115
6.5.1 AC Structural Overlay Alternative	122
6.5.2 Bonded Concrete Overlay Alternative	122
6.5.3 Reconstruct / Restore Alternative	129
6.6 REHABILITATION ALTERNATIVE SELECTION	129
CHAPTER 7 CONCLUSIONS AND RECOMMENDATIONS	133
7.1 CONCLUSIONS	133
7.2 RECOMMENDATIONS	134
APPENDIX A JRCP	136
APPENDIX B JPCP	239
APPENDIX C CRCP	343
REFERENCES VOLUME III	400

VOLUME IV APPENDIXES

CHAPTER 1. INTRODUCTION	1
1.0 STUDY OBJECTIVE	1
1.1 FIELD STUDIES	1
CHAPTER 2. DATABASE DESCRIPTION	2
2.1 DATA COLLECTION PROCEDURES	2
2.1.1 Field Condition Surveys	2
2.1.2 Original Pavement and Rehabilitation Design Factors	6
2.1.3 Traffic Data	6
2.1.4 Environmental Data	6
2.2 LABORATORY STUDIES	6
2.3 ANALYTICAL STUDIES	6
2.4 EVALUATION AND REHABILITATION SYSTEM	6
2.5 EXTENT OF DATABASE	7
2.6 DESCRIPTION OF DATABASE VARIABLES	7
CHAPTER 3. LABORATORY SHEAR TESTING OF DOWELS ANCHORED IN CONCRETE. .	26
3.1 EXPERIMENTAL DESIGN	26
3.1.1 Preparation of the Test Specimens	26
3.1.2 Description of the Test and Related Equipment	33
3.2 LABORATORY STUDY RESULTS	36
3.2.1 Preliminary Results and Observations	36
3.2.2 Factors Affecting Dowel Deflection and Looseness	40
3.2.3 Dowel Deflection and Looseness Models	51
3.2.4 Conclusions	67
REFERENCES VOLUME IV	84

LIST OF FIGURES

Figure		Page
VOLUME I REPAIR REHABILITATION TECHNIQUES		
1	General location of all rehabilitation projects surveyed	2
2	Location of diamond grinding sections included in the database .	10
3	Age distribution for diamond grinding sections	13
4	ESAL distribution for diamond grinding sections	14
5	Transverse cracking distribution for diamond grinding sections .	17
6	Longitudinal cracking distribution for diamond grinding sections	19
7	Faulting distribution for diamond grinding sections.	20
8	Estimated project faulting history for standard JRCP section for new construction and after restoration with diamond grinding.	25
9	Faulting projections for standard JRCP and standard plus drains and PCC shoulders (Estimated faulting for new section also shown for comparison)	27
10	Faulting projections for standard JPCP and standard plus drains and PCC shoulders (Estimated faulting for new section also shown for comparison)	28
11	Faulting projections for standard JRCP and standard plus drains and PCC shoulders	29
12	Faulting projections for standard JPCP and standard plus drains and PCC shoulders	30
13	Illustration of predicted faulting for various restoration techniques for JPCP.	31
14	Illustration of predicted faulting for various restoration techniques for JRCP.	32
15	Location of load transfer restoration sample units by State. . .	43
16	Climatic zone factorial for load transfer restoration uniform sections	45
17	Diagram of retrofit dowel or I-beam device and installation	47
18	Distribution of retrofit dowel performance	48

List of Figures (cont)

Figure	Page
19 Diagram of double-vee shear device and installation	50
20 Distribution of double-vee shear device performance	52
21 Distribution of I-beam device performance	53
22 Diagram of figure-eight device and installation	54
23 Distribution of figure-eight device performance	55
24 Sensitivity plot depicting model-predicted faulting vs. accumulated 18-kip [80 kN] ESALs for JRCP	59
25 Sensitivity plot depicting model-predicted faulting vs. accumulated 18-kip [80 kN] ESALs for JPCP	60
26 Installation pattern for retrofit dowels in Florida	62
27 Installation pattern for double-vee shear devices in Florida. .	64
28 Layout plan of treatment configurations and locations by joint number in Florida project	66
29 Comparison of JPCP joint faulting: new pavement vs. rehabilitated pavement	71
30 Comparison of JRCP joint faulting: new pavement vs. rehabilitated pavement	72
31 Recommended retrofit dowel design for heavy traffic (6)	74
32 Location of edge support sample units by States	79
33 Climatic zone factorial for edge support uniform sections . . .	82
34 Faulting projections for standard JPCP and standard plus drains and PCC shoulders (Estimated faulting for new section also shown for comparison)	84
35 Illustration of predicted faulting for various restoration techniques for JPCP	85
36 Diagram of different edge support designs (6)	99
37 Effect of lane/shoulder tie on deflection of PCC traffic lane (6)	101
38 The effect of lane/shoulder tie and width of PCC shoulder on tensile stress of traffic lane (6)	102

List of Figures (cont)

Figure	Page
39 Effect of edge support on slab corner deflection with a stabilized subbase (6)	103
40 Effect of edge beam on slab corner deflection with a granular subbase (6)	104
41 Recommended tie bar spacing (No. 5 deformed rebar or equivalent) (6)	107
42 Elongation of transverse repair joint dowel holes after 1 year of heavy traffic	114
43 Full-depth repair projects surveyed	120
44 Distribution of full-depth repair ages	121
45 Illustration of the development of faulting at transverse joints (7)	125
46 Illustration of possible mechanism for repair faulting where leave joint faulting exceeds approach joint faulting)	127
47 Full-depth repair loading and faulting mechanism	128
48 Illustration of possible development of faulting at overfilled repairs	129
49 Plot of leave joint load transfer vs. time for varying numbers of 1.25-in [3.2-cm] dowels per wheelpath	134
50 Plot of approach joint load transfer vs. time for tied and dowelled joints	135
51 Effect of tied and dowelled approach joints on leave joint load transfer	136
52 Effect of varying anchor materials and number of dowels per wheelpath on repair leave joint load transfer	137
53 Effects of varying anchor materials and number of dowels per wheelpath on repair leave joint faulting	138
54 Sensitivity of repair leave joint faulting model to traffic and base support.	141
55 Sensitivity of repair leave joint faulting model to climatic factors (Freezing Index and age).	142
56 Sensitivity of repair approach joint spalling model to traffic and the use and maintenance of repair joint seals	146

List of Figures (cont)

Figure	Page
57 Sensitivity of repair approach joint spalling model to contraction joint spacing and the use and maintenance of repair joint seals	147
58 Illustration of grout retention disk used in lab experiment. . .	154
59 Illustration of load function used for lab testings	156
60 Repeated dowel load test assembly	157
61 Illustration of for estimation of dowel looseness from load-deflection curve (47)	160
62 Measured load-deflection profile after 300,000 load cycles for specimen D10R (1-in [2.5 cm] dowel, 1/32-in [0.08 cm] annular gap, 9-in [23-cm] embedment, low-energy drill, epoxy mortar) . .	165
63 Computed dowel looseness vs. log load cycles for specimen D10R (1-in [2.5-cm] dowel, 1/32-in [0.08-cm] annular gap, 9-in [23-cm] embedment, low-energy drill, epoxy mortar)	166
64 Transverse joint evaluation and rehabilitation selection for jointed concrete pavements (34)	171
65 General flow chart for determining joint rehabilitation needs (34)	172
66 Full-depth repair recommendations for plain jointed concrete pavements under heavy traffic (6)	175
67 Full-depth repair recommendations for jointed reinforced concrete pavements under heavy traffic (6)	176
68 Recommended dowel bar layout for heavy traffic loadings (6). . .	177
69 Recommended designs for full-depth repairs for jointed plain concrete pavements (6)	179
70 Recommended designs for full-depth repairs for jointed reinforced concrete pavements (6)	180
71 Saw cut locations for lift out method of concrete removal (6). .	183
72 Transverse and longitudinal joint reservoir designs (6).	188
73 Location of partial-depth repair projects in the database. . . .	196
74 Steps in partial-depth repair operation (6)	210
75 Placement of partial-depth repair over a joint or crack (6). . .	211

List of Figures (cont)

Figure		Page
VOLUME II OVERLAY REHABILITATION TECHNIQUES		
1	General locations of all rehabilitation projects surveyed	2
2	General locations of bonded PCC overlays	10
3	Age distribution of bonded concrete overlays	14
4	Distribution of the overlay thickness of concrete overlays	15
5	Distribution of severity of transverse cracking in the outer lane on bonded concrete overlays	19
6	Development of reflective transverse cracking in bonded concrete overlays from thermal contraction at low temperatures .	21
7	Development and deterioration of reflective transverse cracking in bonded concrete overlays from shearing stresses and bending stresses created by traffic loadings	22
8	Distribution of severity of longitudinal cracking in the outer lane on bonded concrete overlays	24
9	Development of secondary joint cracking in bonded concrete overlays when the overlay joint is not sawed prior to crack propagation past the adjustment point	26
10	Development of secondary joint cracking in bonded concrete overlays from the propagation at a location away from the underlying pavement joint	28
11	Shear stress distribution at the slab edge (30)	30
12	Shear stress distribution for a 1-in bonded concrete overlay from drying shrinkage effects (30)	31
13	Shear stress induced by drying shrinkage of the bonded overlay at various ambient relative humidity levels (30)	32
14	Maximum shear stresses due to drying shrinkage vs. the overlay thickness for various water-cement ratios (30)	33
15	The temperature profile through a concrete slab (mid-may)	34
16	Maximum shear stresses due to shrinkage and differential temperature effects (30)	36

List of Figures (cont)

Figure	Page
17 Sensitivity of bonded overlay faulting model to subbase type and freezing index	39
18 Sensitivity of bonded overlay faulting model to dowel diameter and freezing index	40
19 Comparison of predicted faulting on bonded overlays to predicted new pavement faulting	42
20 Sensitivity of bonded overlay cracking model to Cracking Index and Freezing Index, at high traffic (1 million ESAL/yr)	45
21 Sensitivity of bonded overlay cracking model to Cracking Index and Freezing Index, at moderate traffic (1/2 million ESAL/yr)	46
22 Typical fatigue cracking development curve	47
23 Edge load stress and corner deflection versus overlay thickness on a standard 9-in concrete pavement. (Developed by ILLI-SLAB modelling of a 9 kip wheel load [Tire pressure = 75 psi] positioned at free edge and corner	49
24 Comparison of free edge stress for bonded concrete overlay to equivalent thickness of asphalt concrete overlay (Computed by ILLI-SLAB finite element program for 12 x 20 ft slab with 18 kip single axle-load at edge)	50
25 General locations of unbonded PCC overlays	64
26 Age distribution of unbonded concrete overlays	65
27 Distribution of the overlay thickness for unbonded concrete overlays	66
28 Distribution of severity of transverse cracking in the outer lane on unbonded concrete overlays	70
29 The temperature profile (for mid-May) through an unbonded overlay cross-section	72
30 Development of the void under unbonded concrete pavements from the differential curling phenomena	73
31 Distribution of severity of longitudinal cracking in the outer lane on unbonded concrete overlays	74
32 The effectiveness of mismatched joints in inhibiting the development of faulting and pumping	76

33	Sensitivity of the unbonded overlay faulting model to dowel bar diameter	78
34	Comparison of predicted faulting on unbonded overlays to predicted new pavement faulting (similar design conditions) . .	79
35	Details for mismatching of overlay joints with joints in the existing pavement	86
36	Distribution of crack and seat projects in the database	92
37	Age comparisons for the crack and seat projects in the database	93
38	Thickness comparisons for crack and seat projects in the database	94
39	Amount and severity of reflection cracking present on crack and seat projects (JPCP)	99
40	Amount and severity of reflection cracking present on crack and seat projects (JRCP)	100
41	Present serviceability rating (PSR) for the crack and seat projects	102
42	Distribution of rut depths in the database	103
43	Relationship between rut depth and number of 18-kip ESALs on the overlay	104
44	Influence of cracking pattern on reflection cracking	110
45	Influence of Freezing Index on reflection cracking	111
46	Influence of original concrete pavement thickness on reflection cracking	112
47	Influence of seating roller weight on reflection cracking	113
48	Influence of subgrade type on reflection cracking	114
49	Influence of joint spacing on reflection cracking	115
50	Influence of annual precipitation in inches on reflection cracking	116
51	Influence of annual precipitation in inches and average monthly temperature range on rutting	119
52	Influence of overlay thickness and percent trucks on rut depth	120

List of Figures (cont)

Figure		Page
VOLUME III CONCRETE PAVEMENT EVALUATION AND REHABILITATION SYSTEM		
1	Structural adequacy decision tree for JRCP	7
2	Main rehabilitation approach decision tree	22
3	Project survey sheets for I-74 example	29
4	Evaluation of present condition for I-74 example	41
5	Evaluation of future condition of I-74 without rehabilitation .	48
6	Project survey sheets for I-10 example	62
7	Evaluation of present condition for I-10 example	77
8	Evaluation of future condition of I-10 without rehabilitation .	84
9	Project survey sheets for I-57 example	104
10	Evaluation of present condition for I-57 example	116
11	Evaluation of future condition of I-57 example without rehabilitation	121
VOLUME IV APPENDIXES		
1	Concrete pavement field data collection forms	4
2	Asphalt concrete pavement field data collection forms	5
3	Illustration of grout retention disk used in lab experiment . . .	31
4	Illustration of dowel bar prepared for installation with grout retention disk in place	32
5	Illustration of load function used for lab testing	34
6	Photo of load collar and LVDT attachment	35
7	Repeated dowel load test assembly	37
8	Photo of voids in cement grout anchor material.	39
9	Illustration of estimation of dowel looseness from load-deflection curve (47).	41
10	Plot of ANOVA data for sensor deflection (All specimens).	48

List of Figures (Cont.)

Figures	Page
11 Plot of ANOVA data for dowel looseness (All specimens)	50
12 Predicted effect of annular gap and load cycles on sensor deflection of epoxy mortar specimens with 1-in [2.5-cm] dowels and 9 in [23 cm] of embedment	57
13 Predicted effect of annular gap and bearing stress on sensor deflection of epoxy mortar specimens with 9 in [23 cm] of embedment after 600,000 load cycles	58
14 Predicted effect of annular gap and embedment length on sensor deflection for epoxy mortar specimens	59
15 Predicted effect of annular gap and drill energy on sensor deflection for epoxy mortar specimens	60
16 Predicted effect of annular gap and load cycles on sensor deflection for cement grout specimens	62
17 Predicted effect of annular gap and drill impact energy on sensor deflection for cement grout specimens.	64
18 Predicted effect of annular gap and bearing stress on sensor deflection for cement grout specimens	65
19 Measured load-deflection profile after 300,000 load cycles for specimen D10R (1-in [2.5-cm] dowel, 1/32-in [0.08-cm] annular gap, 9-in [23-cm] embedment, low-energy drill, epoxy mortar)	68
20 Measured load-deflection profile after 300,000 load cycles for specimen D6 (1-in [2.5-cm] dowel, 1/8-in [0.3-cm] annular gap, 9-in [23-cm] embedment, low-energy drill, epoxy mortar)	69
21 Measured load-deflection profile after 300,000 load cycles for specimen A8R (1-in [2.5-cm] dowel, 1/8-in [0.3-cm] annular gap, 9-in [23-cm] embedment, low-energy drill, cement grout)	70
22 Measured load-deflection profile after 300,000 load cycles for specimen B18 (1.5-in [3.8-cm] dowel, 1/8-in [0.3-cm] annular gap, 9-in [23-cm] embedment, low-energy drill, cement grout)	71
23 Measured load-deflection profile after 300,000 load cycles for specimen D20 (1.5-in [3.8-cm] dowel, 1/8-in [0.3-cm] annular gap, 9-in [23-cm] embedment, High-energy drill, cement grout)	72
24 Measured load-deflection profile after 300,000 load cycles for specimen A10 (1.5-in [3.8-cm] dowel, 1/8-in [0.3-cm] annular gap, 7-in [18-cm] embedment, low-energy drill, cement grout).	73
25 Computed dowel looseness vs. log load cycles for specimen D10R (1-in [2.5-cm] dowel, 1/32-in [0.08-cm] annular gap, 9-in [23-cm] embedment, low-energy drill, epoxy mortar)	74

List of Figures (Cont.)

Figures	Page
26 Computed dowel looseness vs. log load cycles for specimen D6 (1-in [2.5-cm] dowel, 1/8-in [0.3-cm] annular gap, 9-in [23-cm] embedment, low-energy drill, epoxy mortar)	75
27 Computed dowel looseness vs. log load cycles for specimen A8R (1-in [2.5-cm] dowel, 1/8-in [0.3-cm] annular gap, 9-in [23-cm] embedment, low-energy drill, cement grout)	76
28 Computed dowel looseness vs. log load cycles for specimen B18 (1.5-in [3.8-cm] dowel, 1/8-in [0.3-cm] annular gap, 9-in [23-cm] embedment, low-energy drill, cement grout)	77
29 Computed dowel looseness vs. log load cycles for specimen D20 (1.5-in [3.8-cm] dowel, 1/8-in [0.3-cm] annular gap, 9-in [23-cm] embedment, high-energy drill, cement grout).	78
30 Computed dowel looseness vs. log load cycles for specimen A10 (1.5-in [3.8-cm] dowel, 1/8-in [0.3-cm] annular gap, 7-in [18-cm] embedment, low-energy drill, cement grout)	79
31 Measured load-deflection profile after 300,000 load cycles for cast-in-place specimen (1-in [2.5-cm] dowel, 9-in [23-cm] embedment)	80
32 Computed dowel looseness vs. log load cycles for cast-in-place specimen (1-in [2.5-cm] dowel, 9-in [23-cm] embedment)	81
33 Measured load-deflection profile after 300,000 load cycles for stainless steel pipe (1.625-in [4.1-cm] by 1/8-in [0.3-cm] wall thickness pipe, 7-in [18-cm] embedment, medium-energy drill, epoxy mortar)	82
34 Computed dowel looseness vs. log load cycles for for stainless steel pipe (1.625-in [4.1-cm] by 1/8-in [0.3-cm] wall thickness pipe, 7-in [18-cm] embedment, medium-energy drill, epoxy mortar) .	83

LIST OF TABLES

TABLE		Page
VOLUME I REPAIR REHABILITATION TECHNIQUES		
1	Breakdown of rehabilitation technique by state	3
2	Summary of monitoring and design data for each rehabilitation technique	4
3	Pavement condition variables collected in the field surveys	11
4	Original pavement construction and design variables	12
5	Summary of distress types identified for diamond grinding projects (Outer traffic lane only)	16
6	Typical "standard" pavement characteristics for faulting sensitivity analysis	26
7	Load transfer restoration database design variables	42
8	Performance summary for all devices evaluated	49
9	Description of treatment configurations for retrofit dowels in Florida	63
10	Description of treatment configurations for double-vee shear devices in Florida	65
11	Edge support database design and monitoring variables	78
12	Design variability by edge support project site	81
13	Edge beam project variability	86
14	Full-width PCC shoulder project variability	87
15	Edge support project variability as part of a concrete overlay	90
16	Pavement condition variables collected during field survey	116
17	Original pavement design and construction variables	117
18	Full-depth repair design and construction variables	118
19	Distribution of cumulative 18-kip [80-kN] ESALs (millions) and load transfer system designs for the surveyed repairs	122
20	Illinois I-70 experimental patch design data	123

List of Tables (Cont)

Table	Page
21 Correlation coefficients and their significances for key variables related to repair leave joint faulting (Outer lane, dowelled repairs only - 699 cases)	131
22 Summary of Illinois DOT experimental repair project faulting and load transfer data	132
23 Correlation coefficients and their significances for key variables related to repair approach joint spalling (Outer lane - 1113 cases)	143
24 Correlation coefficients and their significances for key variables related to transverse cracking of full-depth repairs (Outer lane - 1113 cases)	148
25 Correlation coefficients and their significances for key variables related to longitudinal cracking of full-depth repairs (Outer lane - 1113 cases)	150
26 Summary of test values used in dowel bar repeated shear tests	152
27 Advantages and disadvantages of methods for removal of concrete in patch area (6)	184
28 Early opening guidelines for full-depth repairs (60)	189
29 Summary of partial-depth repair projects	196
30 Original pavement design data for partial-depth repair projects	198
31 Partial-depth repair construction data	199

VOLUME II OVERLAY REHABILITATION TECHNIQUES

1 Breakdown of rehabilitation techniques by State	3
2 Summary of monitoring and design data for each rehabilitation technique	4
3 Pavement condition variables collected in the field surveys . .	11
4 Original pavement construction and design variables	12
5 Overlay construction and design variables	13
6 Design and construction data for bonded concrete overlays . . .	16
7 Summary of bonded concrete overlay faulting and cracking observed on each uniform section surveyed	18

List of Tables (Cont)

Table	Page
8 Design and construction data for unbonded concrete overlays . . .	67
9 Summary of unbonded concrete overlay faulting and cracking observed on each uniform section surveyed	69
10 Crack and seat overlay design variables	91
11 Distresses in each sample unit in the database	96

**VOLUME III CONCRETE PAVEMENT EVALUATION AND
REHABILITATION SYSTEM**

1 Future condition predictions for I-74 example	46
2 Restoration strategy for I-74 example including estimated quantities	50
3 Restoration performance prediction for I-74 example	51
4. AC overlay strategy for I-74 example including estimated quantities	54
5 AC overlay performance prediction for I-74 example	55
6 Unbonded PCC overlay strategy for I-74 example	57
7 Unbonded PCC overlay performance prediction for I-74 example . .	58
8 Future condition predictions for I-10 example	82
9 AC structural overlay strategy for I-10 example	86
10 AC overlay performance prediction for I-10 example	87
11 Crack and seat strategy for I-10 example	89
12 Crack and seat performance prediction for I-10 example	90
13 Bonded PCC overlay strategy for I-10 example	93
14 Bonded PCC overlay performance prediction for I-10 example . . .	94
15 Unbonded PCC overlay strategy for I-10 example	96
16 Unbonded PCC overlay performance prediction for I-10 example . .	97
17 Reconstruction/restore strategy for I-10 example	99
18 Reconstruction/restore performance prediction for I-10 example .	100
19 Future condition predictions for I-57 example	119

List of Tables (Cont)

Table	Page
20 AC structural overlay strategy for I-57 example	123
21 AC overlay performance prediction for I-57 example	124
22 Bonded concrete overlay strategy for I-57 example	126
23 Bonded concrete overlay performance prediction for I-57 example	127
24 Reconstruct/restore strategy for I-57 example	130
25 Reconstruct/restore performance prediction for I-57 example . .	131

VOLUME IV APPENDIXES

1 Breakdown of rehabilitation techniques by state	8
2 Climatic zone factorial for each rehabilitation technique . . .	9
3 Original pavement design variables for all projects	11
4 Database design variables for diamond grinding	12
5 Database monitoring variables for diamond grinding	13
6 Database design variables for load transfer restoration	14
7 Database monitoring variables for load transfer restoration . .	15
8 Database design variables for edge support	16
9 Database monitoring variables for edge support	17
10 Database design variables for full-depth repair	18
11 Database monitoring variables for full-depth repair	19
12 Database design variables for partial-depth repair	20
13 Database monitoring variables for partial-depth repair	21
14 Database design variables for concrete overlays	22
15 Database monitoring variables for concrete overlays	23
16 Database design variables for crack and seat	24
17 Database monitoring variables for crack and seat	25
18 Summary of test values used in dowel bar repeated shear tests .	27
19 Experimental test matrix of specimens actually tested	28

List of Tables (Cont)

Table	Page
20 Summary of results of material property tests performed on I-70 slabs	30
21 Analysis of variance computation table	32
22 Summary of ANOVA data for sensor deflection (All specimens) . .	47
23 Summary of ANOVA data for dowel looseness (All specimens) . . .	49
24 Summary of ANOVA data for sensor deflection (Cement grout specimens)	52
25 Summary of ANOVA data for dowel looseness (Cement grout specimens)	53
26 Summary of ANOVA data for sensor deflection (Epoxy mortar specimens)	54
27 Summary of ANOVA data for dowel looseness (Epoxy mortar specimens)	55

CHAPTER 1

INTRODUCTION

1.0 STUDY OBJECTIVE

The overall objective of this study was to develop improved evaluation procedures and rehabilitation techniques for concrete pavements. This objective was accomplished through extensive field, laboratory and analytical studies that have provided new knowledge and understanding of the performance of rehabilitated concrete pavements. New and unique evaluation and rehabilitation procedures and techniques were developed that will be very useful to practicing pavement engineers.

This final report, presented in four volumes, documents all of the results developed under the contract, "Determination of Rehabilitation Methods For Rigid Pavements", conducted for the Federal Highway Administration. This volume documents the data collection procedures and database description for the rehabilitation projects. Also included is a detailed chapter describing the laboratory shear testing of dowels anchored in concrete. A brief discussion of the laboratory dowel shear testing can be found in volume I, chapter 5.

1.1 FIELD STUDIES

The field studies involved a large and extensive field survey of 349 rehabilitation sections of jointed plain and reinforced concrete pavement. These sections were located in 24 States. Eight rehabilitation techniques were selected for detailed study:

- Diamond grinding.
- Load transfer restoration.
- Edge support.
- Full-depth repair.
- Partial-depth repair.
- Bonded concrete overlays.
- Unbonded concrete overlays.
- Crack and seat and AC overlay.

CHAPTER 2

DATABASE DESCRIPTION

2.1 DATA COLLECTION PROCEDURES

The 349 uniform sections (from 267 different projects) included in the database represent many of the concrete pavement rehabilitation projects in existence today within the United States that have utilized at least one of the eight rehabilitation techniques of interest. These pavements were surveyed between June 1985 and August 1986.

There were five basic data types that were deemed necessary for the development of performance prediction models and the development and improvement of design and construction procedures. These include:

- Field condition data.
- Original pavement structural design, in situ conditions, and historical improvement data.
- Rehabilitation design data.
- Historical traffic volumes, vehicle classifications and accumulated 18-kip [80-kN] equivalent single-axle loadings.
- Environmental data.

The data sources and collection procedures used in this research study are described below.

2.1.1 Field Condition Surveys

A standard field condition survey was performed on each project or uniform section. The procedures used in the collection of condition data closely follow those described in NCHRP Project 1-19 (COPES) study for field data collection.⁽¹³⁾ The distress identification manual developed for the COPES study was used as a standard for the identification and measurement of distresses and their severity levels.

The term "uniform section" was defined in the COPES study as a section of pavement with "uniform characteristics along its length including structural design, joint design and spacing, reinforcement, truck traffic, subgrade conditions, and distress".⁽¹⁴⁾ To properly incorporate rehabilitation technique variation (e.g., different full-depth repair designs, different overlay thicknesses, etc.) into the uniform section concept, it was necessary to expand the definition of a uniform section to include uniformity of rehabilitation design.

Preliminary Work

The first step in project selection was to contact State department of transportation personnel to determine their interest in participating in the study. Project description forms were then sent to those States who were interested and willing to participate. The State personnel then selected representative rehabilitation projects that included one or more of the eight techniques, and filled out a project description form for each section.

The project description forms from all over the country were reviewed by the Contractor, any inappropriate sections were excluded (where one or more of the eight rehabilitation techniques were not included for example), and detailed data collection forms were sent to the State personnel for the selected projects in their State. Upon completion of these data collection forms, data entry into the database was begun. If important data items were missing, an additional written request was sent to the State personnel for this information. In some cases, this information was retrieved in person through a trip to the State department of transportation office.

In preparation for the field work, the beginning and ending markers (stations, mileposts, landmarks) of the project were determined as best as possible in the office by verbal communication with state department of transportation personnel, prior to the commencement of surveying procedures. These steps ensured that any changes in uniform section pertaining to variations in the design of the original pavement or rehabilitation design would not be overlooked.

Field Work

After the preliminary identification of the uniform sections to be surveyed, the following procedures were used in the field data collection process.

- A two-person trained survey crew made at least one pass over the project areas at the posted speed. During the pass, changes in the pavement condition, in situ foundation conditions (cut/fill) and drainage were noted. This pass was used to determine whether one or more uniform sections were necessary on the basis of pavement distress, grade or drainage variation.
- The uniform sections were surveyed by representative sampling. Usually two 1000-ft [305 m] sample units were surveyed per uniform section. If the section was of considerable length (greater than 10 miles [16.1 km]), a third sample unit was taken to ensure reasonable coverage. The location of the sample units was selected randomly; however, sample units were selected such that grade conditions (cut/fill) along their lengths were as uniform as possible. Also, in consideration of the fact that a project or sample unit might require additional evaluation at some future date, many of the sample units were located at milepost markers for easier future identification.
- A very comprehensive distress survey was conducted along each sample unit. The condition of both lanes was measured where traffic or other conditions did not pose a serious safety hazard to the survey crew. The outer lane survey was conducted from the outer shoulder of the pavement and, likewise, the inner lane survey was conducted from the inner shoulder. Measurements of faulting and joint widths were taken 1 foot [0.3 m] from the PCC slab lane edge. Samples of the field data collection sheets are shown in figures 1 and 2. Figure 1 was used for the concrete-surfaced rehabilitation techniques, whereas the strip map shown in figure 2 was used for the asphalt-surfaced crack and seat projects. Also, photographs of the pavement, general topography and other distresses were recorded.
- The presence of subsurface drainage and the condition of subsurface drainage facilities were noted.

stations

DISTRESS SURVEY FOR TRANSVERSE JOINT

	OUTER LAANE						INNER LAANE					
	STATION	STATION	STATION	STATION	STATION	STATION	STATION	STATION	STATION	STATION	STATION	STATION
	PATCH ID	PATCH ID	PATCH ID	PATCH ID	PATCH ID	PATCH ID	PATCH ID	PATCH ID	PATCH ID	PATCH ID	PATCH ID	PATCH ID
REGULAR JOINT PATCH WITH APPROACH JOINT WITH PATCH JOINT LEAVE JOINT PRESSURE RELIEF JOINT												
DISTRESSES												
SPALLING (TR. JOINT)												
(APPROACH SIDE 1)	L M E	L M E	L M E	L M E	L M E	L M E	L M E	L M E	L M E	L M E	L M E	L M E
(LEAVE SIDE 2)	L M E	L M E	L M E	L M E	L M E	L M E	L M E	L M E	L M E	L M E	L M E	L M E
SPALLING (CORNER)												
(APPROACH SIDE 1)	L M E	L M E	L M E	L M E	L M E	L M E	L M E	L M E	L M E	L M E	L M E	L M E
(LEAVE SIDE 2)	L M E	L M E	L M E	L M E	L M E	L M E	L M E	L M E	L M E	L M E	L M E	L M E
PUMPING	L M E	L M E	L M E	L M E	L M E	L M E	L M E	L M E	L M E	L M E	L M E	L M E
FAULTING (in inches)	---	---	---	---	---	---	---	---	---	---	---	---
JOINT WIDTH (in inches)	---	---	---	---	---	---	---	---	---	---	---	---
CORNER BREAKS												
(APPROACH SIDE 1)	Y / N	Y / N	Y / N	Y / N	Y / N	Y / N	Y / N	Y / N	Y / N	Y / N	Y / N	Y / N
(LEAVE SIDE 2)	Y / N	Y / N	Y / N	Y / N	Y / N	Y / N	Y / N	Y / N	Y / N	Y / N	Y / N	Y / N
"D" CRACKING	Y / N	Y / N	Y / N	Y / N	Y / N	Y / N	Y / N	Y / N	Y / N	Y / N	Y / N	Y / N
REACTIVE AGGREGATE	Y / N	Y / N	Y / N	Y / N	Y / N	Y / N	Y / N	Y / N	Y / N	Y / N	Y / N	Y / N
SEALANT CONDITIONS												
ABSENCE	Y / N	Y / N	Y / N	Y / N	Y / N	Y / N	Y / N	Y / N	Y / N	Y / N	Y / N	Y / N
COHESION FAILURE	Y / N	Y / N	Y / N	Y / N	Y / N	Y / N	Y / N	Y / N	Y / N	Y / N	Y / N	Y / N
ADHESION FAILURE	Y / N	Y / N	Y / N	Y / N	Y / N	Y / N	Y / N	Y / N	Y / N	Y / N	Y / N	Y / N
EXTRUSION	Y / N	Y / N	Y / N	Y / N	Y / N	Y / N	Y / N	Y / N	Y / N	Y / N	Y / N	Y / N
OXIDATION (HARDENED)	Y / N	Y / N	Y / N	Y / N	Y / N	Y / N	Y / N	Y / N	Y / N	Y / N	Y / N	Y / N
INCOMPRESSIBLES	Y / N	Y / N	Y / N	Y / N	Y / N	Y / N	Y / N	Y / N	Y / N	Y / N	Y / N	Y / N

DISTRESS SURVEY FOR REHABILITATION PATCH AREA

	OUTER LAANE			INNER LAANE		
	PATCH ID	PATCH ID	PATCH ID	PATCH ID	PATCH ID	PATCH ID
	PCC AC OTHER	PCC AC OTHER	PCC AC OTHER	PCC AC OTHER	PCC AC OTHER	PCC AC OTHER
TYPE OF MATERIAL TYPE OF PATCH PATCH LOCATION PATCH LENGTH PATCH WIDTH SUBSEALANT USED	FULL / PARTIAL DEPTH AT A JOINT BETWEEN JOINTS FULL SLAB REPLACEMENT	FULL / PARTIAL DEPTH AT A JOINT BETWEEN JOINTS FULL SLAB REPLACEMENT	FULL / PARTIAL DEPTH AT A JOINT BETWEEN JOINTS FULL SLAB REPLACEMENT	FULL / PARTIAL DEPTH AT A JOINT BETWEEN JOINTS FULL SLAB REPLACEMENT	FULL / PARTIAL DEPTH AT A JOINT BETWEEN JOINTS FULL SLAB REPLACEMENT	FULL / PARTIAL DEPTH AT A JOINT BETWEEN JOINTS FULL SLAB REPLACEMENT
DISTRESSES	Y / N	Y / N	Y / N	Y / N	Y / N	Y / N
PCC or other material						
TRANSVERSE CRACKING	L M E	L M E	L M E	L M E	L M E	L M E
LONGITUDINAL CRACKING	L M E	L M E	L M E	L M E	L M E	L M E
SCALING	Y / N	Y / N	Y / N	Y / N	Y / N	Y / N
AC Patch material						
RUTTING	L M E	L M E	L M E	L M E	L M E	L M E
ALLIGATOR CRACKING	L M E	L M E	L M E	L M E	L M E	L M E
RAVELING	Y / N	Y / N	Y / N	Y / N	Y / N	Y / N
SHOWING	Y / N	Y / N	Y / N	Y / N	Y / N	Y / N
Partial depth patches						
LOSS OF PATCH MATERIAL (percent of patch area)	---	---	---	---	---	---

Figure 1. Concrete pavement field data collection forms.

Present Lane Width _____

Start Pt. Mile Mark _____

Start Pt. Station No. _____

The figure displays three identical vertical data collection forms for asphalt concrete pavement. Each form is a tall rectangle with a vertical scale on the left side, marked with the numbers 20, 40, 60, and 80. A dashed vertical line runs down the center of each form, representing a lane centerline. Below the first form, the labels "Left Ln" and "Right Ln" are positioned to indicate the left and right lanes relative to the centerline. The forms are intended for field data collection, likely for measuring lane width and other pavement characteristics.

Figure 2. Asphalt concrete pavement field data collection forms.

2.1.2 Original Pavement and Rehabilitation Design Factors

For the collection of this data, the as-built original construction and rehabilitation construction plans, as well as special provisions for the rehabilitation projects, were obtained for each project. Much of the required data was obtained from these records; however, consultation with State department of transportation personnel was also necessary to collect additional information. Finally, data from other sources such as published reports was also used.

A detailed listing of the variables collected under this study pertaining to original pavement and rehabilitation design and rehabilitation field monitoring is included in section 2.6.

2.1.3 Traffic Data

Values for the average annual daily traffic and percent heavy commercial truck traffic were also collected from the State department of transportation records. Historical information was collected where the data was available; however, in some instances only current traffic levels were obtained. For the determination of the number of equivalent 18-kip [80 kN] single-axle loadings (ESALs) accumulated on each project, Federal Highway Administration W-4 truck axle load distribution data were utilized to compute the truck factors over the life of the pavements. The number of accumulated axle loads from the time of original pavement construction until the time each rehabilitation technique was applied, and from then until the time of survey, was calculated for each project.

2.1.4 Environmental Data

The average monthly precipitation and average daily minimum, maximum and mean temperatures were taken from National Oceanic and Atmospheric Administration data. The nearest weather station was assumed to be representative of the conditions at the project site. The mean Freezing Index was interpolated from the contour map developed by the Corps of Engineers for the continental United States.(14) The climatic zone as classified by Carpenter was also determined for each site.(14)

2.2 LABORATORY STUDIES

Laboratory studies included the first comprehensive testing of dowel anchoring procedures and designs. Full-scale repeated shear loading of dowels was conducted for up to one million load repetitions using slabs cut from I-70 in Illinois. Many different design, material and construction variables were considered in a factorial type experimental design.

2.3 ANALYTICAL STUDIES

Analytical studies were accomplished primarily to develop prediction models for rehabilitated pavement deterioration so that the service life of different rehabilitation techniques could be estimated. Twelve distress models were developed including reflective cracking, faulting, rutting, and serviceability for most of the above rehabilitation techniques. These models were incorporated into the evaluation and rehabilitation system.

2.4 EVALUATION AND REHABILITATION SYSTEM

A comprehensive concrete pavement evaluation and rehabilitation system was developed for jointed plain, jointed reinforced and continuously reinforced concrete

pavements. This system is intended to assist the design engineer in the following rehabilitation project design activities:

- Project data collection.
- Evaluation of present condition.
- Prediction of future condition without rehabilitation.
- Physical testing recommendations.
- Selection of feasible rehabilitation approaches.
- Development of detailed rehabilitation recommendations.
- Prediction of performance of the rehabilitation strategy.
- Cost analysis and selection of the preferred rehabilitation alternative.

The results of this research are published in four volumes:

- Volume I Repair Rehabilitation Techniques
- Volume II Overlay Rehabilitation Techniques
- Volume III Concrete Pavement Evaluation/Rehabilitation System
- Volume IV Appendixes

Each of these volumes are stand alone volumes that present the data, analyses and conclusions for each of the rehabilitation techniques and the evaluation and rehabilitation system.

2.5 EXTENT OF THE DATABASE

The database is comprehensive, containing as many projects as were available or that could be included within available resources. This was done to provide a wide range of data to facilitate regression analysis for the development of performance models.

An indication of the extent of this database is shown in tables 1 and 2. Table 1 represents the number of different project designs in the database by State and rehabilitation technique. In addition, there are typically two replicate sample units for each different design. Table 2 illustrates the climatic zone factorial for all of the rehabilitation sections defined in this study.

2.6 DESCRIPTION OF DATABASE VARIABLES

Tables 3 through 17 contain all of the variables collected for this rehabilitation study which pertain to the original pavement design, the design of each rehabilitation technique and the field monitoring of each rehabilitation technique. For each rehabilitation technique, the monitoring data collected applies to different sections of the rehabilitated pavement. For instance, edge support monitoring data was collected not only for the outer and inner traffic lanes, but also for the PCC tied shoulder, whereas the full-depth repair monitoring data applies to individual repairs and individual repair joints. The section headings for the database monitoring variables contain a description concerning the proper application of the field monitoring data to the various pavement sections.

The traffic database contains the annual average daily traffic, percent heavy commercial trucks, truck factor and accumulated 18-kip [80 kN] equivalent single-

Table 1. Breakdown of rehabilitation techniques by State.

STATE	FDR	PDR	DGD	LTR	CAS	UNBOL	BOL	ES	TOTAL
Arizona	1	1	3	0	0	0	0	0	5
Arkansas	1	0	1	0	1	0	0	1	4
California	3	0	7	0	6	0	0	0	16
Colorado	2	0	1	1	2	3	0	2	11
Florida	3	0	2	0	5	0	0	0	10
Georgia	5	6	16	2	0	2	0	0	31
Illinois	11	1	6	2	12	2	0	1	35
Iowa	5	0	2	0	0	0	25	0	32
Kentucky	0	0	0	0	9	0	0	0	9
Louisiana	1	1	1	1	0	0	1	0	5
Michigan	8	1	0	0	0	2	0	2	13
Minnesota	7	5	7	0	2	0	0	1	22
Nebraska	6	3	0	0	0	0	0	0	9
New York	1	1	2	2	10	0	2	0	18
Ohio	6	1	6	1	0	3	0	1	18
Oklahoma	1	0	2	2	0	0	0	0	5
Pennsylvania	5	2	3	1	2	2	0	2	17
South Carolina	2	1	2	0	0	0	0	1	6
South Dakota	0	3	3	0	3	0	1	0	10
Texas	6	3	0	0	0	0	0	0	9
Virginia	10	5	2	1	0	0	0	0	18
West Virginia	2	0	0	0	3	0	0	0	5
Wisconsin	8	1	5	0	15	0	0	0	29
Wyoming	2	1	5	0	0	0	2	2	12
Total	96	36	76	13	70	14	31	13	349

NOTE: FDR = full-depth repair
PDR = partial-depth repair
DGD = diamond grinding
LTR = load transfer restoration
CAS = crack and seat and AC overlay
UNBOL = unbonded concrete overlay
BOL = bonded concrete overlay
ES = edge support (tied PCC shoulder or edge beam)

* Represents the number of different uniform sections in the database. In addition, there are typically two replicate sample units for each different design.

Table 2. Climatic zone factorial for each rehabilitation technique.

DETERMINATION OF REHABILITATION METHODS FOR RIGID PAVEMENTS

FACTORIAL OF CLIMATIC ZONES FOR EACH REHABILITATION TECHNIQUE

	FDR	PDR	DGD	LIR	CAS	UNBOL	BOL	ES
WET-FREEZE	40	11	27	5	40	10	20	6
WET-FREEZE-THAW	11	6	22	2	12	0	1	1
WET-NO FREEZE	22	8	10	3	9	1	0	1
INTERMEDIATE-FREEZE	8	7	2	0	3	0	8	1
INTER. FREEZE-THAW	1	0	2	2	0	0	0	0
INTERMEDIATE-NO FREEZE	5	3	5	0	3	0	0	0
DRY-FREEZE	6	0	5	1	2	3	2	4
DRY-FREEZE-THAW	0	1	1	0	0	0	0	0
DRY-NO FREEZE	3	0	2	0	1	0	0	0
TOTAL UNIFORM SECTIONS	96	36	76	13	70	14	31	13

axle loads (ESALs) for the outer and inner lane. This information was calculated for each year since the project was rehabilitated with any of the eight techniques under consideration. The accumulated ESALs correspond to the loadings applied from the year of rehabilitation to the year of survey. An approximate value for the ESALs accumulated since original pavement construction was also determined.

The climatic database contains the average monthly temperature, the average daily maximum temperature, the average daily minimum temperature and the average monthly precipitation for each month of the year for each project site. These values correspond to the weather station nearest to the project site, which was assumed to represent the conditions at the project site. Also included in this database was an entry for the climatic zone and mean Freezing Index at the project site.

Table 3. Original pavement design variables for all projects.

Identification Number (State Code, Highway #, Milepost, Direction)

Beginning and Ending Mile Marker (station)

Number of Through Lanes in One Direction

Type of Original Pavement (JPCP, JRCP)

Layer Descriptions, Thicknesses, Material Types

Date of Original Pavement Construction

Dates and Description of Major Pavement Improvements

Average Contraction Joint Spacing

Skewness of Joints

Expansion Joint Spacing, if any

Transverse Contraction Joint Load Transfer System

Dowel Diameter, Spacing and Length

Type of Slab Reinforcement (welded-wire fabric, deformed rebar)

Longitudinal Bar/Wire Diameter, Spacing and Length

Type of Subgrade Soil (fine-grained, coarse-grained)

Outer Shoulder Surface Type

Original Subsurface Drainage Type

Original Subsurface Drainage Location

Table 4. Database design variables for diamond grinding.

Project Identification Number

Sample Unit

Primary Reason for Diamond Grinding

Extent of Diamond Grinding (entire pavement, at joints only)

Friction Number Before Grinding and Measurement Date

Friction Number After Grinding and Measurement Date

Equipment Used For Friction Testing

Roughness of Pavement Before Grinding and Measurement Date

Roughness of Pavement After Grinding and Measurement Date

Equipment Used For Roughness Measurement

Speed at Which Roughness Measurements Taken

Table 5. Database monitoring variables for diamond grinding.

GENERAL FIELD DATA:

Sample Unit Length

Foundation of Sample Unit (cut, fill or at grade)

Condition of Drainage Ditches

Subsurface Drainage Functional

Number of Regular and Patch Joints

PAVEMENT DISTRESS DATA: (for outer lane and inner lane)
(low, medium and high severities)

Centerline Joint Longitudinal "D" Cracking (Outer Lane Only)

Transverse and Longitudinal Cracking

Transverse and Longitudinal "D" Cracking

Longitudinal Joint Spalling

Scaling, Crazeing, Map Cracking

Mean Regular Joint Faulting over Sample Unit

Mean Patch Joint Faulting over Sample Unit

Mean Transverse Crack Faulting over Sample Unit

JOINT DISTRESS SUMMARY: (for outer lane and inner lane)
(low, medium and high severities)

Transverse Joint Spalling (approach side, leave side)

Transverse Joint Corner Spalling (approach side, leave side)

Mean Pumping over Sample Unit

Mean Joint Width over Sample Unit

Corner Breaks (approach side, leave side)

"D" Cracking along Joint and/or Reactive Aggregate in Slab

Sealant Conditions (Cohesion Failure, Oxidized, etc.)

Incompressibles in Joint

Table 6. Database design variables for load transfer restoration.

Project Identification Number

Sample Unit

Load Transfer Device Type (retrofit dowels, Double-vee shear devices)

Frequency of Installation (all joints, selected joints)

Lane in Which Load Transfer was Restored

Number of Devices Per Lane

Location of Load Transfer Devices Across the Lane

Diameter and Length of Retrofit Dowel Bars

Material Used to Backfill Slot/Core Hole

Bonding Agent Between Existing Slab and Backfill Material

Table 7. Database monitoring variables for load transfer restoration.

GENERAL FIELD DATA:

Sample Unit Length

Foundation of Sample Unit (cut, fill or at grade)

Condition of Drainage Ditches

Subsurface Drainage Functional

LOAD TRANSFER DEVICE DISTRESS DATA: (for individual restored joints and cracks)

Load Transfer Device Type

Station of Restored Joint or Crack

Type of Joint

Location of Joint (outer lane, inner lane)

Number of Devices on Joint or Crack

Device Performance (debonding of core, material failure, etc.)

JOINT DISTRESS SUMMARY: (for individual restored joints and cracks)

Transverse Joint Spalling (approach side, leave side)

Transverse Joint Corner Spalling (approach side, leave side)

Mean Pumping at Restored Joint

Mean Joint Faulting and Joint Width at Restored Joint

Corner Breaks (approach side, leave side)

"D" Cracking along Joint

Reactive Aggregate

Sealant Conditions (Cohesion Failure, Oxidized, etc.)

Incompressibles in Joint

Table 8. Database design variables for edge support.

Project Identification Number
Sample Unit
Type of Edge Support System
Matching of Shoulder and Mainline Pavement Joints
Lane/Shoulder Tie System
Diameter of Tie Bars
Length of Tie Bars
Spacing of Tie Bars
Shoulder Width and Design Thickness
Shoulder Thickness Tapering, if any
Thickness of Undercut, if any
Type of Lane/Shoulder Joint
Lane/Shoulder Joint Forming Method

Table 9. Database monitoring variables for edge support.

GENERAL FIELD DATA:

Sample Unit Length

Foundation of Sample Unit (cut, fill or at grade)

Condition of Drainage Ditches

Subsurface Drainage Functional

Number of Transverse Joints on the Mainline Pavement

Number of Transverse Joints on the Shoulder

PAVEMENT DISTRESS DATA: (for outer lane, inner lane and shoulder)
(low, medium and high severities)

Centerline Joint Longitudinal "D" Cracking (Outer Lane Only)

Transverse Cracking

Transverse "D" Cracking

Longitudinal Cracking

Longitudinal "D" Cracking

Longitudinal Joint Spalling

Scaling, Crazeing, Map Cracking

Lane/Shoulder Dropoff (Shoulder Only)

JOINT DISTRESS SUMMARY: (for outer lane, inner lane and shoulder)
(low, medium and high severities)

Transverse Joint Spalling (approach side, leave side)

Transverse Joint Corner Spalling (approach side, leave side)

Mean Pumping over Sample Unit

Mean Joint Faulting and Joint Width over Sample Unit

Corner Breaks (approach side, leave side)

"D" Cracking along Joint and/or Reactive Aggregate in Slab

Sealant Conditions (Cohesion Failure, Oxidized, etc.)

Incompressibles in Joint

Table 10. Database design variables for full-depth repair.

Project Identification Number

Sample Unit

Number of Different Patch Designs in Sample Unit

Patch Type Design Number

Equipment Used for Cutting Boundaries

Depth of Typical Boundary Saw Cut

Concrete Breakup Method and Removal Method

Foundation Repair

Transverse Joint Design

Type of Transverse Joint at Repair Boundaries

Type of Transverse Joint Within Repair, if any

Type of Load Transverse System at Approach Joint

Type of Load Transverse System at Leave Joint

Type of Load Transverse System at Longitudinal Joint

Patch Joint Skew, if any

Transverse Boundary Joint Bar Diameter, Spacing and Length

Location of Transverse Bars

Load Transfer Bar Grouting Material

Reinforcement Steel Placed in Patch

Transverse Repair Sealing Method (at boundaries)

Type of Seal Forming (at the within joint)

Repair Curing Method

Typical Time Between Patch Placement and Opening to Traffic

Table 11. Database monitoring variables for full-depth repair.

PATCH DISTRESS DATA:	(by individual patches) (low, medium and high severities)
Patch Designation Number	
Patch Location by Lane (outer lane or inner lane)	
Type of Material (PCC, AC)	
Patch Location within Lane (at a joint, mid-slab)	
Patch Length and Width	
Subsealing of Patch Evident	
Transverse and Longitudinal Cracking	
Scaling	
Rutting	
Alligator Cracking	
Raveling of Patch Material (yes, no)	
Shoving of Patch Material (yes, no)	
Percent Loss of Patch Material	
JOINT DISTRESS SUMMARY:	(by individual patch joints) (patch approach, leave and within joints) (low, medium and high severities)
Transverse Joint Spalling (approach side, leave side)	
Transverse Joint Corner Spalling (approach side, leave side)	
Mean Pumping at Joint	
Mean Joint Faulting and Joint Width at Joint	
Corner Breaks (approach side, leave side)	
"D" Cracking along Joint and/or Reactive Aggregate in Slab	
Sealant Conditions (Cohesion Failure, Oxidized, etc.)	
Incompressibles in Joint	

Table 12. Database design variables for partial-depth repair.

Project Identification Number
Sample Unit
Patch Boundary Determination
Equipment for Cutting Boundaries
Depth of Typical Boundary Saw Cut
Deteriorated Concrete Breakup and Removal Method
Maximum Airhammer Size
Method Used to Clean Patch Area
Bonding Agent
Patch Material Used
Typical Air Temperature at Time of Placement
Joint Forming Method
Patch Curing Method
Time Between Patch Placement and Opening to Traffic

Table 13. Database monitoring variables for partial-depth repair.

PATCH DISTRESS DATA:	(by individual patches) (low, medium and high severities)
Patch Designation Number	
Joint Station of Patched Joint or Crack	
Location of Joint (outer lane, inner lane)	
Type of Joint (regular joint, repair joint, transverse crack)	
Type of Patch Material and Number of Patches on the Joint	
Patch Location (approach side, leave side)	
Average Patch Length and Width	
Presence of Subsealing Holes near the Joint	
Transverse and Longitudinal Cracking	
Scaling	
Rutting	
Alligator Cracking	
Raveling and/or Shoving of Patch Material (yes, no)	
Percent Loss of Patch Material	
JOINT DISTRESS SUMMARY:	(by individual patch joints) (low, medium and high severities)
Transverse Joint Spalling (approach side, leave side)	
Transverse Joint Corner Spalling (approach side, leave side)	
Mean Pumping at Joint	
Mean Joint Faulting and Joint Width at Joint	
Corner Breaks (approach side, leave side)	
"D" Cracking along Joint and/or Reactive Aggregate in Slab	
Sealant Conditions (Cohesion Failure, Oxidized, etc.)	
Incompressibles in Joint	

Table 14. Database design variables for concrete overlays.

Project Identification Number

Sample Unit

Type of PCC Overlay (JPCP or JRCP)

Bonding Condition of Overlay (bonded, unbonded or partially bonded)

Initial Surface Preparation

Final Surface Preparation

Type of Grout Used For Bonding Overlays

Material Used to Prevent Bonding

Matching of Overlay and Existing Pavement Joints

Average Overlay Contraction Joint Spacing

Expansion Joint Spacing

Skewness of Joint

Contraction Joint Load Transfer System (dowels, aggregate interlock)

Dowel Diameter, Spacing and Length

Method used to Form Transverse Joints

Lane/Shoulder Joint Tie Bar Diameter, Spacing and Length

Type of Slab Reinforcement

Longitudinal Bar Diameter, Spacing and Length

Table 15. Database monitoring variables for concrete overlays.

GENERAL FIELD DATA:

Sample Unit Length

Foundation of Sample Unit (cut, fill or at grade)

Condition of Drainage Ditches

Subsurface Drainage Functional

Number of Transverse Joints in the Sample Unit

PAVEMENT DISTRESS DATA: (for outer lane, inner lane and shoulder)
(low, medium and high severities)

Centerline Joint Longitudinal "D" Cracking (Outer Lane Only)

Transverse Cracking

Transverse "D" Cracking

Longitudinal Cracking

Longitudinal "D" Cracking

Longitudinal Joint Spalling

Scaling, Crazeing, Map Cracking

JOINT DISTRESS SUMMARY: (for outer lane, inner lane and shoulder)
(low, medium and high severities)

Transverse Joint Spalling (approach side, leave side)

Transverse Joint Corner Spalling (approach side, leave side)

Mean Pumping over Sample Unit

Mean Joint Faulting over Sample Unit

Mean Joint Width over Sample Unit

Corner Breaks (approach side, leave side)

"D" Cracking along Joint and/or Reactive Aggregate in Slab

Sealant Conditions (Cohesion Failure, Oxidized, etc.)

Incompressibles in Joint

Table 16. Database design variables for crack and seat.

Project Identification Number
Sample Unit
Presence of "D" cracking on Existing Pavement
Original Slab Repair
Pavement Breaker Type
Average PCC Breakage Size -- WIDTH
Average PCC Breakage Size -- LENGTH
Wire Mesh Cut or Broken
Seating Roller Type
Seating Roller Weight
Broken Pavement Exposure Time to Traffic

Table 17. Database monitoring variables for crack and seat.

GENERAL FIELD DATA:

Sample Unit Length

Foundation of Sample Unit (cut, fill or at grade)

Condition of Drainage Ditches

Subsurface Drainage Functional

PAVEMENT DISTRESS DATA: (for outer lane and inner lane)
(low, medium and high severities)

Centerline Longitudinal Cracking (Outer Lane Only)

Transverse Cracking

Joint Reflective Cracking

Longitudinal Cracking

Lane Edge Cracking

Mean Pumping over Sample Unit

Alligator Cracking

Block Cracking

Raveling/Weathering

Bleeding

Potholes

Rutting Inner Wheelpath (100-ft [30.5 m] intervals)

Rutting Outer Wheelpath (100-ft [30.5 m] intervals)

CHAPTER 3

LABORATORY SHEAR TESTING OF DOWELS ANCHORED IN CONCRETE

3.1 EXPERIMENTAL DESIGN

The general concept of the study involved the application of repeated shear loads to dowels of various dimensions anchored in holes drilled in concrete specimens obtained from an inservice Interstate highway and the collection and analysis of dowel load and deflection data at several points during the load history of each dowel.

The effects of five design and construction variables -- dowel diameter, annular gap (the width of the void to be filled with anchor material when the dowel is placed in the exact center of the drilled hole), anchor material, embedment length and drill type (varying drill impact energy) -- on the deflection response of dowels in full-depth repairs to repeated shear loads were investigated. Two test levels, one "high" and one "low," based on the current range of design and construction practice, were selected for each variable except for drill type, for which three "levels" or types were selected. Table 18 summarizes the test values that were selected for each of the variables.

Tests were also conducted on a number of "special" specimens, including two specimens with dowels cast in place in the lab, two specimens with dowels turned on a lathe to provide a very tight friction fit, and one specimen with a large diameter hollow stainless steel dowel. These tests were conducted for comparison purposes and to provide an indication of needs for future research.

Most test specimens were subjected to approximately 600,000 load cycles, although a few specimens received 2 million or more load cycles to more accurately document the development of dowel looseness.

A replicated half-fraction factorial experimental design was employed to provide a statistical basis for determining the main effects and interaction effects of the five variables under consideration. The use of a half-fraction factorial allows the estimation of main effects and two-way interaction effects while testing only half of the cells in the complete factorial matrix. Three-way and higher order interaction effects are considered negligible.(1)

The original replicated half-fraction factorial design was modified as testing progressed. Test cells and replicates were added to provide estimates of test result variability over various test factors. Specimen preparation and testing errors resulted in the deletion of some specimens from the testing program and adjustments were also made to the test matrix based on availability of specimens. Table 19 presents the matrix of specimens that were actually tested.

3.1.1 Preparation of the Test Specimens

Portland cement concrete slabs for fabricating test specimens were obtained from the outside eastbound lane of Interstate 70 near milepost 89, west of Effingham, Illinois. This pavement is a four-lane divided highway constructed of 10-in [25 cm] reinforced PCC pavement with contraction joints at 100-ft [30.5 m] intervals. The highway was constructed in 1962, and had accommodated approximately 13.8 million 18-kip [80-kN] single-axle loads in the design (outside) lane from the date of construction to the date of removal.

Table 18. Summary of test values used in dowel bar repeated shear tests.

<u>VARIABLE</u>	<u>Low Value</u>	<u>Medium</u>	<u>High Value</u>
Dowel Diameter	1" [2.5 cm]		1.5" [3.8 cm]
Annular Gap	1/32" [0.08 cm]		1/8" [0.3 cm]
Anchor Material	Cement Grout (Dayton Superior Sure-Grip -- "Flowable" Mix)		Epoxy Resin (Hilti HIT C-10)
Embedment Length	7" [17.8 cm]		9" [22.9 cm]
Drill Type	Standard Pneumatic	Hydraulic Percussion (TAMROCK)	Electro- Pneumatic (Hilti, Inc.)

Table 19. Experimental test matrix of specimens actually tested.

	1 in DOWEL BAR				1-1/2 in DOWEL BAR			
	1/32 in ANNULAR GAP		1/8 in ANNULAR GAP		1/32 in ANNULAR GAP		1/8 in ANNULAR GAP	
	CEMENT GROUT	EPOXY RESIN	CEMENT GROUT	EPOXY RESIN	CEMENT GROUT	EPOXY RESIN	CEMENT GROUT	EPOXY RESIN
TAMROCK HYDRAULIC DRILL		2 B2(CPR) D4	2	B1(CPR) C15(CPR) D7(CPR)	2 B5			3 C6(CPR) D16(TEST) A6(CPR)
7 in EMBED	2 A16			2 A4 D2		2 B13 C10	2	
HILTI ELECTRIC DRILL		3 C19 D10 D10R	2 A8R D7R	3 B21 C15R D6	3 C21	3 A5 C19R	3 D13 B18 C6R C22	3 C3R A6R B17
7 in EMBED	2 A18 B4	A16R(cpr) A19R(cpr)	A12	2 A8 C3	C17	2 B11R(5in)	2 A10 D5	
SULLAIR PNEUMATIC DRILL	2 A1 B14			2 B7 D18		2 A2 D19	2 C12 D20	3 A13 B3 D22
7 in EMBED		2 C2 D8	2 A20	C8	2 B20 C16			2 C7

Note: 1 in = 2.54 cm

Four-in [10.2 cm] pressure relief joints were cut near mid-panel at 1000-ft [305 m] intervals in 1972. In July 1985 these relief joints were being replaced with 4-ft [1.2 m] bituminous concrete pressure relief joints/repairs. Using the existing relief joint as one transverse repair joint, the remaining transverse joint and the pavement centerline joint were cut with a diamond blade saw. The undamaged slabs were lifted out and loaded onto flat bed trucks for disposal.(2) Four of these slabs were transported and cut into 18 in by 12 in [31 cm by 46 cm] test specimens. Concrete located near the old relief joint, the lane/shoulder joint and the drilled lift-out holes was discarded. Eighteen usable test specimens were obtained from each slab. Eight 6-in [15.2 cm] diameter (nominal size) cores were also obtained from each slab for compression, split tensile, and elastic modulus testing in accordance with ASTM specifications C 39-72, C 496-71 and C 469-65. Test results are summarized in table 20.

Sand-cement mortar "caps" (generally less than 0.5 in [1.3 cm] thick) were cast on the bottom of each specimen to provide a level base for drilling and testing.

A steel drilling frame was assembled to hold the specimens and drill rigs in place during drilling and to ensure that the holes were drilled perpendicular and centered within one of the 12-in [31 cm] faces of the test specimens. Drilling dust and loose particles were removed from the holes using a large test tube brush and compressed air.

The uncoated steel dowels were washed with soap and water to remove dirt and oil buildups accumulated during shipping which might affect the curing and material properties of the anchor materials, dried with hand towels and allowed to air dry.

The dowels were installed horizontally in the test specimens by injecting sufficient anchor material into the backs of the drilled holes to cause material extrusion when the dowels were inserted. A tight-fitting nylon disk, 2 in larger than the dowel diameter and approximately 3/32 in [0.24 cm] thick was fixed on each dowel at a distance equal to the embedment length from one end of the dowel (see figures 3 and 4). These disks were used to prevent the anchor material from flowing out of the holes and creating voids around the dowels. They also force the anchor material to fill spalls near the dowel hole on the concrete face caused by the drill. One small "weep" hole was provided in each disk to allow excess anchor material to extrude.

The dowels were inserted up to the nylon disks with a back-and-forth twisting action (as recommended by Lippert) to ensure complete and uniform coverage of the dowel and filling of the annular gap with the anchor material.(3) The dowels were allowed to settle or tip in the holes as the anchor material cured.

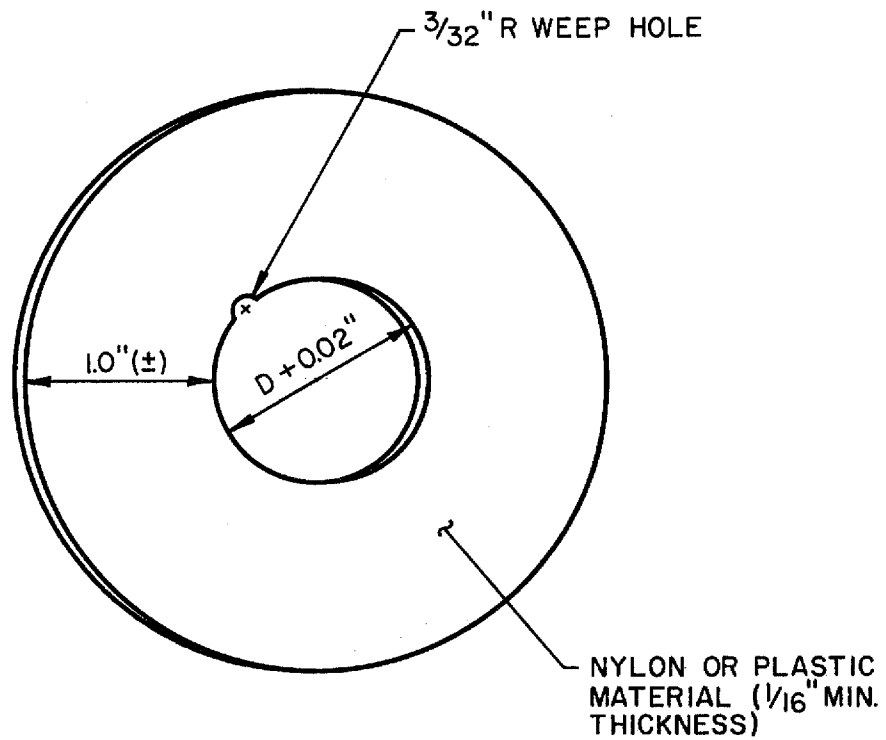
The nylon disks were removed after 24 hours and the anchor material was inspected for surface voids or other visible faults that would affect test results.

An effort was made to test the cement grout specimens no sooner than 7 days and no later than 14 days after preparation. A similar effort was made to test the epoxy resin mortar specimens no sooner than 24 hours and no later than 7 days after preparation. Failures of the test equipment and other delays did result in exceptions, however. Analyses of replicate specimens of each type that were tested at different ages found that the effect of delaying testing beyond the time frames described above was insignificant.

Table 20. Summary of results of material property tests performed on I-70 slabs.

	SLAB DESIGNATION			
	A	B	C	D
Compressive Strength (psi)				
n	3	3	3	3
mean	6283	5320	5819	7471
std. dev.	471	355	527	361
Split Tensile Strength (psi)				
n	3	3	3	3
mean	635	515	689	698
std. dev.	67	50	82	98
Elastic Modulus (psi x 10 ⁶)				
n	1	1	1	1
result	4.8	4.4	4.6	5.2

Note: Multiply psi by 0.0068947 to get MPa.



D = DOWEL DIAMETER
 (INCLUDING
 PROTECTIVE
 COATINGS, IF ANY)

Note: 1 in = 2.54 cm.

Figure 3. Illustration of grout retention disk used in lab experiment.

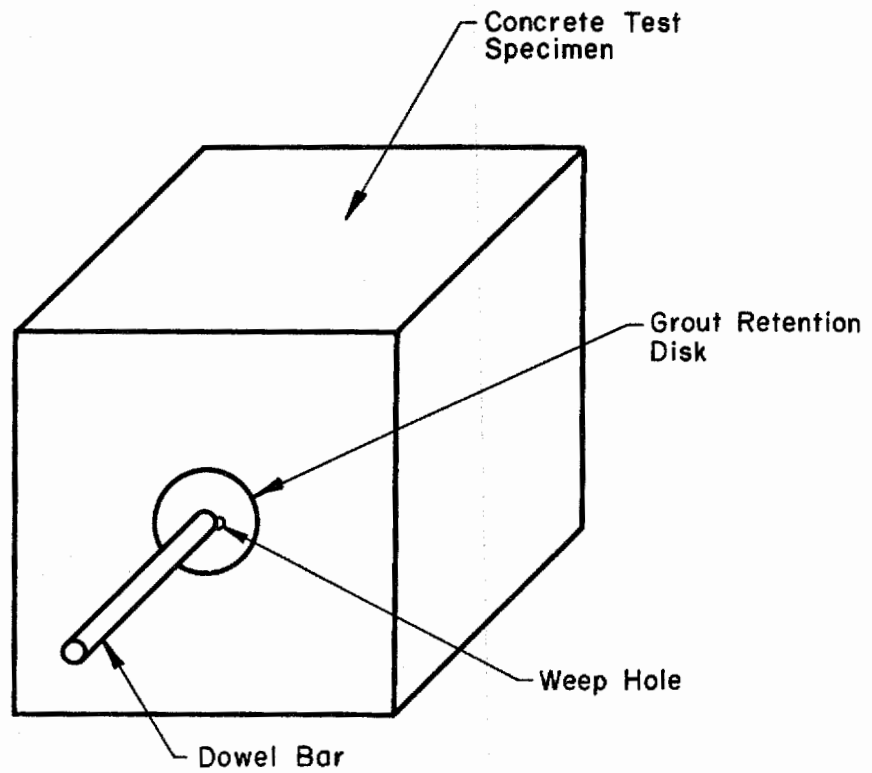


Figure 4. Illustration of dowel bar prepared for installation with grout retention disk in place.

Two specimens were prepared with 1-in [2.5 cm] diameter dowels cast-in-place with 9 in [22.9 cm] of embedment. The concrete mix was designed according to Portland Cement Association procedures for a 3000-psi [20.7 MPa] mix using 1.50-in [3.8 cm] top size crushed stone and sand from the contractor's concrete lab, a type I cement, and a water/cement ratio of 0.45.(4) These specimens were cured for 24 hours, subjected to 5000 load cycles (to simulate early opening of the repair), cured for an additional 27 days, and subjected to an additional 595,000 load cycles. The purpose of these specimens was to set a standard of deflection performance against which to compare the anchored dowels, and to simulate the conditions imposed on the end of the dowel embedded in the repair.

Specimens were also prepared to test the performance of dowels installed to an embedment length of 9 inches [22.9 cm] in very close-fitting holes. The inside diameter of holes drilled in two specimens using 1.0625-in [2.7 cm] nominal diameter drill steels mounted in the Hilti drill was measured and 1.25-in [3.2 cm] dowels were turned on a metal lathe to achieve dowel diameters 0.02 in [0.05 cm] less than the smallest diameter measured in each hole. The finished dowels were 1.06 and 1.10 inches [2.7 and 2.8 cm] in diameter. Insertion of the dowels showed that the smaller of the two was loose enough to be moved slightly in any direction. The larger could not be inserted to full-depth by hand. The larger dowel was forcibly inserted without anchor material using a large hammer. Before testing of the larger dowel, a vertical crack was noted through the center of the face of the specimen, although the crack did not deteriorate under test conditions.

3.1.2 Description of the Test and Related Equipment

Repeated bidirectional vertical shear loads were applied to the dowels installed in the test specimens. The magnitude and rise time of the loads were originally selected to simulate the response of the critical dowel installed in a transverse repair joint to the passage of a tandem-axle dual-wheel load with 18 kips [80-kN] per axle (AASHTO WB-50) at 55 miles per hour [90 km/h]. This simulation was accomplished using the finite-element slab analysis program ILLISLAB.(5) The load format was then modified to reflect the results of previous research efforts and test equipment limitations.(6,7) The load function finally utilized was a continuous sinusoidal form with a peak magnitude of ± 3000 pounds [13.4 kN] and a frequency of 6 Hz (see figure 5). Loads were thus applied at the rate of nearly 520,000 per day, allowing the application of about a years worth of heavy traffic loads to a single dowel installation each day.

The specimens were clamped to a thick steel plate using two sets of thick steel straps which were bolted to the plate and could be adjusted to accommodate specimens of varying width and height. The applied loads were generated hydraulically using an MTS Model 661 ram with an 11 kip [50 kN] capacity, which was controlled by a simple sine wave function generator. The load was applied to the dowel through a specially fabricated high-strength steel loading collar which was clamped to the dowel using large "set" screws. This collar allowed vertical deflection and associated angular movement of the dowel about a lateral axis. The collar contacted 2.5 in [6.5 cm] of the length of the dowel and was positioned 0.25 in [0.6 cm] from the concrete face.

A linearly varying deflection transducer (LVDT) was mounted on a bracket attached to the face of each specimen (using the HIT-C10 material) and connected to the load collar using a small nylon screw. This device was used to measure the movement of the dowel relative to the PCC specimen. The MTS load cell data was also collected for analysis and was used to assist in the computer control of the test. Figure 6 shows the load collar and LVDT attachment.

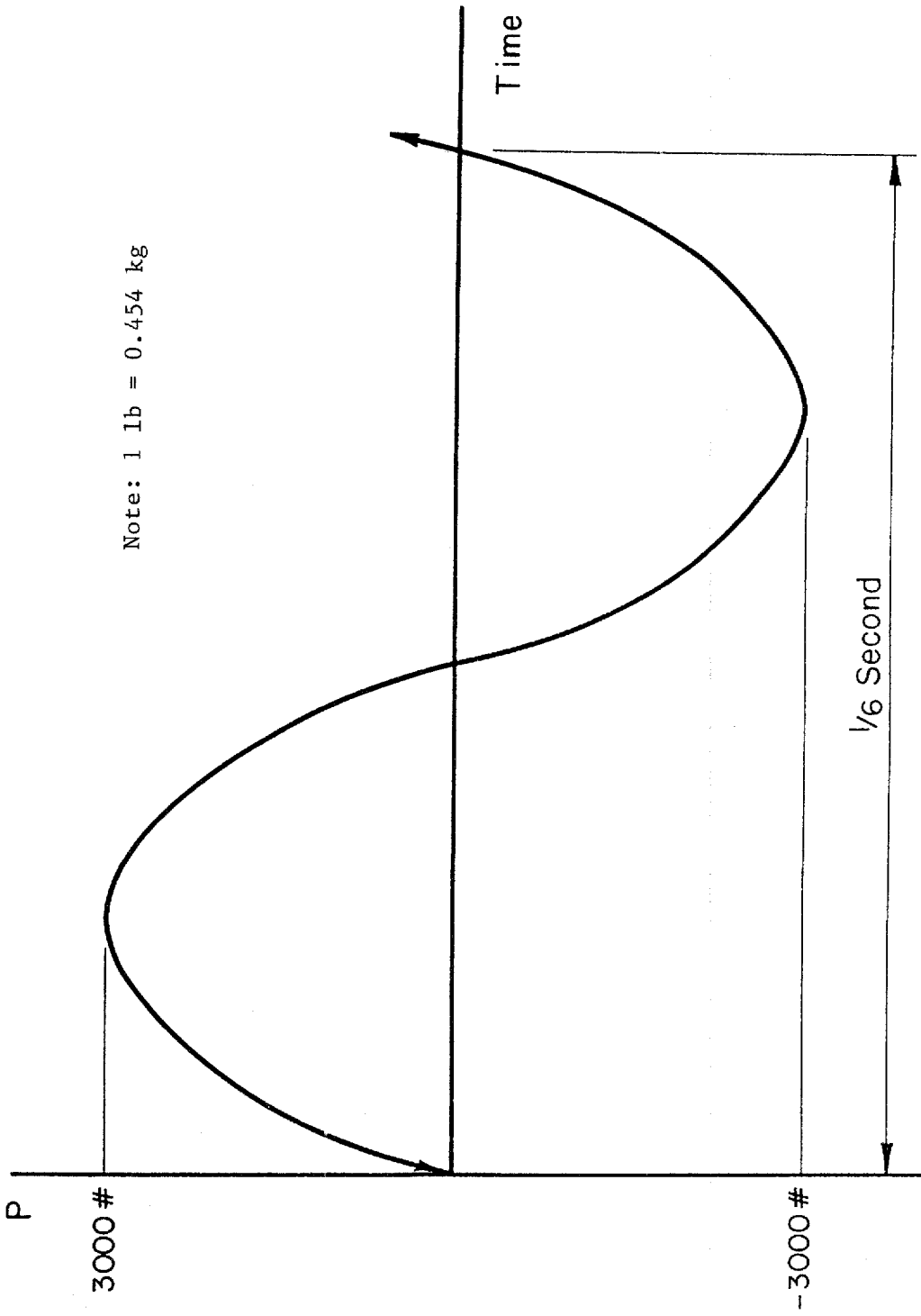


Figure 5. Illustration of load function used for lab testing.

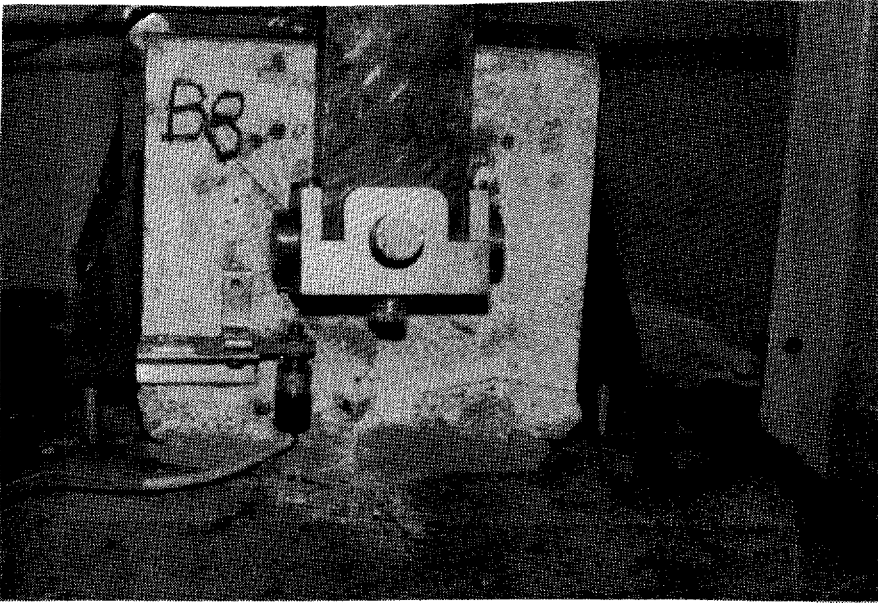


Figure 6. Photo of load collar and LVDT attachment.

The entire test operation was controlled by an IBM Personal Computer using a Data Translations DT-2801A Analog/Digital (A/D) board and a controlling program written in BASIC using the PCLAB library of A/D board control subroutines.(8) Figure 7 shows the entire test assembly arrangement.

The execution of the test control program produces a series of prompts requesting information concerning test specimen identification, design values, and test parameters, including magnitude and frequency of load, and timing, duration and frequency of data collection. Test initiation includes zeroing and calibrating the data collection channels and test operation allows the user to interrupt the test at any time, collect additional data at any time, and change certain test parameters, such as load cycle frequency.

Deflection and load data were typically collected during 10 load cycles immediately after the completion of 1, 2000, 5000, 20000, 100000, 300000 and 600000 load cycles. Extended test data was also collected after 1,200,000, 2,000,000 and 4,000,000 load cycles for certain specimens. Deflection and load data were collected 400 times per second (each) and stored on floppy disk with appropriate identification and test initiation data for later analysis. Data reduction programs were written and used to identify peak load, deflection, and dowel looseness conditions during each load cycle and average the results for each set of ten readings.

The reduced and summarized design and performance data was loaded into an SPSS database and a Lotus 1-2-3 spreadsheet for analysis, production of graphs, etc.(9,10)

3.2 LABORATORY STUDY RESULTS

3.2.1 Preliminary Results and Observations

Observations of the preparation and testing (and occasional failure) of the test specimens provided some insight into the performance of full-depth repairs.

Effect of Drill Impact Energy on Spalling

Drills that impart high impact energy produce more spalling on the concrete face near the drilled hole than drills using low impact energy. The hydraulic drills produced significantly less spalling than the pneumatic drills and the electric-pneumatic drills produced very little spalling at all.

Even relatively minor spalling around the drilled hole can result in a loss of dowel support. If the spall is not filled with dowel anchor material or PCC repair material, the effective joint width will increase in the vicinity of the dowel, producing increased pavement and dowel deflections and increased bearing stresses. Since nylon dowel rings were used to retain the anchor material in the drilled holes and spalled areas, the effect of spalling on dowel deflection could not be determined directly. However, increased deflections were recorded where the anchor material did not completely fill the dowel hole or the spalled area.

The electric-pneumatic drill was most acceptable in minimizing spalling, but the reduced impact energy resulted in a three to fourfold increase in the time required to drill each hole. The hydraulic drills provided a substantial reduction in spalling with no discernible increase in drilling time. The excessive spalling produced by the pneumatic drill was usually repaired easily by using the nylon dowel rings to retain the anchor material and the performance of these "repaired" specimens was equal to similar specimens prepared using other drills.

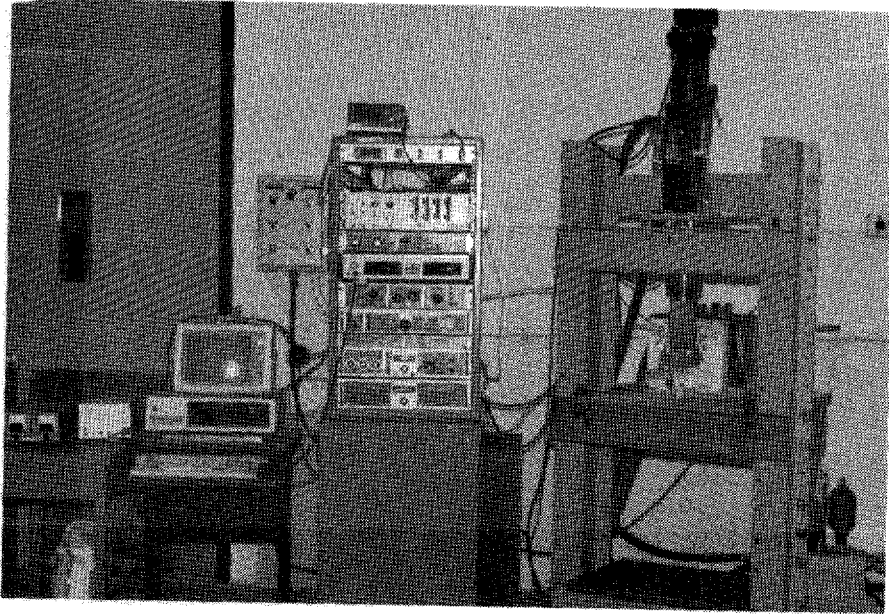


Figure 7. Repeated dowel load test assembly.

Consistency of Dowel Anchor Materials

The installation of dowels using cement grout was often difficult. Small batches of grout (sufficient for about four dowel installations) were carefully prepared in the lab to produce a "flowable" mix and appropriate quantities were delivered to the backs of the drilled holes. Specimens prepared immediately after mixing the grout received a grout that was almost "pourable," and retention of the grout was difficult, even using the nylon rings. Large voids were often observed around these dowels prior to testing (see figure 8) and their deflection profiles were often exaggerated. Specimens that were prepared around 5 minutes after the grout was mixed received a grout that was of the desired consistency, were found to have no voids (or only very small voids), and performed relatively well. Specimens that were prepared 10 minutes or more after mixing the grout received a very stiff grout that often compacted at the back of the hole, preventing proper installation of the dowels, rather than extruding out as the dowels were inserted. These specimens had to be cleaned out and grouted again using a more flowable grout.

The wide variation in grout consistency over a relatively short period of time in the highly controlled environment of the laboratory makes questionable the use of the same material in the field, where conditions can be much more harsh and quality control often takes a back seat to production. Field installations require a reliable, easy-to-use dowel installation material. Cement grout does not consistently meet these requirements.

The epoxy mortar used was almost always proportioned accurately and mixed thoroughly using a hand-held double-barrel caulking gun delivery system which produced a mortar that was the desired consistency. The mortar "set up" in about 5 minutes, which was more than enough time to install the dowel. Curing was complete in about 24 hours (according to the manufacturer), although the dowels could not be moved or removed by any means after about an hour of curing.

The cost of the epoxy mortar is currently substantially higher than the cost of the cement grout, but the reliability and the uniform consistency of the epoxy should make it the preferred material.⁽³⁾ Recently-developed epoxy delivery equipment using much larger cartridges and typical discounts for the purchase of large quantities should reduce the cost of the epoxy for field installations.

It should be noted that not all epoxy mortar materials perform like the one tested. Different "gel," "set" and cure times, and physical and chemical properties affect the suitability of a given material for pavement repair applications. Additional testing should be accomplished before using any unproven material.

Dowel Failures

Five of the 1-in [2.5 cm] diameter dowels tested experienced brittle fatigue failures at locations 0.75 to 1.5 in [1.9 to 3.8 cm] inside the face of the PCC specimens. This location corresponds approximately with the predicted point of maximum moment in the dowel (0.75 in [1.9 cm] inside the face), as presented by Friberg based on the work of Timoshenko.^(11,12) Variations from the predicted location are probably due to nonuniform support of the dowel at the face due to spalling of the concrete during drilling and spalling of the cement grout mortar during testing due to high dowel bearing stress.

Some of these failures occurred after as few as 40,000 load cycles while others occurred after nearly 600,000 load cycles. Four of the failed dowels were anchored using cement grout while one was anchored using epoxy mortar. Large voids were visible above three of the four grouted dowels prior to testing.

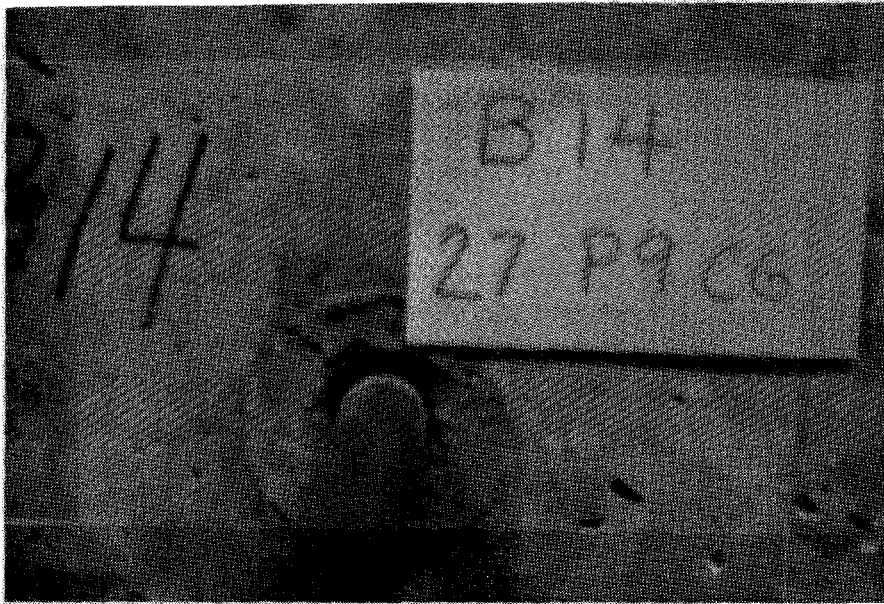


Figure 8. Photo of voids in cement grout anchor material.

These observations indicate the variability of quality of the cement grout anchor material (in spite of the use of the nylon grout retaining rings) and demonstrate the importance of providing void-free uniform dowel support in pavement joints.

Effectiveness of Nylon Grout Retention Rings

The nylon grout retention rings were clearly very effective in reducing the outflow of anchor materials from the drilled holes and ensuring more uniform dowel support. They also forced excess anchor material into the spalled area created by drilling, effectively repairing the spall and reducing dowel deflections.

The effectiveness of the rings was highly dependent on the fluidity of the anchor material being used. Very fluid cement grouts were difficult to work with and were not retained well, even with the rings. Excellent results were obtained using materials that were "flowable" (e.g., using the cement grout about 5 minutes after mixing or the epoxy mortar, as delivered), because they were fluid enough to be moved into the voids, yet viscous enough not to flow appreciably under gravity alone. A smooth, void-free face resulted in these cases.

The use of the grout retention rings represented part of the effort to use the "best" repair preparation and construction techniques so that the maximum potential of each installation would be achieved. The use of these rings, therefore, also probably reduces the difference in performance that would have been observed between the two anchor materials and the three drill types if the rings hadn't been used. Based on initial observations, it would be expected that the elimination of the retention rings would result in much more variability of performance for the cement grout specimens. Higher deflections would be associated with more spalling around the drill hole, so better performance would be expected from holes drilled using low-impact energy drills.

3.2.2 Factors Affecting Dowel Deflection and Looseness

For the purposes of this study, dowel deflection refers to the dowel deflection (under an applied shear load of ± 3000 pounds [13.4 kN]) measured using the LVDT attached to the load collar at a point approximately 1/2 in [1.3 cm] from the face of the specimen.

Dowel looseness was estimated by plotting measured dowel deflection vs. shear load and projecting the slopes of the loading and reverse loading portions of the load-deflection curve at ± 3000 pounds [13.4 kN] back to intercept the deflection axis. This technique was conceptualized by Teller and Cashell and is shown in figure 9.(6)

The half-fraction factorial experimental design employed in the lab tests allowed direct identification of significant effects through analysis of variance (ANOVA) techniques. Table 21 presents the analysis of variance computation sheet.

The six main variables of effects under consideration are number of load cycle repetitions, dowel bar diameter, annular gap, anchor material, embedment length, and drill type and these are referred to as effects 1 through 6, respectively. Interactions between effects are indicated by combinations of these numbers (e.g., the two-way interaction effect of load cycle applications, which is effect 1, and dowel diameter, which is effect 2, is called interaction effect 12). Since a half-fraction factorial experimental design was used, each computed main or interaction effect also represents a higher order interaction effect, or alias, which is listed below the primary effect being considered. As discussed previously,

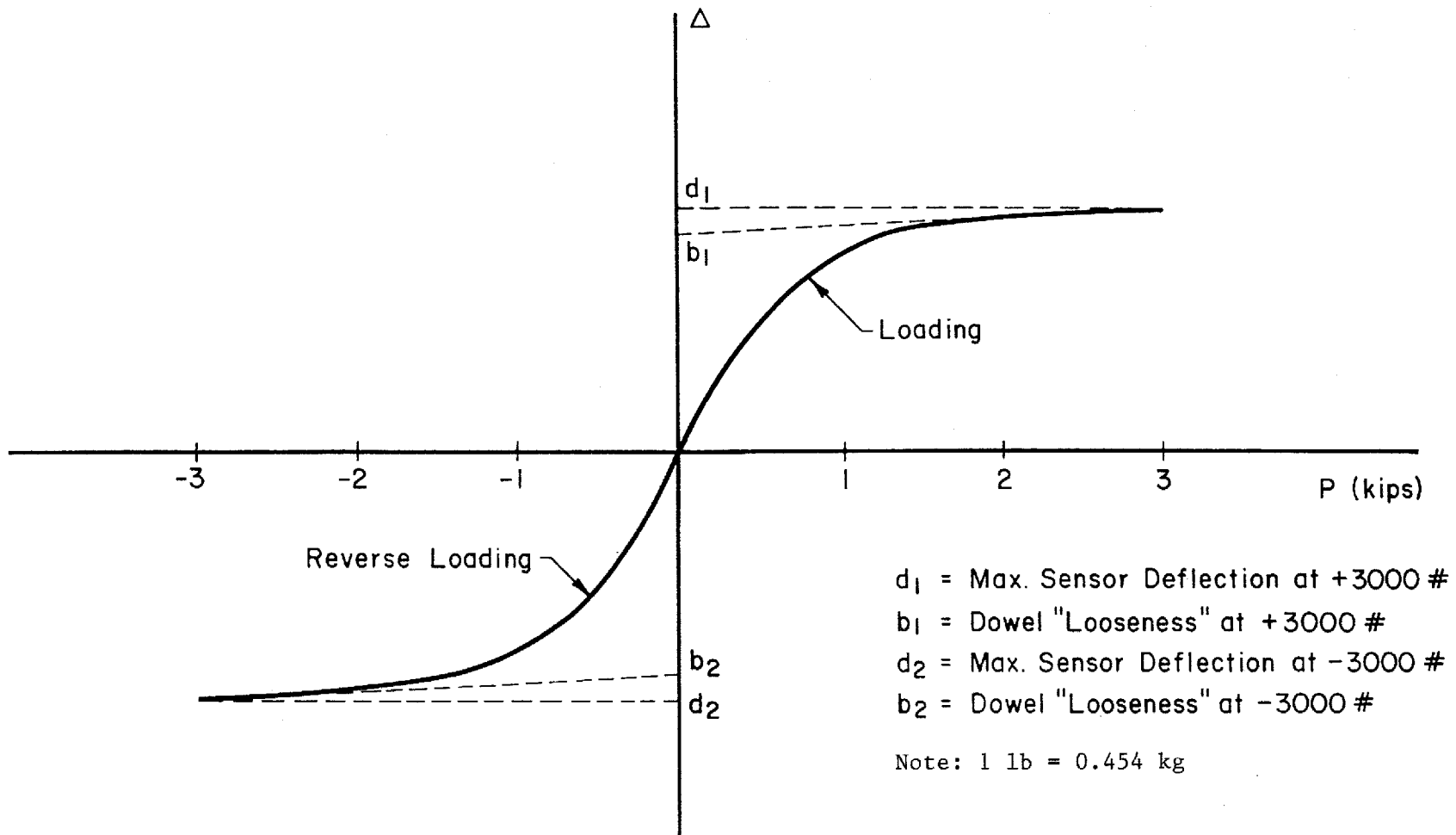


Figure 9. Illustration of estimation of dowel looseness from load-deflection curve.(47)

Table 21. Analysis of variance computation table.

Effect:	LOAD REPS 1 123456	DWLDIA 2 3456	ANNGAP 3 2456	ANKMAIL 4 2356	EMBED 5 2346	DRLTYP 6=2345 2345	BMAXMIN	B-SE	DMAXMIN	D-SE
Level -1:	2000	1.0"	1/32"	CG	7"	Pneumatic				
Level +1:	100000	1.5"	1/8"	C10	9"	Electric				
Specimen										
A18, B4	-1	-1	-1	-1	-1	1	14.45	3.08	20.04	1.73
	1	-1	-1	-1	-1	1	22.11	9.68	29.84	4.59
B20, C16	-1	1	-1	-1	-1	-1	1.64	0.49	5.88	1.38
	1	1	-1	-1	-1	-1	2.08	0.82	6.28	1.47
A20	-1	-1	1	-1	-1	-1	8.05		18.82	
	1	-1	1	-1	-1	-1	10.54		21.00	
A10, D5	-1	1	1	-1	-1	1	4.74	1.18	9.27	1.62
	1	1	1	-1	-1	1	5.88	0.87	10.10	1.75
C2, D8	-1	-1	-1	1	-1	-1	4.63	0.41	17.06	2.60
	1	-1	-1	1	-1	-1	8.76	1.15	17.38	1.38
B11R	-1	1	-1	1	-1	1	7.09		12.53	
	1	1	-1	1	-1	1	7.83		12.87	
A8	-1	-1	1	1	-1	1	15.61		26.80	
	1	-1	1	1	-1	1	19.63		31.12	
C7	-1	1	1	1	-1	-1	10.79		18.72	
	1	1	1	1	-1	-1	13.81		19.96	
A1	-1	-1	-1	-1	1	-1	7.80		15.00	
	1	-1	-1	-1	1	-1	9.06		16.39	
C21	-1	1	-1	-1	1	1	3.07		5.52	
	1	1	-1	-1	1	1	3.33		5.90	
A8R	-1	-1	1	-1	1	1	7.76		18.04	
	1	-1	1	-1	1	1	13.50		23.33	
C12, C20	-1	1	1	-1	1	-1	1.83	1.55	5.28	0.22
	1	1	1	-1	1	-1	3.01	4.95	5.47	0.52
C19, D10, D10R	-1	-1	-1	1	1	1	6.02	3.75	16.71	6.62
	1	-1	-1	1	1	1	8.96	4.70	17.13	6.53
A2, D19	-1	1	-1	1	1	-1	4.18	0.01	10.96	0.74
	1	1	-1	1	1	-1	4.95	0.12	11.07	0.86
B7, D18	-1	-1	1	1	1	-1	12.33	0.07	31.42	1.45
	1	-1	1	1	1	-1	17.43	2.41	32.53	1.04
A6R, B17 C3R	-1	1	1	1	1	1	6.56	0.51	19.79	4.32
	1	1	1	1	1	1	10.00	1.12	19.52	4.90
Effects:										
Bmaxmin:	2.77	-5.99	2.84	2.48	-2.37	2.23	8.67			
Dmaxmin:	1.75	-10.84	5.66	6.21	-1.48	1.58			16.62	

Table 21. Analysis of variance computation table (cont'd).

Effect:	12	13	14	15	16	23	24	25	26	34	
	13456	12456	12356	12346	12345	456	356	346	345	256	
Level -1:											
Level +1:											
Specimen											
A18, B4	73	1	1	1	1	-1	1	1	1	-1	1
	59	-1	-1	-1	-1	1	1	1	1	-1	1
B20, C16	38	-1	1	1	1	1	-1	-1	-1	-1	1
	47	1	-1	-1	-1	-1	-1	-1	-1	-1	1
A20		1	-1	1	1	1	-1	1	1	1	-1
		-1	1	-1	-1	-1	-1	1	1	1	-1
A10, D5	62	-1	-1	1	1	-1	1	-1	-1	1	-1
	75	1	1	-1	-1	1	1	-1	-1	1	-1
C2, D8	60	1	1	-1	1	1	1	-1	1	1	-1
	38	-1	-1	1	-1	-1	1	-1	1	1	-1
B11R		-1	1	-1	1	-1	-1	1	-1	1	-1
		1	-1	1	-1	1	-1	1	-1	1	-1
A8		1	-1	-1	1	-1	-1	-1	1	-1	1
		-1	1	1	-1	1	-1	-1	1	-1	1
C7		-1	-1	-1	1	1	1	1	-1	-1	1
		1	1	1	-1	-1	1	1	-1	-1	1
A1		1	1	1	-1	1	1	1	-1	1	1
		-1	-1	-1	1	-1	1	1	-1	1	1
C21		-1	1	1	-1	-1	-1	-1	1	1	1
		1	-1	-1	1	1	-1	-1	1	1	1
A8R		1	-1	1	-1	-1	-1	1	-1	-1	-1
		-1	1	-1	1	1	-1	1	-1	-1	-1
C12, C20	22	-1	-1	1	-1	1	1	-1	1	-1	-1
	52	1	1	-1	1	-1	1	-1	1	-1	-1
C19, D10,	62	1	1	-1	-1	-1	1	-1	-1	-1	-1
D10R	53	-1	-1	1	1	1	1	-1	-1	-1	-1
A2, D19	74	-1	1	-1	-1	1	-1	1	1	-1	-1
	86	1	-1	1	1	-1	-1	1	1	-1	-1
B7, D18	45	1	-1	-1	-1	1	-1	-1	-1	1	1
	04	-1	1	1	1	-1	-1	-1	-1	1	1
A6R, B17	32	-1	-1	-1	-1	-1	1	1	1	1	1
C3R	90	1	1	1	1	1	1	1	1	1	1
Effects:											
Bmaxmin:		-1.40	0.50	0.25	-0.18	0.47	-0.04	2.47	0.25	-1.45	3.87
Dmaxmin:		-1.35	0.11	-0.80	-0.68	0.89	-1.03	2.75	-0.04	-0.10	4.86

Table 21. Analysis of variance computation table (cont'd).

Effect:	35	36	45	46	56					
	246	245	236	235	234	123	124	125	126	134
						1456	1356	1346	1345	1256
Level -1:										
Level +1:										
Specimen										
A18, B4	1	-1	1	-1	-1	-1	-1	-1	1	-1
	1	-1	1	-1	-1	1	1	1	-1	1
B20, C16	1	1	1	1	1	1	1	1	1	-1
	1	1	1	1	1	-1	-1	-1	-1	1
A20	-1	-1	1	1	1	1	-1	-1	-1	1
	-1	-1	1	1	1	-1	1	1	1	-1
A10, D5	-1	1	1	-1	-1	-1	1	1	-1	1
	-1	1	1	-1	-1	1	-1	-1	1	-1
C2, D8	1	1	-1	-1	1	-1	1	-1	-1	1
	1	1	-1	-1	1	1	-1	1	1	-1
B11R	1	-1	-1	1	-1	1	-1	1	-1	1
	1	-1	-1	1	-1	-1	1	-1	1	-1
A8	-1	1	-1	1	-1	1	1	-1	1	-1
	-1	1	-1	1	-1	-1	-1	1	-1	1
C7	-1	-1	-1	-1	1	-1	-1	1	1	-1
	-1	-1	-1	-1	1	1	1	-1	-1	1
A1	-1	1	-1	1	-1	-1	-1	1	-1	-1
	-1	1	-1	1	-1	1	1	-1	1	1
C21	-1	-1	-1	-1	1	1	1	-1	-1	-1
	-1	-1	-1	-1	1	-1	-1	1	1	1
A8R	1	1	-1	-1	1	1	-1	1	1	1
	1	1	-1	-1	1	-1	1	-1	-1	-1
C12, C20	1	-1	-1	1	-1	-1	1	-1	1	1
	1	-1	-1	1	-1	1	-1	1	-1	-1
C19, D10	-1	-1	1	1	1	-1	1	1	1	1
D10R	-1	-1	1	1	1	1	-1	-1	-1	-1
A2, D19	-1	1	1	-1	-1	1	-1	-1	1	1
	-1	1	1	-1	-1	-1	1	1	-1	-1
B7, D18	1	-1	1	-1	-1	1	1	1	-1	-1
	1	-1	1	-1	-1	-1	-1	-1	1	1
A6R, B17	1	1	1	1	1	-1	-1	-1	-1	-1
C3R	1	1	1	1	1	1	1	1	1	1
Effects:										
Bmaxmin:	0.29	-1.49	0.15	-1.63	-2.40	0.33	0.37	0.22	-0.45	0.38
Dmaxmin:	1.42	-0.98	1.81	-1.91	-1.85	-0.01	0.76	0.38	-0.97	0.54

Table 21. Analysis of variance computation table (cont'd).

Effect:	135 1246	136 1245	145 1236	146 1235	156 1234
Level -1:					
Level +1:					
Specimen					
A18, B4	-1	1	-1	1	1
	1	-1	1	-1	-1
B20, C16	-1	-1	-1	-1	-1
	1	1	1	1	1
A20	1	1	-1	-1	-1
	-1	-1	1	1	1
A10, D5	1	-1	-1	1	1
	-1	1	1	-1	-1
C2, D8	-1	-1	1	1	-1
	1	1	-1	-1	1
B11R	-1	1	1	-1	1
	1	-1	-1	1	-1
A8	1	-1	1	-1	1
	-1	1	-1	1	-1
C7	1	1	1	1	-1
	-1	-1	-1	-1	1
A1	1	-1	1	-1	1
	-1	1	-1	1	-1
C21	1	1	1	1	-1
	-1	-1	-1	-1	1
A8R	-1	-1	1	1	-1
	1	1	-1	-1	1
C12, C20	-1	1	1	-1	1
	1	-1	-1	1	-1
C19, D10, D10R	1	1	-1	-1	-1
	-1	-1	1	1	1
A2, D19	1	-1	-1	1	1
	-1	1	1	-1	-1
B7, D18	-1	1	-1	1	1
	1	-1	1	-1	-1
A6R, B17	-1	-1	-1	-1	-1
	1	1	1	1	1
C3R	1	1	1	1	1
Effects:					
Bmaxmin:	0.78	-0.15	0.23	-0.71	0.04
Dmaxmin:	0.39	-0.20	0.07	-0.63	-0.51

the higher order interaction effects are generally assumed to be insignificant, so the computed effect values are assumed to represent the primary effects being considered.

In each effect column, the presence of a 1 or a -1 indicates that the specimen being described in that row was tested at either a high level (1) or a low level (-1) for the given effect. The high and low levels selected for the main effects are described near the top of their respective columns. Thus, the test configuration of each specimen is described completely in the first seven columns of table 21. The next four columns contain the average computed total dowel looseness from 3000 lb [13.4 kN] loading to 3000 lb [13.4 kN] reverse loading (BMAXMIN), the standard deviation of that number (B-SE), the average measured total dowel deflection from 3000 lb [13.4 kN] loading to 3000 lb [13.4 kN] reverse loading (DMAXMIN), and the standard deviation of that number (D-SE) for each specimen configuration.

The computed values of each main or interaction effect on BMAXMIN and DMAXMIN is tabulated at the bottom of each column and is computed by summing the products of each 1 or -1 value with the value of BMAXMIN or DMAXMIN in the same row. A positive value suggests a positive relationship between the variable or variable combination and the predicted response. A negative value indicates an inverse relationship. A value of zero indicates that no relationship exists.

Nonzero effects that are due to random variation will be normally distributed and, when ranked according to relative magnitude, should plot on probability paper approximately as a straight line. Effects that do not lie on this line may be significant and should be investigated further. This approach is shown in table 22 and figure 10 for measured sensor deflection (DMAXMIN) and in table 23 and figure 11 for computed dowel looseness (BMAXMIN).

These tables and figures suggest that all of the main variables may significantly affect the development of dowel looseness and sensor deflection and sensor deflection as follows:

<u>Variable Changed</u>	<u>Effect on Deflection/Looseness</u>
Increasing Dowel Diameter	Decrease
Increasing Dowel Embedment	Decrease
Increasing Drill Impact Energy	Decrease
Epoxy Anchor Material (Instead of Cement Grout)	Increase
Increase Annular Gap	Increase
Increase Load Repetitions	Increase

These variables all affect dowel deflection and looseness as expected, with the exception of the effect of drill impact energy. As discussed previously, it is believed that the use of the nylon grout retention rings may have reduced (or eliminated) the effect of spalling caused by the use of high impact energy drills. Since the low impact energy drill was guided but hand-held, the apparent increase in dowel deflection could be due to slight increases in actual drilled hole diameter (which must be filled with a grout that is softer than the surrounding concrete).

Several significant two-factor interactions were also noted, including drill impact energy and dowel embedment length, anchor material and drill impact energy, anchor material and dowel diameter (bearing stress), and anchor material and annular

Table 22 Summary of ANOVA data for sensor deflection
(all specimens).

Rank	Plot	Dmaxmin	Effect		Alias
1	1.61	-10.84	DWLDIA	2	3456
2	4.84	-1.91		46	235
3	8.06	-1.85		56	234
4	11.29	-1.48	EMBED	5	2346
5	14.52	-1.03		23	456
6	17.74	-0.98		36	245
7	20.97	-0.97		126	1345
8	24.19	-0.80		14	12356
9	27.42	-0.68		15	12346
10	30.65	-0.63		146	1235
11	33.87	-0.51		156	1234
12	37.10	-0.20		136	1245
13	40.32	-0.10		26	345
14	43.55	-0.04		25	346
15	46.77	-0.01		123	1456
16	50.00	0.00		12	13456
17	53.23	0.07		145	1236
18	56.45	0.11		13	12456
19	59.68	0.38		125	1346
20	62.90	0.39		135	1246
21	66.13	0.54		134	1256
22	69.35	0.76		124	1356
23	72.58	0.89		16	12345
24	75.81	1.42		35	246
25	79.03	1.58	DRLTYP	6=2345	2345
26	82.26	1.75	LOAD REPS	1	123456
27	85.48	1.81		45	236
28	88.71	2.75		24	356
29	91.94	4.86		34	256
30	95.16	5.66	ANNGAP	3	2456
31	98.39	6.21	ANKMATL	4	2356

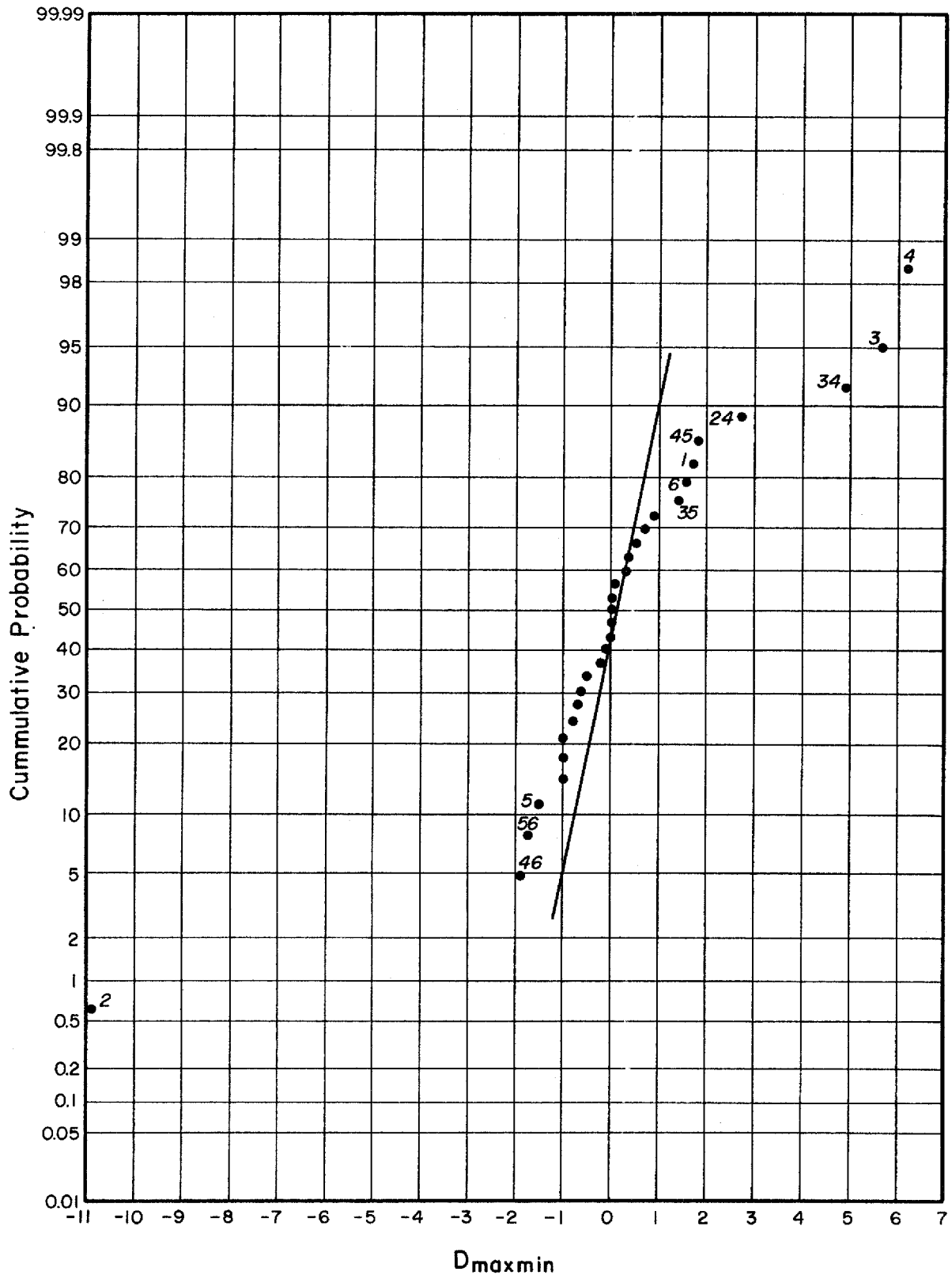


Figure 10. Plot of ANOVA data for sensor deflection (all specimens).

Table 23 Summary of ANOVA data for dowel looseness
(all specimens).

Rank	Plot	Bmaxmin	Effect	Alias
1	1.61	-5.99	DWLDIA	2 3456
2	4.84	-2.40		56 234
3	8.06	-2.37	EMBED	5 2346
4	11.29	-1.63		46 235
5	14.52	-1.49		36 245
6	17.74	-1.45		26 345
7	20.97	-1.40		12 13456
8	24.19	-0.71		146 1235
9	27.42	-0.45		126 1345
10	30.65	-0.18		15 12346
11	33.87	-0.15		136 1245
12	37.10	-0.04		23 456
13	40.32	0.04		156 1234
14	43.55	0.15		45 236
15	46.77	0.22		125 1346
16	50.00	0.23		145 1236
17	53.23	0.25		25 346
18	56.45	0.25		14 12356
19	59.68	0.29		35 246
20	62.90	0.33		123 1456
21	66.13	0.37		124 1356
22	69.35	0.38		134 1256
23	72.58	0.47		16 12345
24	75.81	0.50		13 12456
25	79.03	0.78		135 1246
26	82.26	2.23	DRLTYP	6=2345 2345
27	85.48	2.47		24 356
28	88.71	2.48	ANKMATL	4 2356
29	91.94	2.77	LOAD REPS	1 123456
30	95.16	2.84	ANNGAP	3 2456
31	98.39	3.87		34 256

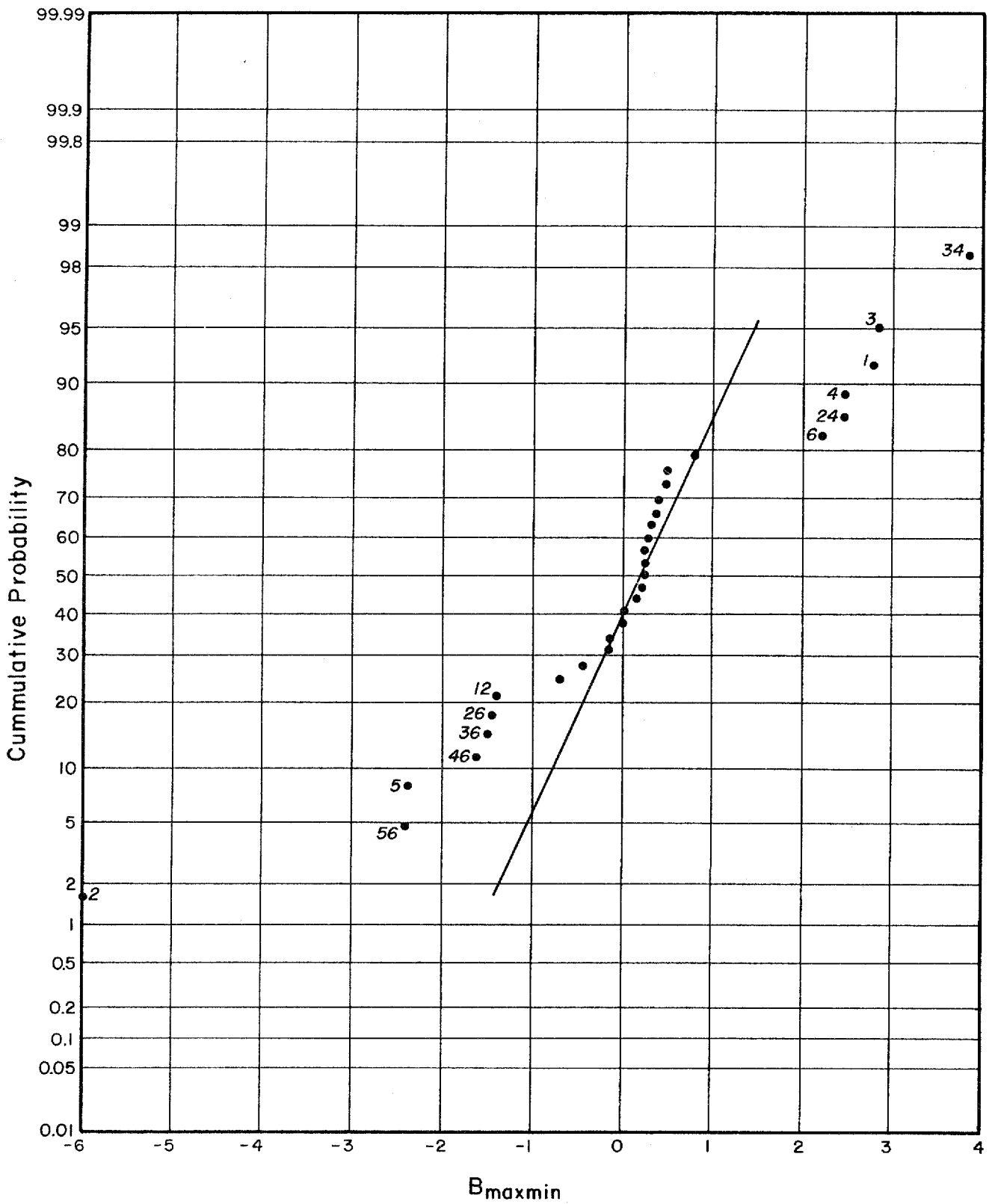


Figure 11. Plot of ANOVA data for dowel looseness (all specimens).

gap. Since many of these two-factor interactions indicated a strong relationship between anchor material and some other variable, the database was subdivided according to anchor material and an analysis of variance was conducted for each of the new data sets. Tables 24 through 27 present the ranked ANOVA results for each anchor material set as they affect DMAXMIN and BMAXMIN. Clearly, the main effects are still among the most significant in each of the anchor material database subsets. Performance models were developed for each of these data sets.

The strength of the main effects and the significance of several two-factor interaction effects point to additional conclusions concerning the stiffness of the anchor materials. Since the cement grout is more rigid than the epoxy mortar, the effects (and interaction effects) of dowel diameter (bearing stress) and embedment on dowel deflection are reduced for this material. Furthermore, it appears that a larger annular gap generally produces better results for cement grout, presumably because it becomes easier to install the bar in a stiffer grout, which provides more uniform dowel support.

Since the epoxy mortar is a softer material than either the cement grout or the concrete specimen, the deflections of bars embedded in this material are more sensitive to dowel diameter (bearing stress) and embedment, with increases in either resulting in decreased deflections. As annular gap increased, deflections generally increased as well due to the use of larger volumes of softer material. Since the epoxy mortar was always delivered at a uniform consistency that allowed easy insertion of the dowels, there is no apparent need (for installation purposes) for a large annular gap, as with the cement grout. It may be appropriate to use epoxy mortar with the smallest annular gap that will allow dowel installation without excessive force. This would allow the mortar to fill voids and spalls using a minimum thickness of the softer material and allowing the bar to be supported directly by the concrete in many places. Additional research should be conducted to verify this.

3.2.3 Dowel Deflection and Looseness Models

The data sets for each anchor material type were used to develop predictive models for sensor deflection and dowel looseness. Although many factors and interactions appear to affect these performance measures, their inclusion often made the models much more complex without significantly improving the accuracy of the models. Satisfactory models were often obtained using nonlinear regression techniques and including only main effects.

The models developed for the epoxy mortar anchor material are presented below:

$$B_{\max\min} = 34840 (AG) + 1167 (CT)^{1.058} - 9.899 (EB)^{1.160} \\ + 1.079 (BS) - 0.6912 (EN)^{1.831} + 8380$$

$$\text{Statistics:} \quad R^2 = 0.594 \\ \text{COV} = 36.9\% \\ n = 178$$

$$D_{\max\min} = 54210 (AG) + 643.3 (CT) - 2117 (EB) \\ + 2.031 (BS) - 8.822 (EB)(EN) + 21210$$

Table 24 Summary of ANOVA data for sensor deflection
(cement grout specimens).

Rank	Plot	Dmaxmin	Effect		Alias
1	1.61	-27.02	ANKMATL	4	2356
2	4.84	-13.60	DWLDIA	2	3456
3	8.06	-3.49		46	235
4	11.29	-3.29	EMBED	5	2346
5	14.52	-2.56		14	12356
6	17.74	-1.52		26	345
7	20.97	-1.52		146	1235
8	24.19	-1.36		126	1345
9	27.42	-0.95		36	245
10	30.65	-0.83		56	234
11	33.87	-0.81		34	256
12	37.10	-0.75		15	12346
13	40.32	-0.58		136	1245
14	43.55	-0.50		156	1234
15	46.77	-0.44		13	12456
16	50.00	0.00		12	13456
17	53.23	0.44		134	1256
18	56.45	0.50		123	1456
19	59.68	0.58		125	1346
20	62.90	0.75		145	1236
21	66.13	0.81	ANNGAP	3	2456
22	69.35	0.83		23	456
23	72.58	0.95		25	346
24	75.81	1.36		135	1246
25	79.03	1.52		16	12345
26	82.26	1.52		35	246
27	85.48	2.11		124	1356
28	88.71	2.56	LOAD REPS	1	123456
29	91.94	3.29		45	236
30	95.16	3.49	DRLTYP	6-2345	2345
31	98.39	13.60		24	356

Table 25 Summary of ANOVA data for dowel looseness
(cement grout specimens).

Rank	Plot	Bmaxmin	Effect	Alias	
1	1.61	-14.86	ANKMATL	4	2356
2	4.84	-8.46	DWLDIA	2	3456
3	8.06	-3.85		46	235
4	11.29	-2.52		14	12356
5	14.52	-2.52	EMBED	5	2346
6	17.74	-2.36		56	234
7	20.97	-1.77		12	13456
8	24.19	-1.74		36	245
9	27.42	-1.74		26	345
10	30.65	-1.23		126	1345
11	33.87	-1.18		146	1235
12	37.10	-1.03	ANNGAP	3	2456
13	40.32	-0.41		15	12346
14	43.55	-0.38		136	1245
15	46.77	-0.29		156	1234
16	50.00	-0.12		134	1256
17	53.23	0.12		13	12456
18	56.45	0.29		123	1456
19	59.68	0.38		125	1346
20	62.90	0.41		145	1236
21	66.13	1.03		34	256
22	69.35	1.18		16	12345
23	72.58	1.23		135	1246
24	75.81	1.74		35	246
25	79.03	1.74		25	346
26	82.26	1.77		124	1356
27	85.48	2.36		23	456
28	88.71	2.52		45	236
29	91.94	2.52	LOAD REPS	1	123456
30	95.16	3.85	DRLTYP	6=2345	2345
31	98.39	8.46		24	356

Table 26 Summary of ANOVA data for sensor deflection
(epoxy mortar specimens).

Rank	Plot	Dmaxmin	Effect	Alias
1	1.61	-8.09		356
2	4.84	-8.09	DWLDIA	2 3456
3	8.06	-2.88		234
4	11.29	-2.88		456
5	14.52	-1.02		346
6	17.74	-1.02		245
7	20.97	-0.61		12346
8	24.19	-0.61		1236
9	27.42	-0.59		1356
10	30.65	-0.57		1246
11	33.87	-0.57		1345
12	37.10	-0.52		1234
13	40.32	-0.52		1456
14	43.55	-0.33	DRLTYP	6-2345 2345
15	46.77	-0.33		235
16	50.00	0.00		13456
17	53.23	0.17		1245
18	56.45	0.17		1346
19	59.68	0.25		12345
20	62.90	0.25		1235
21	66.13	0.34	EMBED	5 2346
22	69.35	0.34		236
23	72.58	0.65		1256
24	75.81	0.65		12456
25	79.03	0.95		12356
26	82.26	0.95	LOAD REPS	1 123456
27	85.48	1.33		345
28	88.71	1.33		246
29	91.94	10.52		256
30	95.16	10.52	ANNGAP	3 2456
31	98.39	39.45	ANKMATL	4 2356

Table 27 Summary of ANOVA data for dowel looseness
(epoxy mortar specimens).

Rank	Plot	Bmaxmin	Effect		Alias
1	1.61	-3.52		24	356
2	4.84	-3.52	DWLDIA	2	3456
3	8.06	-2.44		56	234
4	11.29	-2.44		23	456
5	14.52	-2.22	EMBED	5	2346
6	17.74	-2.22		45	236
7	20.97	-1.24		36	245
8	24.19	-1.24		25	346
9	27.42	-1.17		26	345
10	30.65	-1.17		35	246
11	33.87	-1.03		124	1356
12	37.10	-1.03		12	13456
13	40.32	-0.24		16	12345
14	43.55	-0.24		146	1235
15	46.77	0.04		145	1236
16	50.00	0.04		15	12346
17	53.23	0.07		125	1346
18	56.45	0.07		136	1245
19	59.68	0.33		126	1345
20	62.90	0.33		135	1246
21	66.13	0.36		156	1234
22	69.35	0.36		123	1456
23	72.58	0.60		46	235
24	75.81	0.60	DRLTYP	6=2345	2345
25	79.03	0.87		13	12456
26	82.26	0.87		134	1256
27	85.48	3.02	LOAD REPS	1	123456
28	88.71	3.02		14	12356
29	91.94	6.72		34	256
30	95.16	6.72	ANNGAP	3	2456
31	98.39	19.82	ANKMATL	4	2356

Statistics: R^2 = 0.584
 COV = 28.7%
 n = 178

where:

$B_{\max\min}$ = Total dowel looseness (as defined previously), mils

$D_{\max\min}$ = Total sensor deflection (as defined previously), mils

AG = (Nominal diameter of drilled hole - Nominal dowel diameter), in

CT = Natural log of number of complete load cycle applications

EB = Dowel embedment, in

BS = Friberg's bearing stress, psi

EN = Estimated drill impact energy, ft-lbs/blow

Figures 12 through 15 illustrate the sensitivity of the deflection model to the input parameters. The sensitivity of the "looseness" model is similar, although it is subject to some interpretation since it is a computed (rather than measured) response.

Figure 12 illustrates the relatively large effect of annular gap and the comparatively small effect of number of load applications on dowel deflection when the epoxy mortar was used. This confirms that the epoxy mortar is flexible (when compared to the surrounding concrete) and that thin supporting layers (sufficient to fill drilling voids) are best. It also shows that the material is very resistant to fatigue and undergoes very little permanent deformation or deterioration after many repeated load applications.

Figure 13 further defines the response of the epoxy mortar to applied loads by showing the expected total vertical dowel movement for several values of dowel bearing stress for each of the annular gap values tested. The predicted behavior is linear because of the form of the equation, which in turn reflects the fact that only two levels of bearing stress were examined. Additional data may produce a nonlinear relationship, but the overall indicated effect of increased bearing stress is likely to be similar. This model predicts dowel deflection increases of 60-100 percent or bearing stress increases from 1000 psi to 5000 psi [6.9 to 34.5 MPa].

Figure 14 shows that the flexibility of the epoxy mortar results in increased sensitivity to dowel embedment length because the mortar allows the dowel to deflect slightly inside of the drilled hole, whereas the cement grout has the potential to hold the bar rigidly. The increased deflection that results from decreasing embedment length from 9 to 7 in [23 cm to 18 cm] is approximately 10 percent and is probably not critical. It should be emphasized that the deflection of the bar within the drilled hole is probably due to the flexibility of the material; there is no reason to believe that the epoxy deteriorates within the drilled hole when no deterioration was observed at the joint face where stresses are highest.

Figure 15 shows the unexpected prediction of higher deflections with lower drill impact energy. As discussed before, it is believed that the grout retention rings masked the true effect of drill impact energy by filling the joint face spalls with

Predicted Deflection Range 9" Embed, 1" Dowel, Med Energy Drill

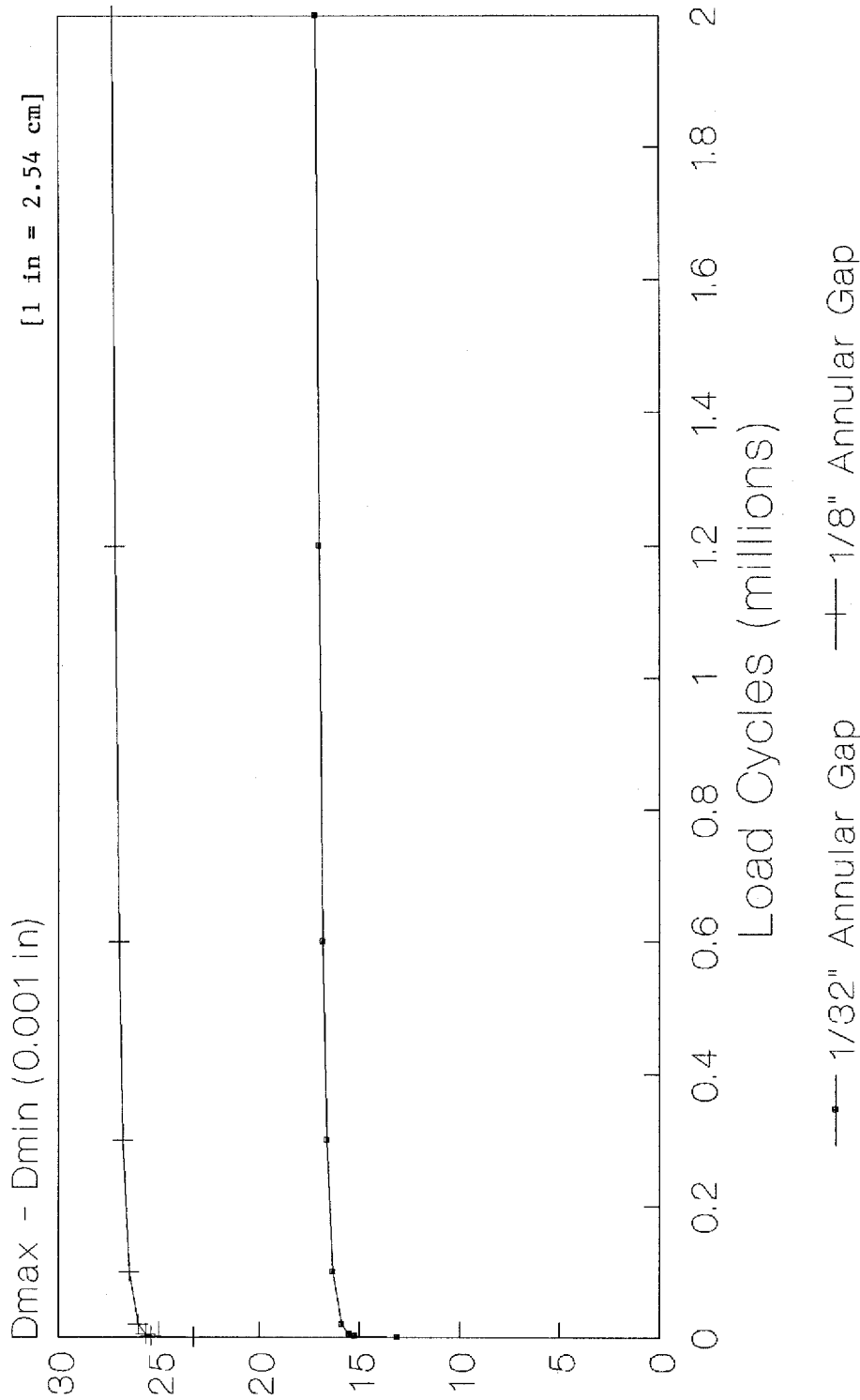


Figure 12. Predicted effect of annular gap and load cycles on sensor deflection of epoxy mortar specimens with 1-in [2.5-cm] dowels and 9 in [23 cm] of embedment.

Predicted Deflection Range

N=600000, 9" Embed, Med Energy Drill

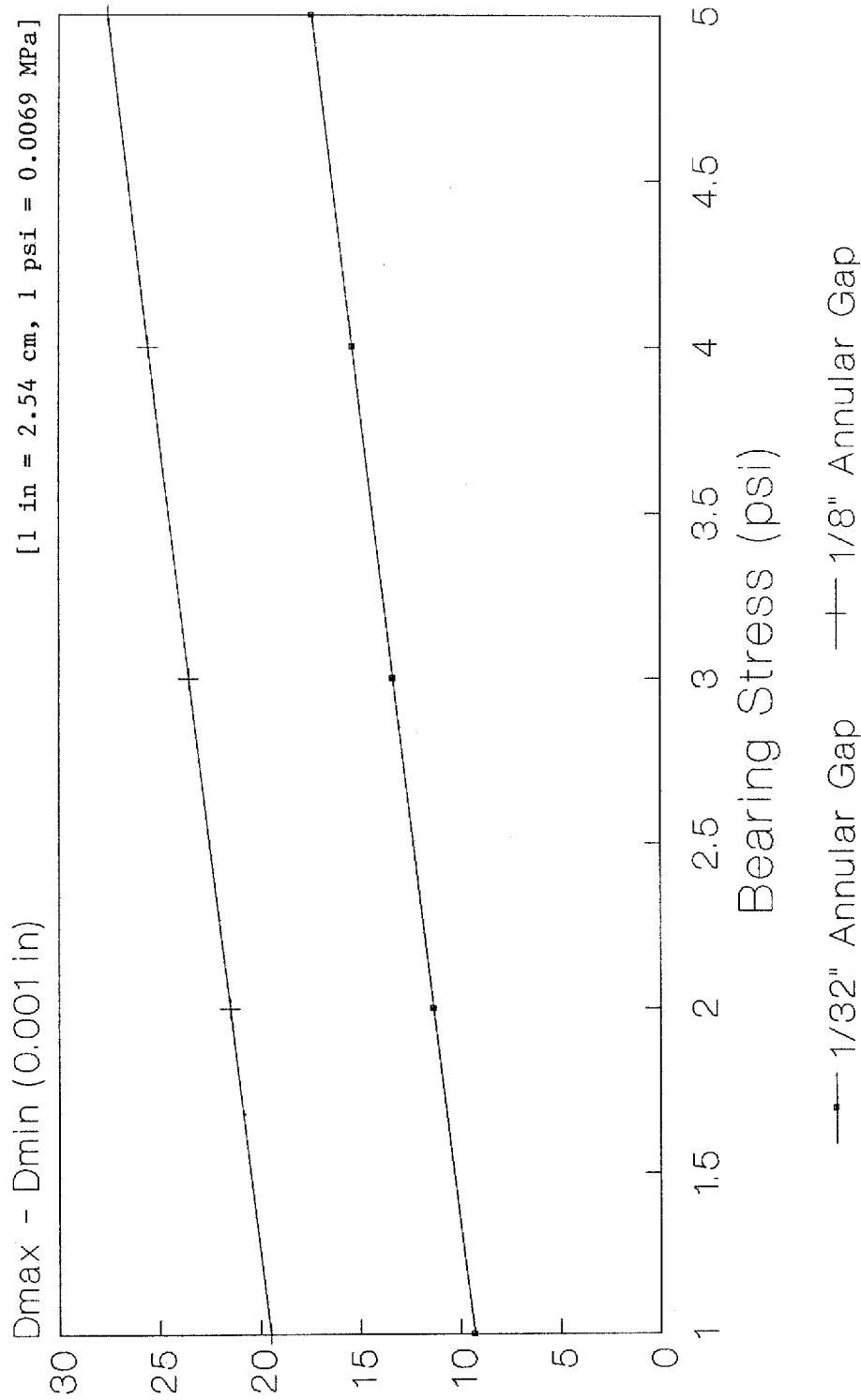


Figure 13. Predicted effect of annual gap and bearing stress on sensor deflection of epoxy mortar specimens with 9 in [23 cm] of embedment after 600,000 load cycles.

Predicted Deflection Range

N=600000, 1" Dowel, Med Energy Drill

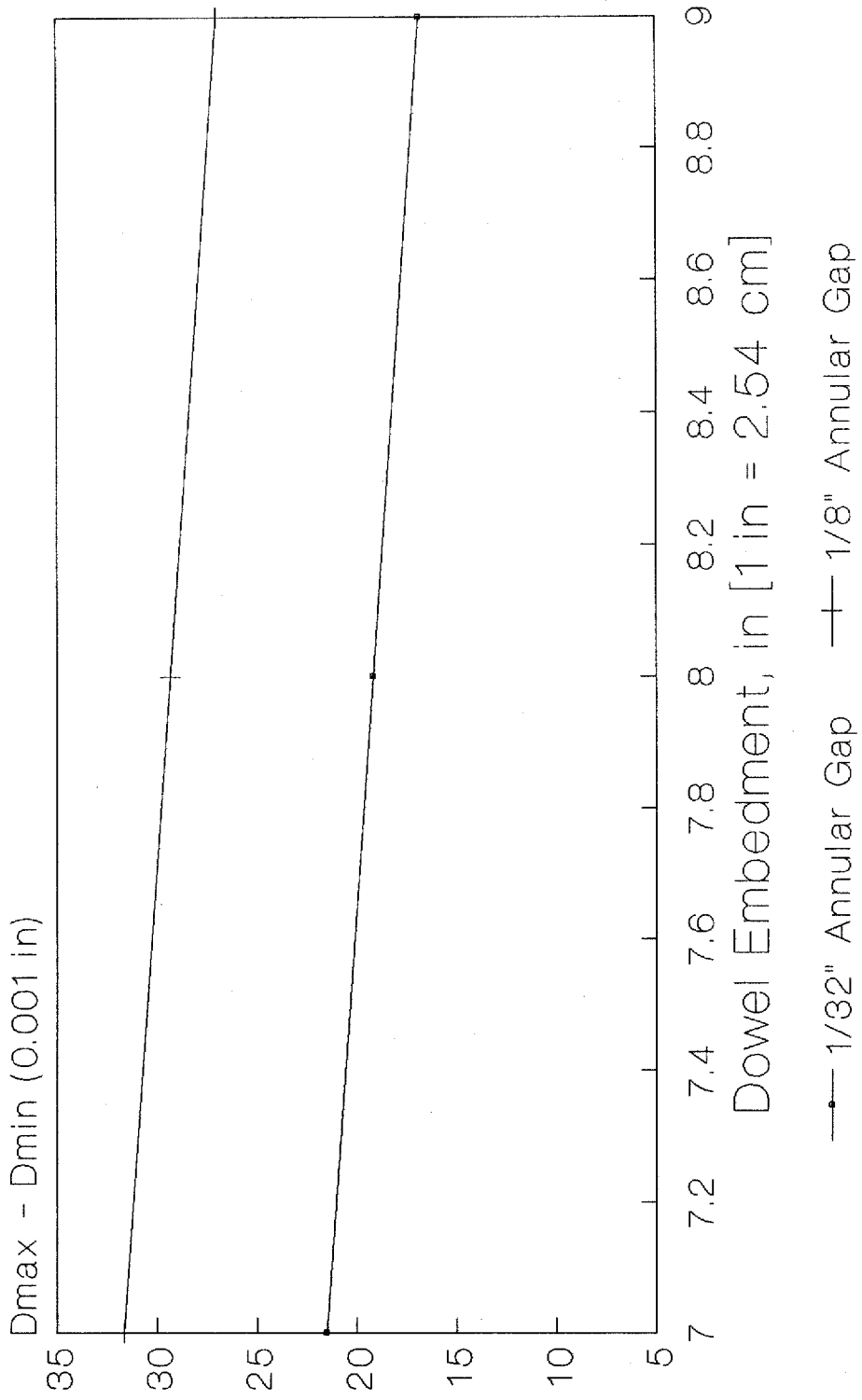


Figure 14. Predicted effect of annular gap and embedment length on sensor deflection for epoxy mortar specimens.

Predicted Deflection Range N=600000, 1 in Dowel, 9 in Embed

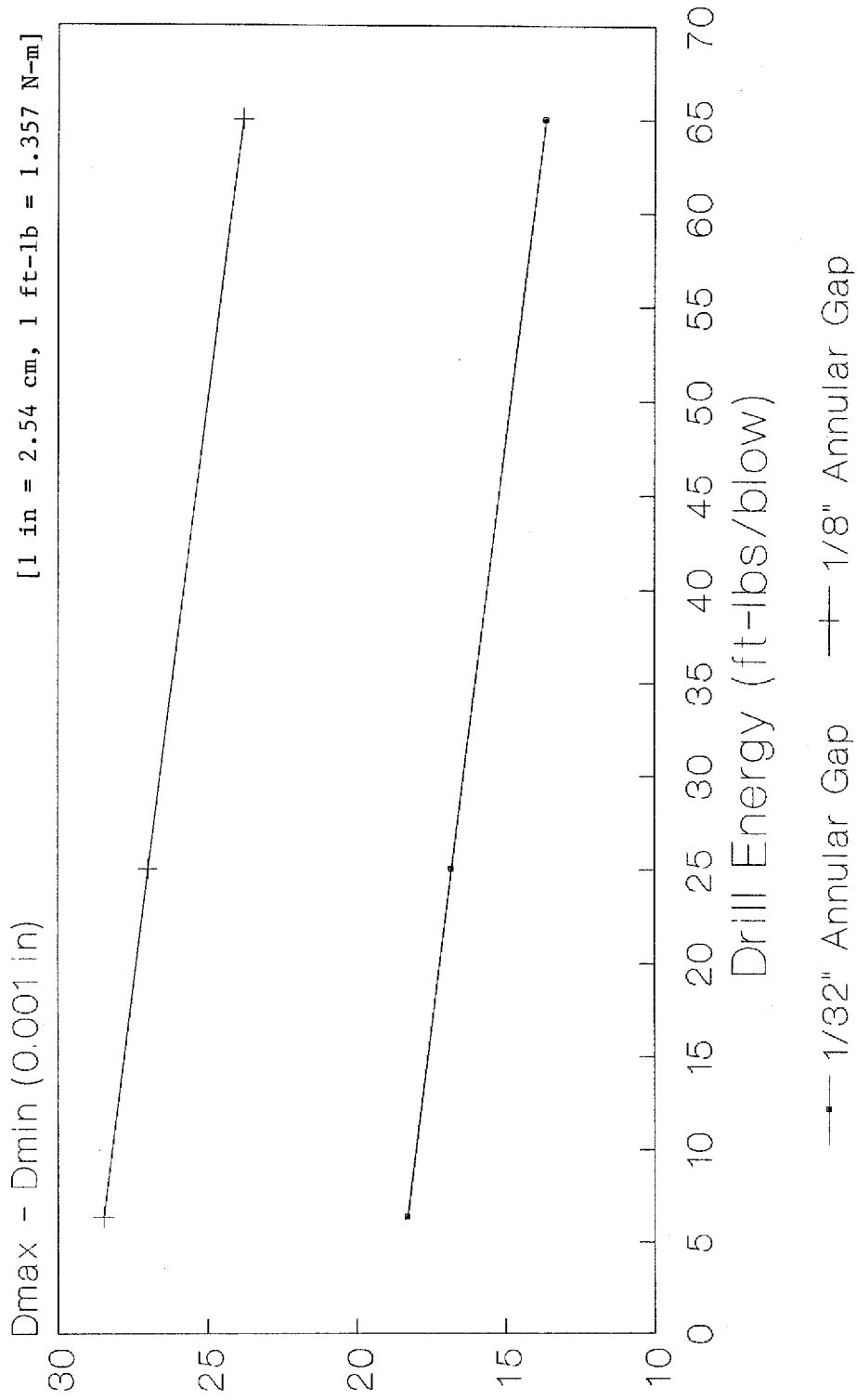


Figure 15. Predicted effect of annular gap and drill energy on sensor deflection for epoxy mortar specimens.

anchor material and reducing all deflections significantly. The effect presented in figure 15 may be due to the use of different drill guide systems for each drill, resulting in more variable drilled hole diameters and shapes.

The models developed for the cement grout anchor system are presented below:

$$B_{\max\min} = [CT (-2347 + BS (0.762 + 2.604 / EN)) + 3883] / 1000$$

Statistics: $R^2 = 0.647$
 $COV = 61.2\%$
 $n = 109$

$$D_{\max\min} = [6.072 (BS) - 66.96 (EN) + 13900 (AG) + 572.7 (CT) - 8946] / 1000$$

Statistics: $R^2 = 0.663$
 $COV = 43.3\%$
 $n = 110$

where:

$B_{\max\min}$ = Total dowel looseness (as defined previously), mils

$D_{\max\min}$ = Total sensor deflection (as defined previously), mils

AG = (Nominal diameter of drilled hole - Nominal dowel diameter), in

CT = Natural log of number of complete load cycle applications

BS = Friberg's bearing stress, psi

EN = Estimated drill impact energy, ft-lbs/blow

Figures 16 through 18 illustrate the sensitivity of the deflection model to the input parameters. The sensitivity of the "looseness" model is similar, although it is subject to some interpretation since it is a computed (rather than measured) response. It should be noted that these models were developed using only data from specimens that did not fail prematurely and therefore they tend to represent "potential" performance rather than average observed performance. The failed specimens were eliminated because their deflections prior to failure (often from the very beginning) exceeded the capacity of the deflection sensor.

Figure 16 shows the sensitivity of the deflection model to annular gap and suggests that increasing the annular gap increases dowel deflection slightly, which is contrary to the conclusion previously drawn for cement grout installations. This is because the model is based primarily on specimens that performed well (i.e., many of the small annular gap/1 inch [2.5 cm] dowel specimens that failed were not included in the development) and the effect of annular gap is actually smaller than the variability between measurements for the large dowel diameters.

Predicted Dowel Deflection Range

Bstress=3000 psi, Energy = 25 ft-lbs

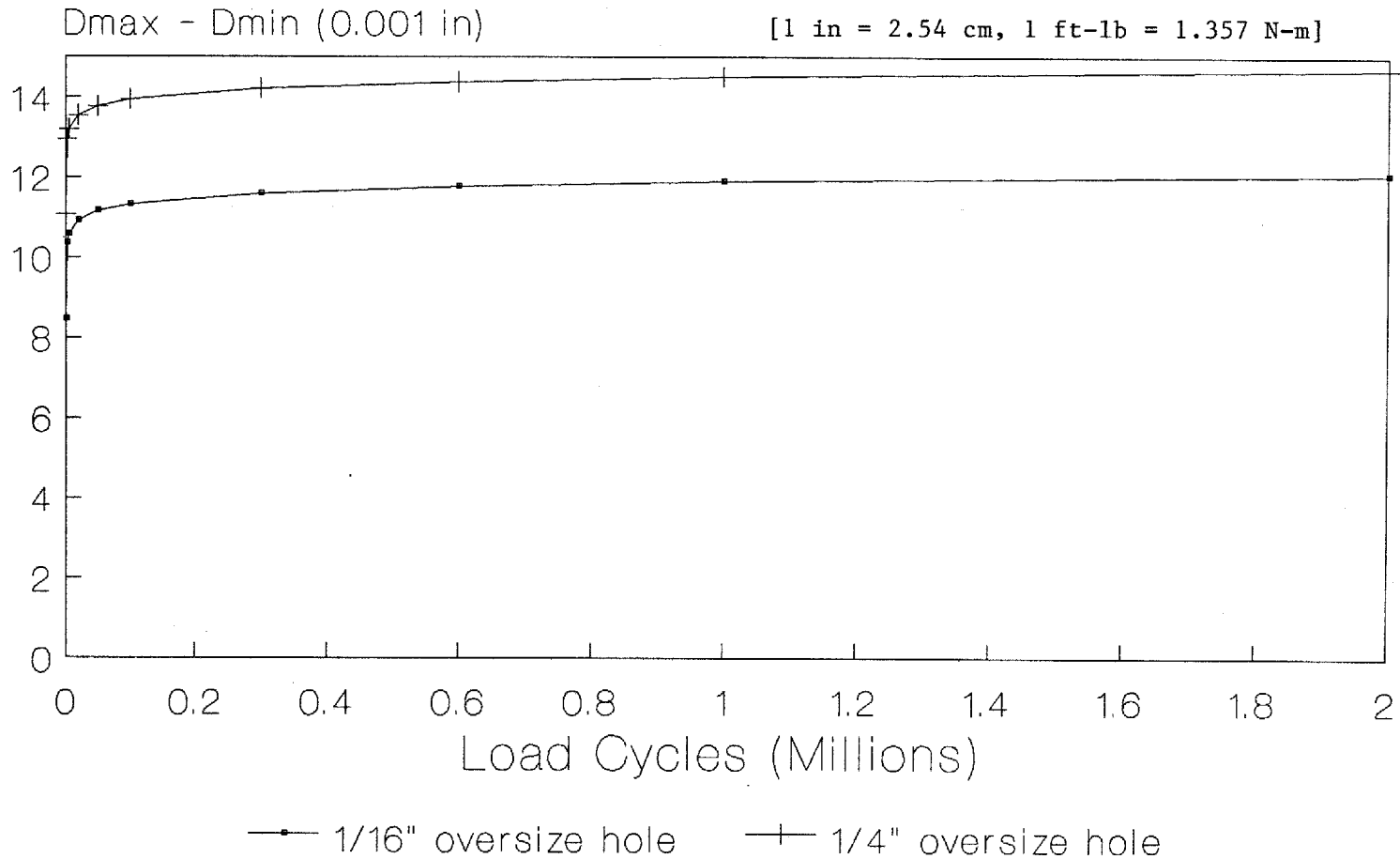


Figure 16. Predicted effect of annual gap and load cycles on sensor deflection for cement grout specimens.

Figure 17 illustrates the sensitivity of the model to both annular gap and drill impact energy. The reversed effect of the annular gap was discussed above and the masking effect of the grout retention ring on the drill energy (spalling) was discussed previously.

Figure 18 shows the sensitivity of the model to bearing stress and annular gap. The large effect of bearing stress on performance is clear and suggests that the bearing stresses that result from the use of 1-in [2.5 cm] dowels result in deterioration of the anchor material at the joint face. The 1.5-in [3.8 cm] dowels are represented by the lowest curves, which suggest acceptable performance.

The effect of increased heavy load repetitions is presented in all three figures. When good installations are achieved, rapid increases in deflection typically occur at first as the dowel becomes "seated" and subsequent increases are generally small. Poor installations were observed to have excessive deflections at the start which increased as the dowel impacted the supporting material, causing it to deteriorate. As stated earlier, these models were developed using only specimens that performed adequately and are not representative of the general lab experience with the use of cement grout anchor material.

The results of the lab study can be further illustrated by looking at the deflection profiles and "looseness" envelopes for various specimens. Figures 19 through 24 are measured deflection profiles for representative specimens after they had been subjected to 300,000 load cycles. Each deflection profile consists of four response curves -- loading (lower curve, right side), load relaxation (upper curve, right side), reverse loading (upper curve, left side) and reverse load relaxation (lower curve, left side). The graph titles include pertinent test information in the form xx ay bbb, where xx is the nominal diameter of the drilled hole in millimeters (27 = 1.0625 in, 32 = 1.25 in, 40 = 1.5625 in, and 44 = 1.75 in), ay is the drill type (E = electric, H = hydraulic, P = pneumatic) and embedment length in inches [1 in = 2.54 cm], and bbb is the type of anchor material used (C10 = epoxy mortar, CG = cement grout).

Figures 25 through 30 are dowel "looseness" envelopes for the same specimens, illustrating the development of looseness over time for each specimen. In these figures the "upstroke looseness" (data plotted as + signs) is the component of total looseness computed from the reverse loading curve, "downstroke looseness" (data plotted as diamonds) is the component of total looseness computed from the normal loading curve, and the "total looseness" (plotted as squares) is the distance between the other two curves and corresponds to $B_{\max\min}$ in the regression models.

A comparison of figures 19 and 20 illustrates the increase in dowel deflection that was observed to accompany increases in annular gap when the epoxy anchor material was used. Figures 25 and 26 show that the larger annular gap consistently produced larger deflections throughout the testing period. These figures also illustrate that the reverse loading mode typically produced higher deflections than normal loading. This is presumably due to settlement of the dowel during curing, which results in the dowel bearing on a very thin layer of anchor material on the bottom and a thicker layer on top. Since the deformations are somewhat dependent on the deformation of the supporting layer, the thicker layer on top allows more deflection in reverse loading.

Comparing figures 20 and 21 illustrates that dowels properly installed using cement grout typically exhibited lower deflections than those installed using the epoxy mortar. Figures 26 and 27 show that similar results were obtained at other

Predicted Dowel Deflection Range

Bstress=3000, Drill Energy/Ann Gap

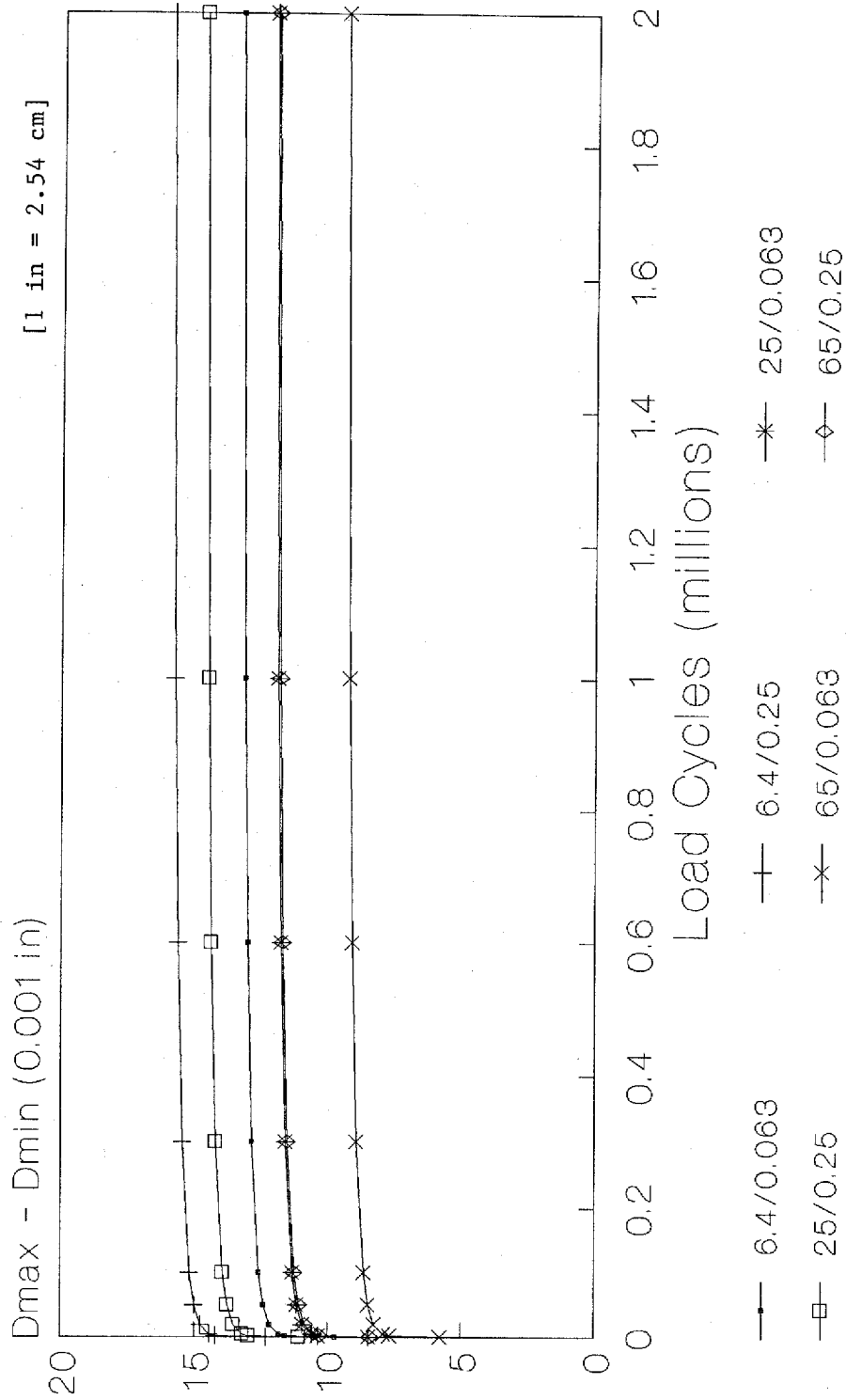


Figure 17. Predicted effect of annual gap and drill impact energy on sensor deflection for cement grout specimens.

Predicted Dowel Deflection Range Energy=25, Bstress/Ann Gap

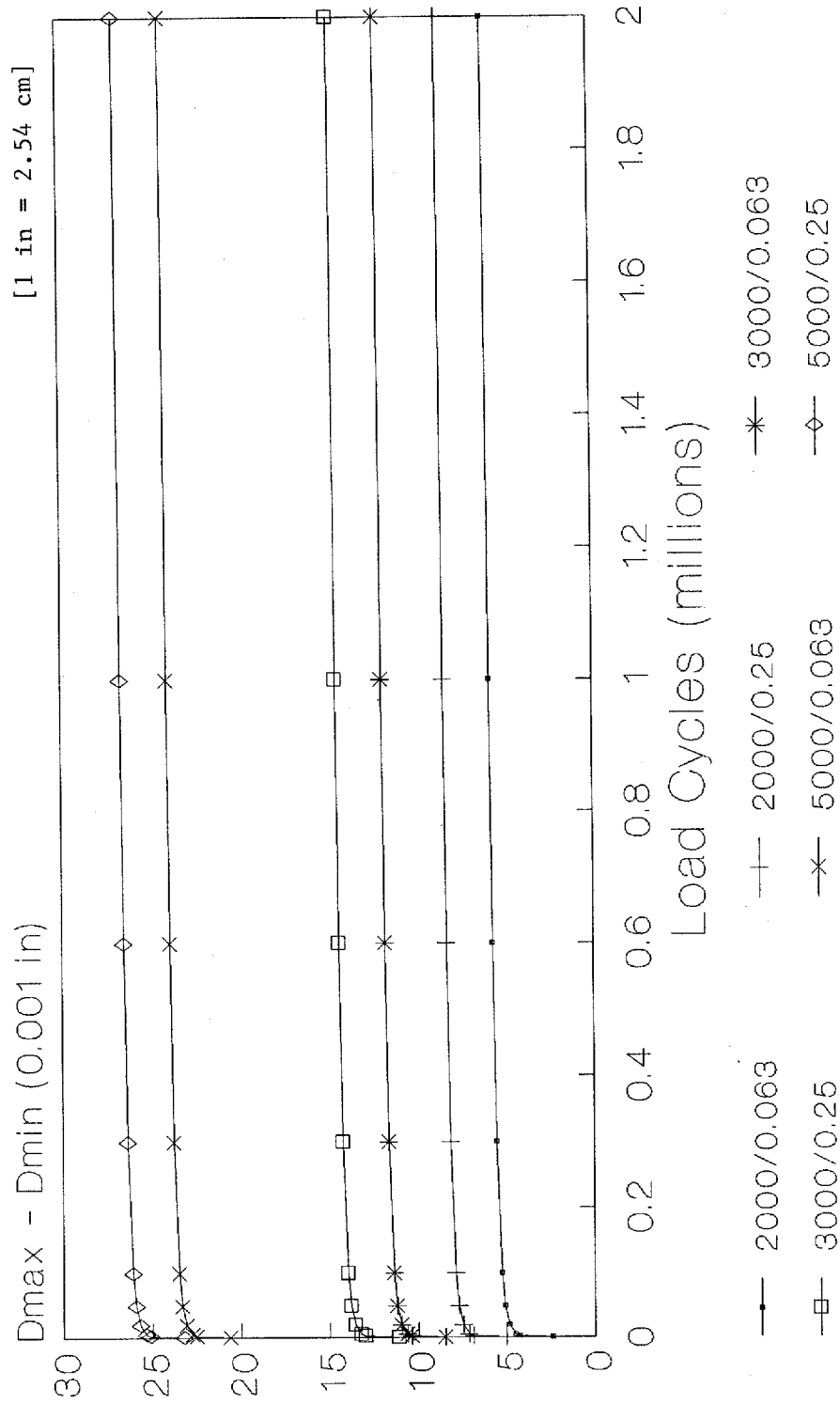


Figure 18. Predicted effect of annual gap and bearing stress on sensor deflection for cement grout specimens.

points in the loading history. It must be emphasized, however, that it was often difficult to obtain good anchoring using cement grout due to the extreme variability of grout consistency over short periods of time.

A comparison of figures 21 and 22 shows the tremendous reduction in deflection that typically accompanied an increase in dowel diameter from 1 in to 1.5 in [2.5 to 3.8 cm]. Figures 27 and 28 compare the load history performance of the same two specimens and show that the 1.5-in [3.8 cm] dowel exhibited a total computed "looseness" of less than 6 mils [0.015 cm] after 600,000 load cycles.

Figures 22 and 23, and figures 28 and 29 show that the difference in deflection profiles actually varied very little for different drill types. A slight improvement is noted for the high-energy drill, but it is suspected that this improvement is due to the difference in drill guidance systems rather than impact energy. The use of the grout retention ring is believed to have eliminated the effects of increased impact energy, which resulted in more spalling around the drilled hole and would reduce dowel support if unrepaired.

Figures 23 and 24, and figures 29 and 30 illustrate that the effect of dowel embedment on dowel deflection was typically very small for the range of embedments tested. This confirms other studies which have suggested that embedment lengths of 6 - 7 in are adequate for the size dowels currently used in highway applications.

Figure 31 presents the deflection profile obtained from one of the specimens that was prepared by casting a 1-in [2.5 cm] diameter dowel (embedded 9 inches [23 cm]) in a block of concrete, curing it 24 hours, applying 5000 load cycles, curing an additional 27 days, and finally applying an additional 595,000 load cycles.

It was believed that a properly prepared cast-in-place specimen would represent the best possible support that could be provided a dowel and would be a "yardstick" against which to compare the performance of similar specimens. The relatively flat deflection profile indicates that no real looseness existed at the time of testing and confirms the use of such specimens as an idealized dowel installation. A comparison of this profile to other 1-in [2.5 cm] dowelled specimens suggests that the cement grout specimens have the potential to most closely approach this level of dowel support, particularly when longer embedment lengths and good grout installations are present.

By comparison, the epoxy mortar specimens performed well when the annular gap was small and the embedment length was 9 in [23 cm]. The epoxy mortar specimens performed much more consistently than the cement grout specimens. Figure 32 presents the history of "looseness" for the cast-in-place specimen. Although it is apparent that the deflection sensor slipped somewhat near the end of the test, the total looseness trend is relatively uniform and suggests good overall performance, and can be compared to similar looseness curves for the other specimens.

Figure 33 presents the deflection curve for the 1.625-in [4.1 cm] O.D. hollow stainless steel dowel that was installed using the epoxy mortar to a depth of 7 inches [18 cm] in a 1.75-in [4.4 cm] diameter hole. The profile is similar to that illustrated in figure 20, which was produced using a 1-in [2.5 cm] diameter dowel with a slightly thicker supporting layer of epoxy mortar. A solid bar (or a tube with thicker walls) would probably have provided a more acceptable deflection

profile. In addition, the stainless steel did not bond to the epoxy mortar, allowing the bar to be twisted freely after testing, although the bar was not necessarily loose. Figure 34 shows the computed "looseness" history for this specimen.

The two specimens that were prepared using "close-fitting holes" and no grout of any type were very loose (compared to the other specimens) and rapidly developed deflections that were beyond the capability of the sensor to measure (>0.05 inches [0.13 cm] in either direction). Neither could be tested to the full 600,000 load repetitions because of possible damage to the test equipment. One of the specimens failed after less than 60,000 load cycles.

3.2.4 Conclusions

Conclusions drawn from the laboratory study are summarized with the field study conclusions in volume I, chapter 5.

Specimen D10R, 27 E9 C10, 300000 Cycles

Sensor Deflection vs. Load

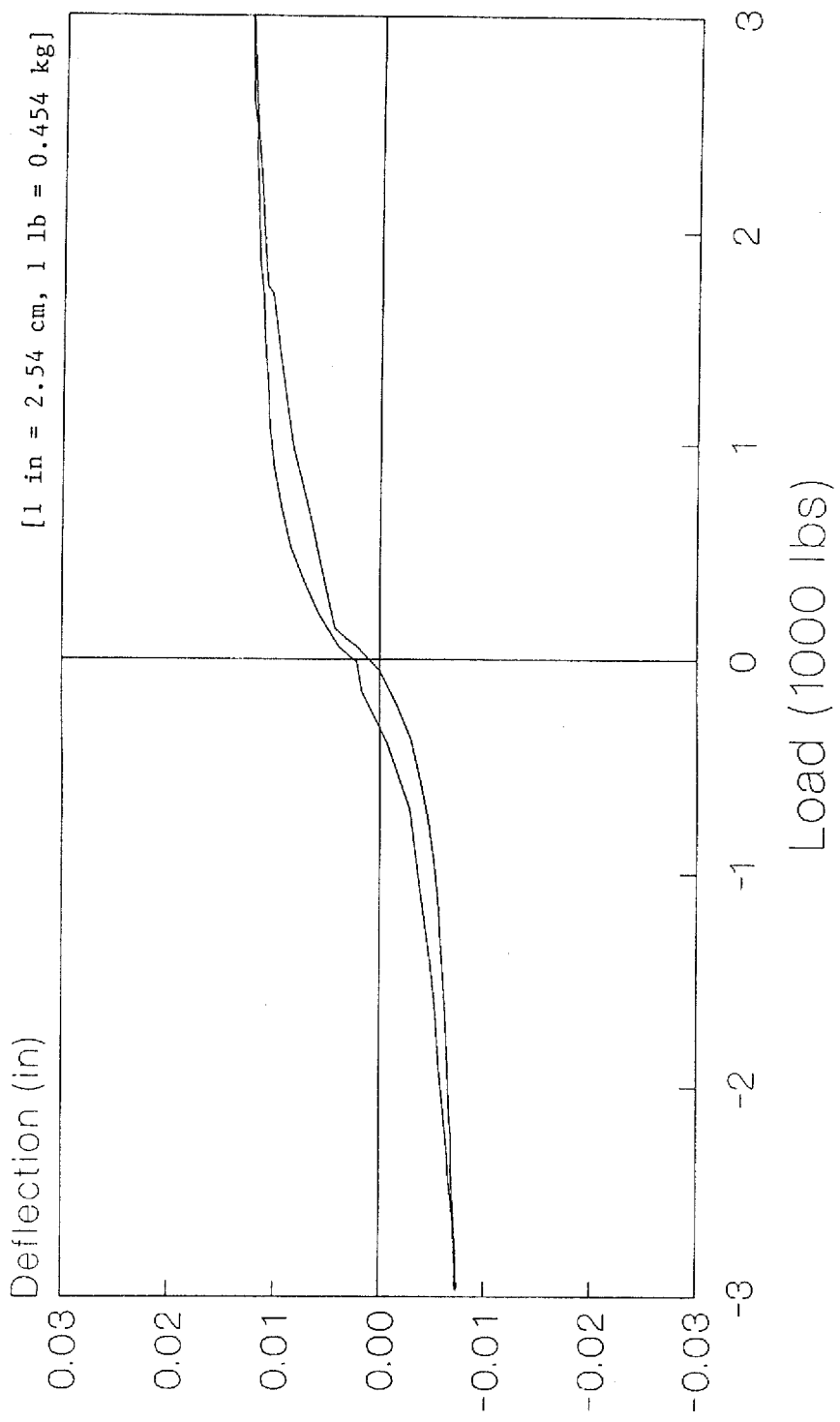


Figure 19. Measured load-deflection profile after 300,000 load cycles for specimen D10R (1-in [2.5-cm] dowel, 1/32-in [0.08-cm] annual gap, 9-in [23-cm] embedment, low-energy drill, epoxy mortar).

Specimen D6, 32 E9 C10, 300000 Cycles

Sensor Deflection vs. Load

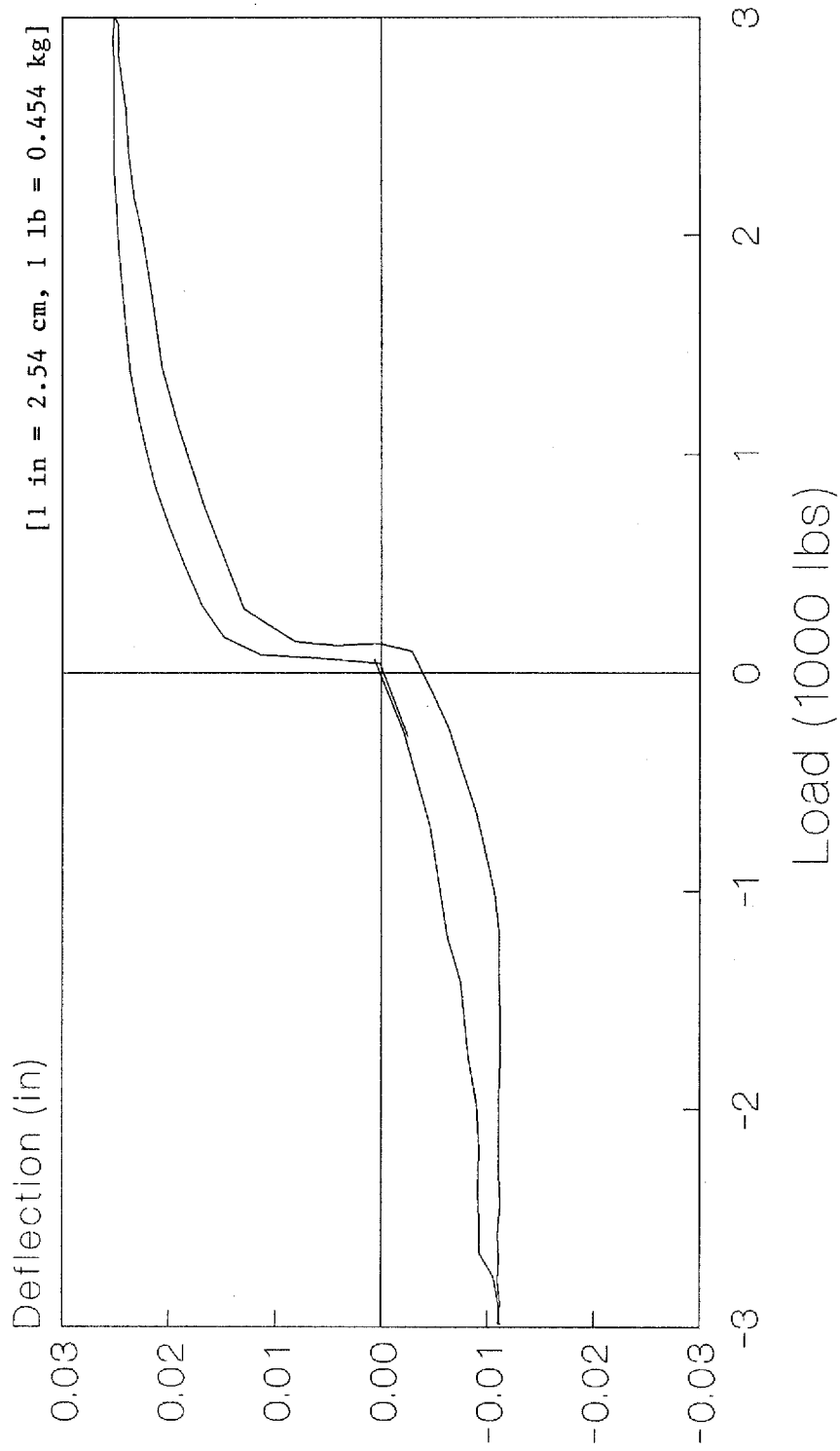


Figure 20. Measured load-deflection profile after 300,000 load cycles for specimen D6 (1-in [2.5-cm] dowel, 1/8-in [0.3-cm] annual gap, 9-in [23-cm] embedment, low-energy drill, epoxy mortar).

Specimen A8R, 32 E9 CG, 300000 Cycles Sensor Deflection vs. Load

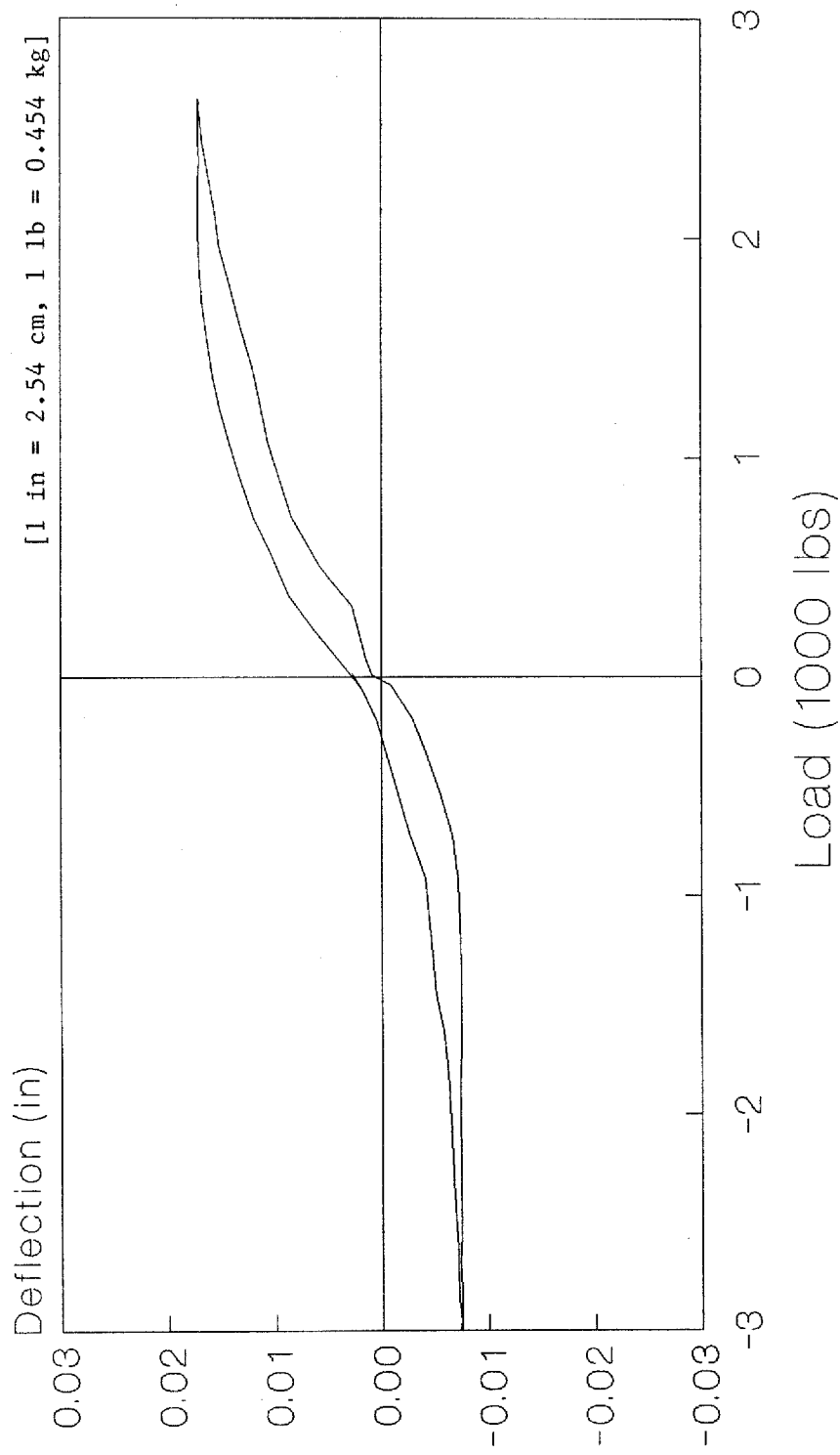


Figure 21. Measured load-deflection profile after 300,000 load cycles for specimen A8R (1-in [2.5-cm] dowel, 1/8-in [0.3-cm] annual gap, 9-in [23-cm] embedment, low-energy drill, cement grout).

Specimen B18, 44 E9 CG, 300000 Cycles Sensor Deflection vs. Load

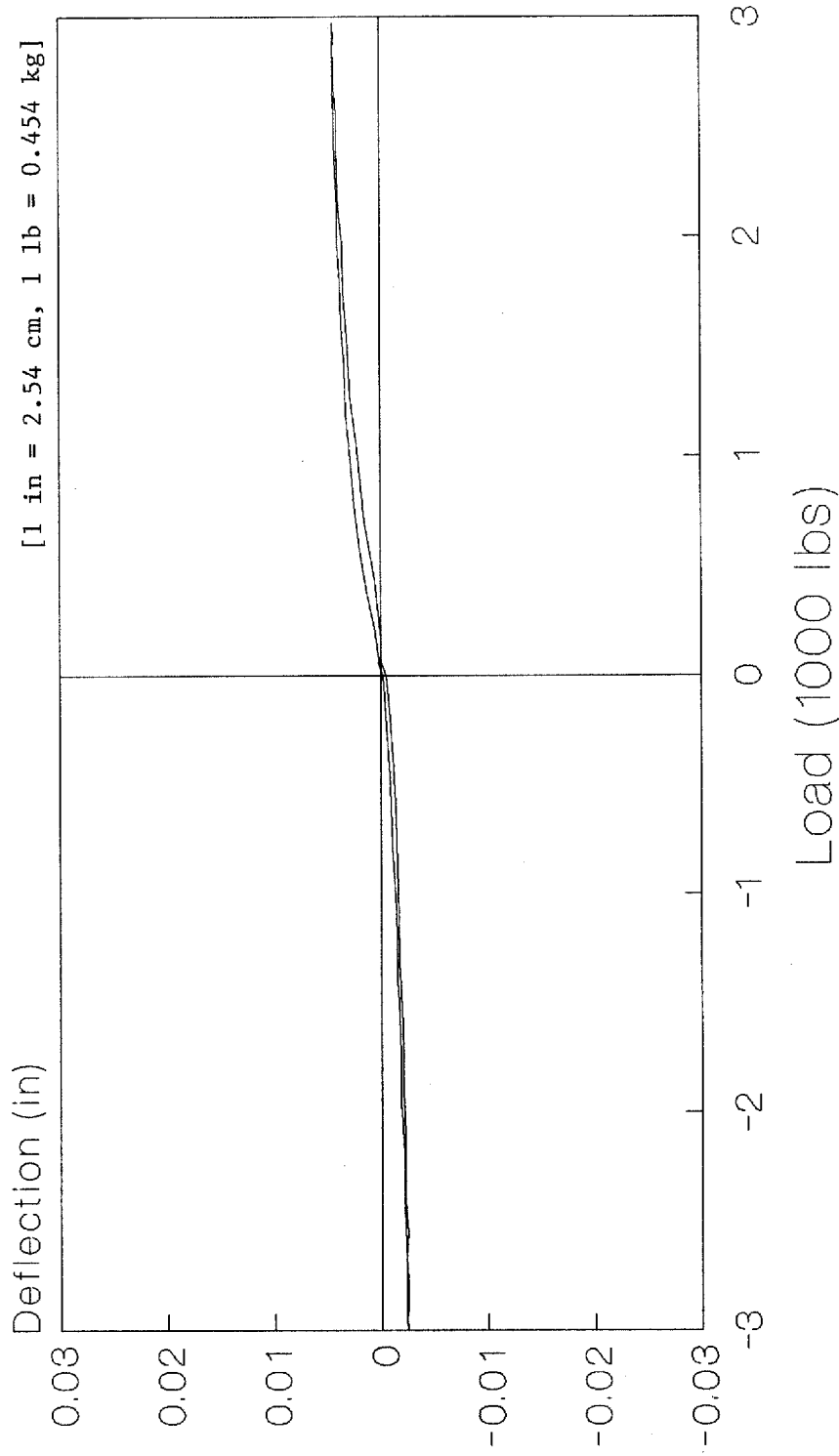


Figure 22. Measured load-deflection profile after 300,000 load cycles for specimen B18 (1.5-in [3.8-cm] dowel, 1/8-in [0.3-cm] annual gap, 9-in [23-cm] embedment, low-energy drill, cement grout).

Specimen D20, 44 P9 CG, 3000 Cycles

Sensor Deflection vs. Load

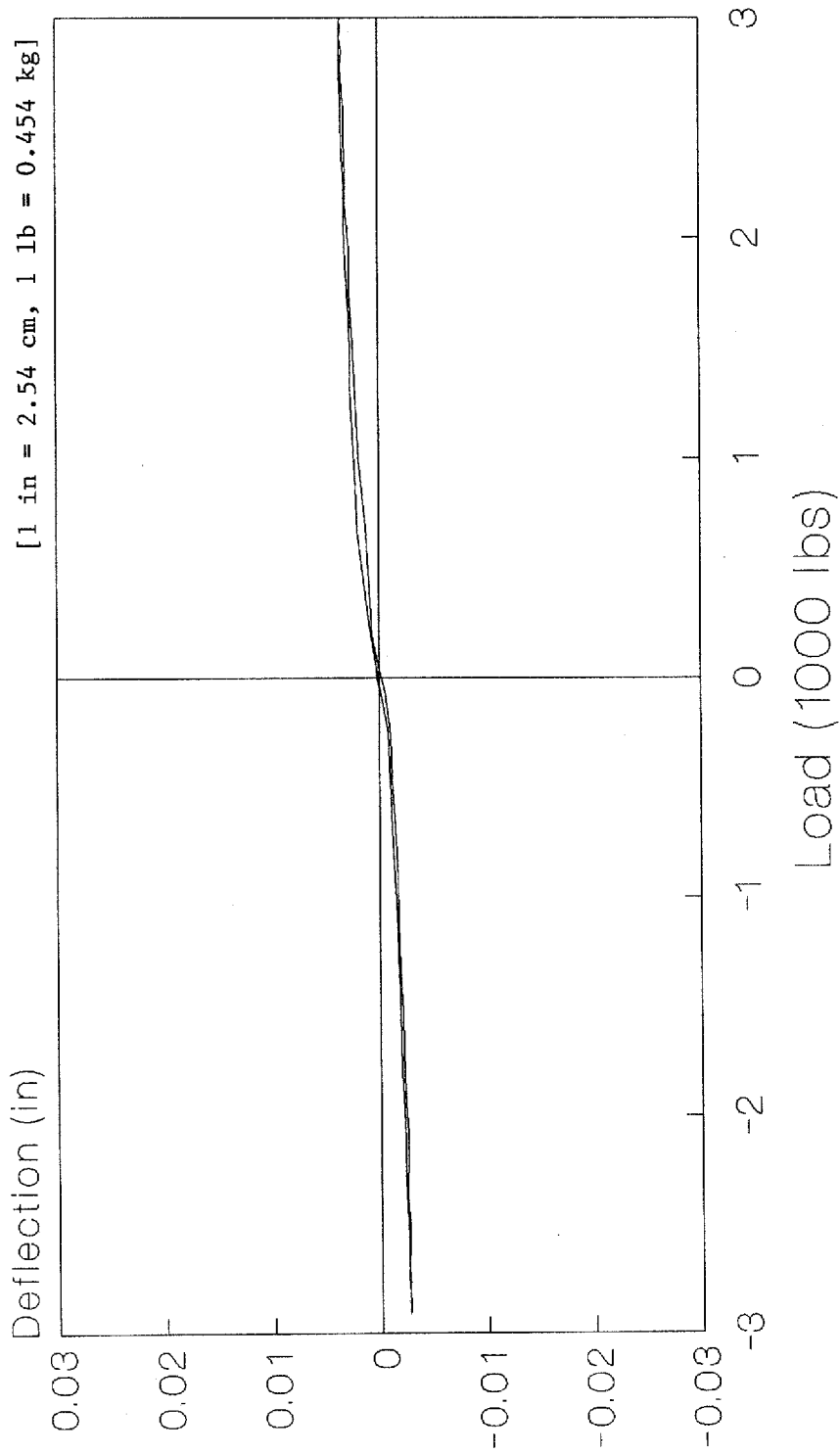
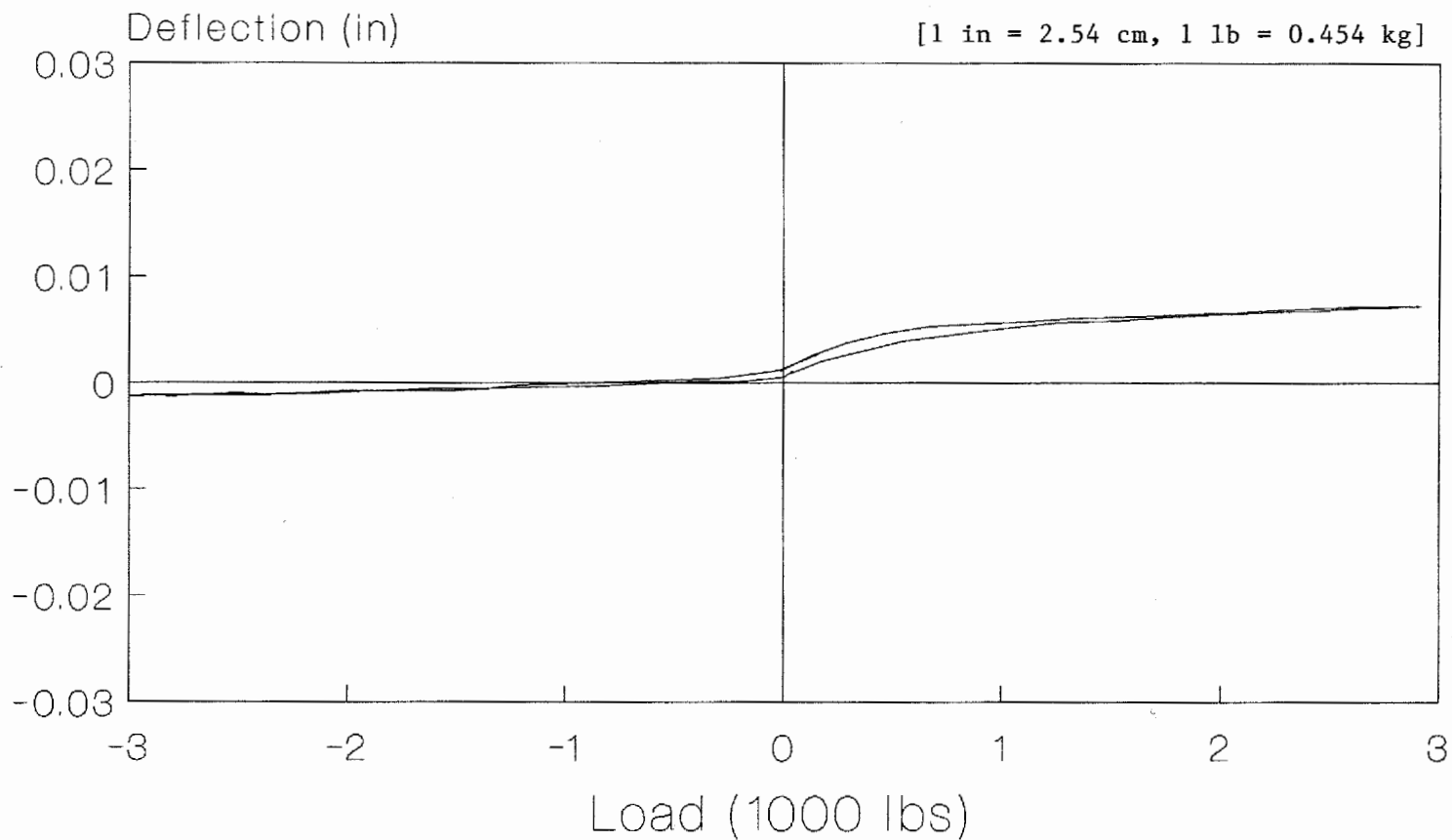


Figure 23. Measured load-deflection profile after 300,000 load cycles for specimen D20 (1.5-in [3.8-cm] dowel, 1/8-in [0.3-cm] annual gap, 9-in [23-cm] embedment, high-energy drill, cement grout).

Specimen A10, 44 E7 CG, 300000 Cycles Sensor Deflection vs. Load



73

Figure 24. Measured load-deflection profile after 300,000 load cycles for specimen A10 (1.5-in [3.8-cm] dowel, 1/8-in [0.3-cm] annual gap, 7-in [18-cm] embedment, low-energy drill, cement grout).

Dowel Looseness vs. Log N Specimen D10R, 27, E9, Epoxy

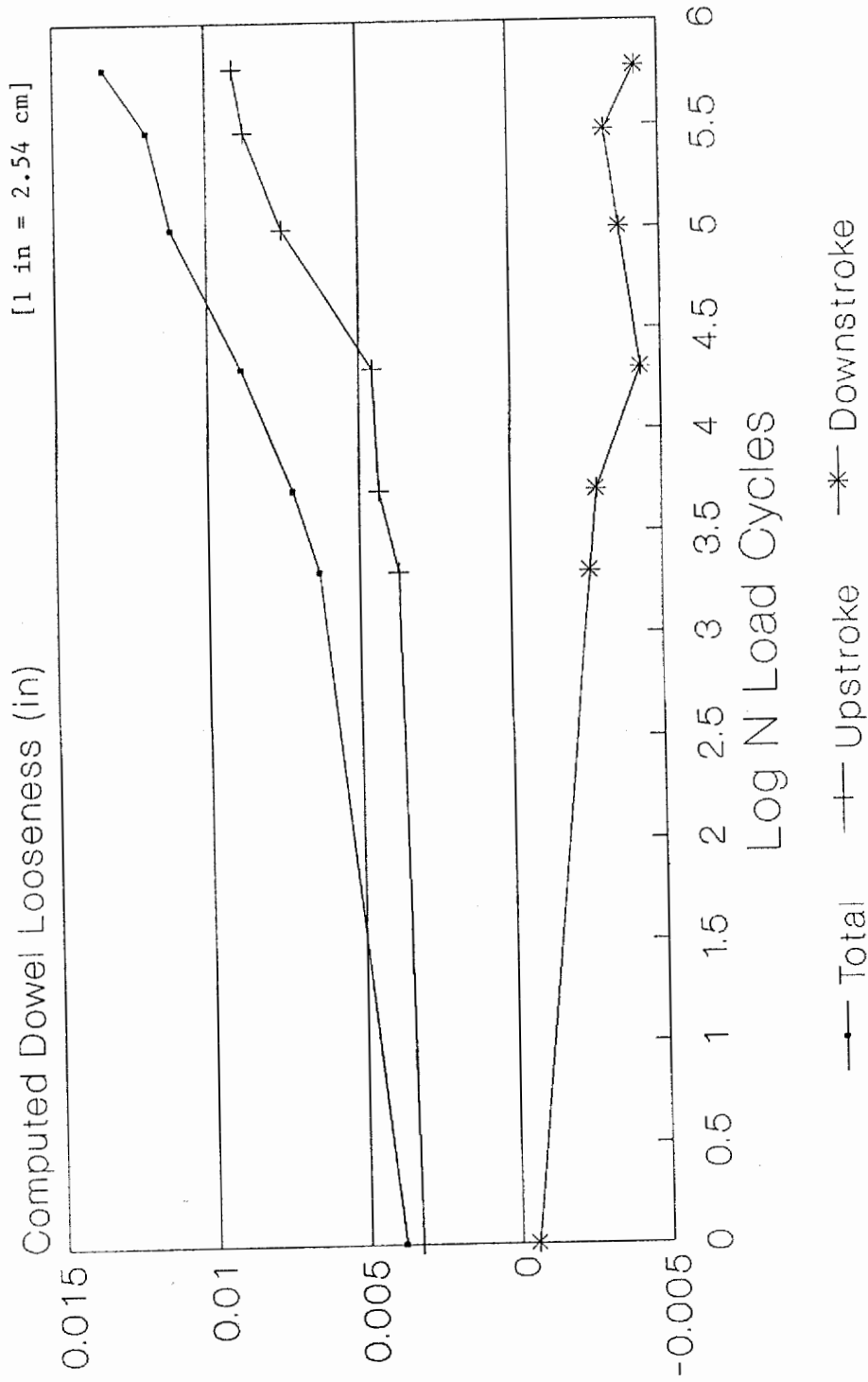


Figure 25. Computed dowel looseness vs. log load cycles for specimen D10R (1-in [2.5-cm] dowel, 1/32-in [0.08-cm] annual gap, 9-in [23-cm] embedment, low-energy drill, epoxy mortar).

Dowel Looseness vs. Log N

Specimen D6, 32, E9, Epoxy

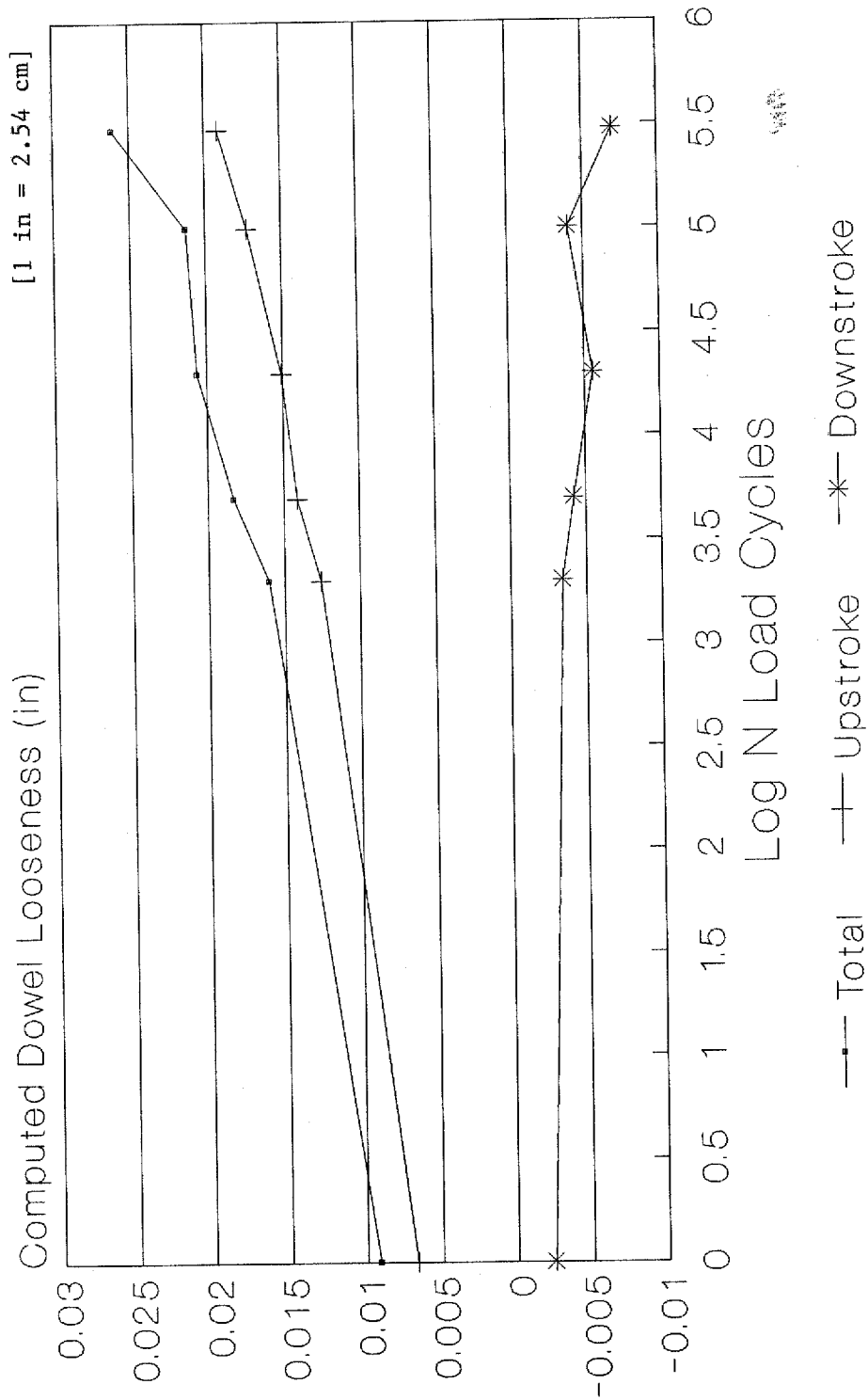


Figure 26. Computed dowel looseness vs. log load cycles for specimen D6 (1-in [2.5-cm] dowel, 1/8-in [0.3-cm] annual gap, 9-in [23-cm] embedment, low-energy drill, epoxy mortar).

Dowel Looseness vs. Log N Specimen A8R, 32, E9, Cement Grout

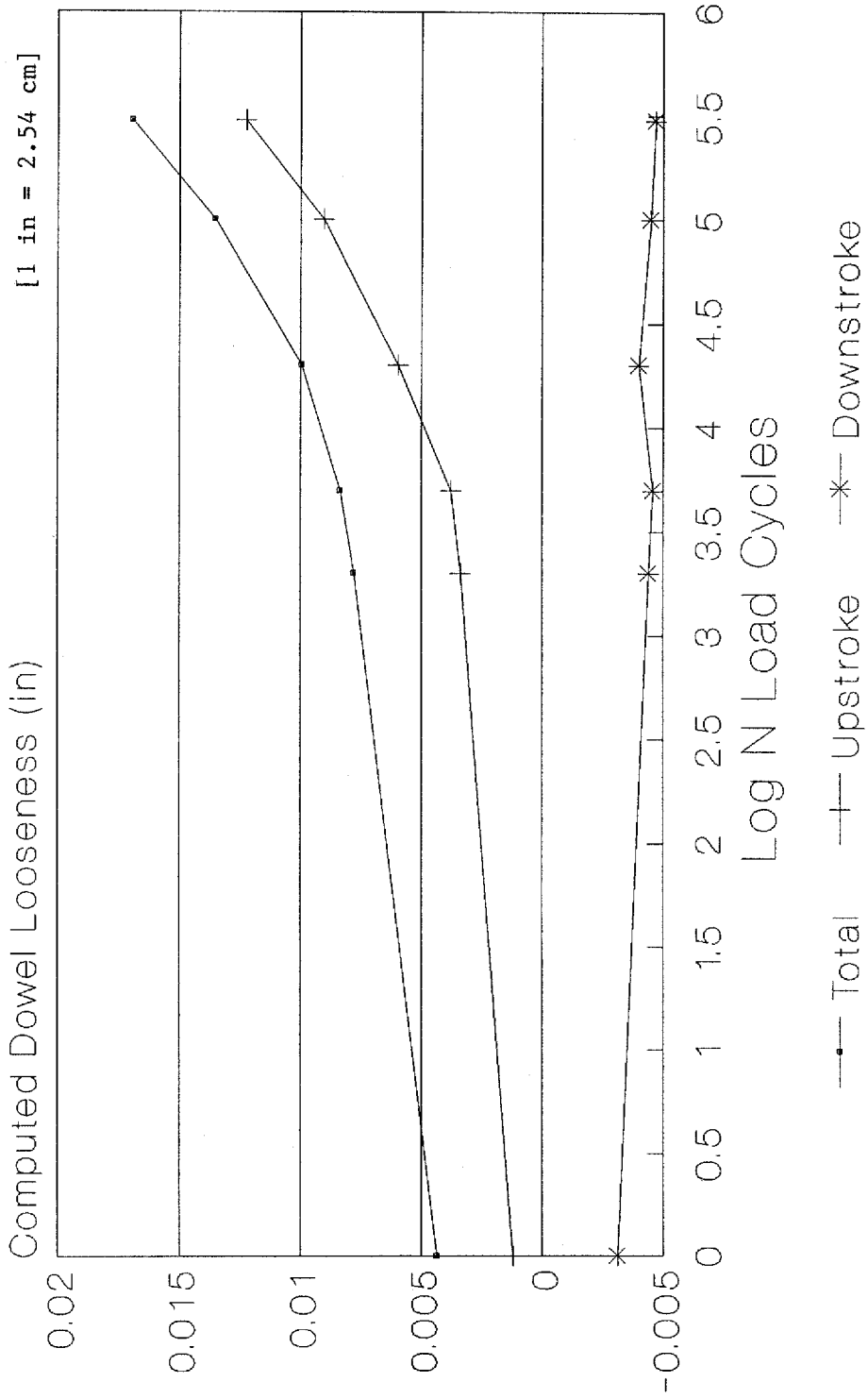


Figure 27. Computed dowel looseness vs. log load cycles for specimen A8R (1-in [2.5-cm] dowel, 1/8-in [0.3-cm] annual gap, 9-in [23-cm] embedment, low-energy drill, cement grout).

Dowel Looseness vs. Log N

Specimen B18, 44, E9, Cement Grout

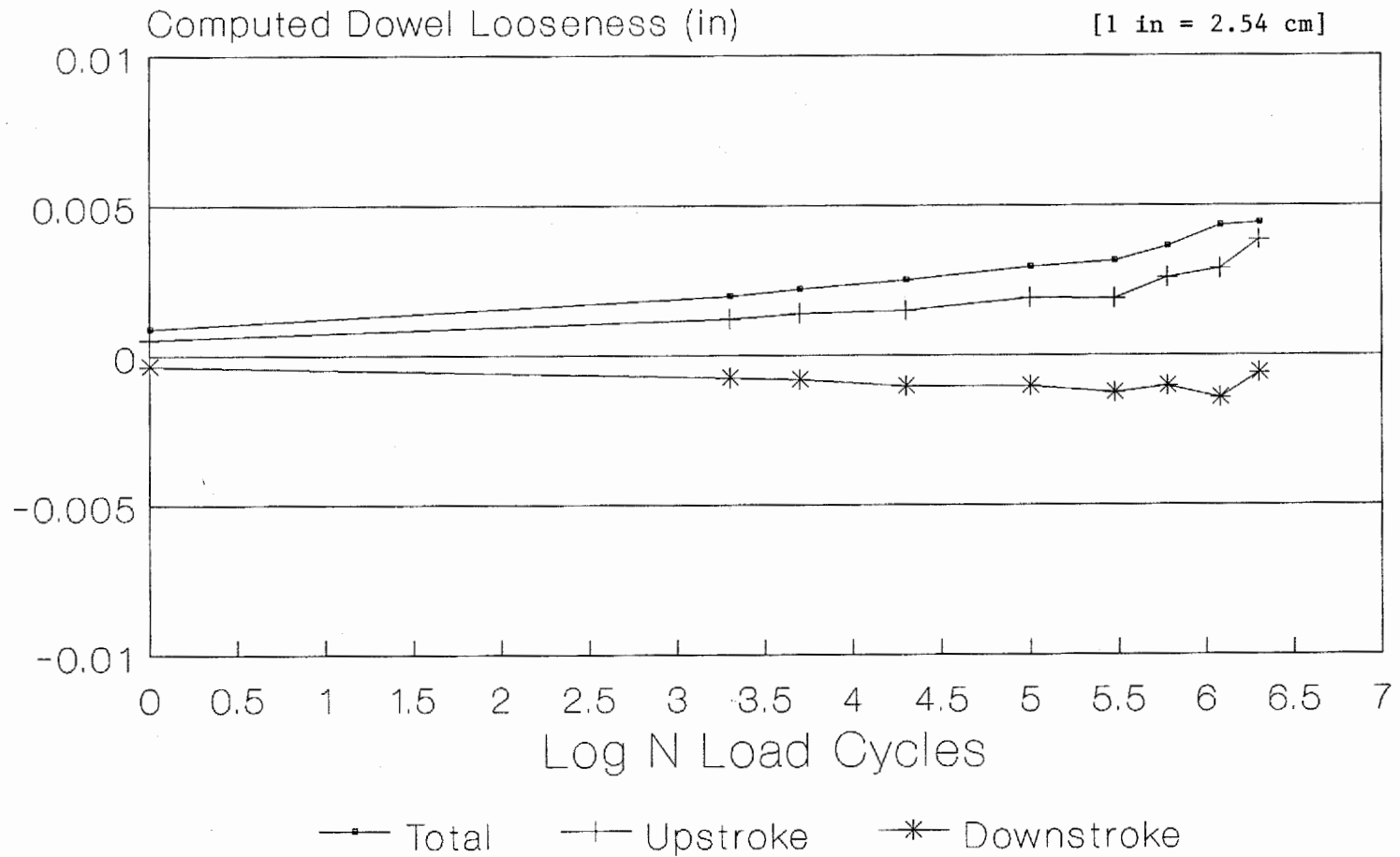


Figure 28. Computed dowel looseness vs. log load cycles for specimen B18 (1.5-in [3.8-cm] dowel, 1/8-in [0.3-cm] annual gap, 9-in [23-cm] embedment, low-energy drill, cement grout).

Dowel Looseness vs. Log N

Specimen D20, 44, P9, Cement Grout

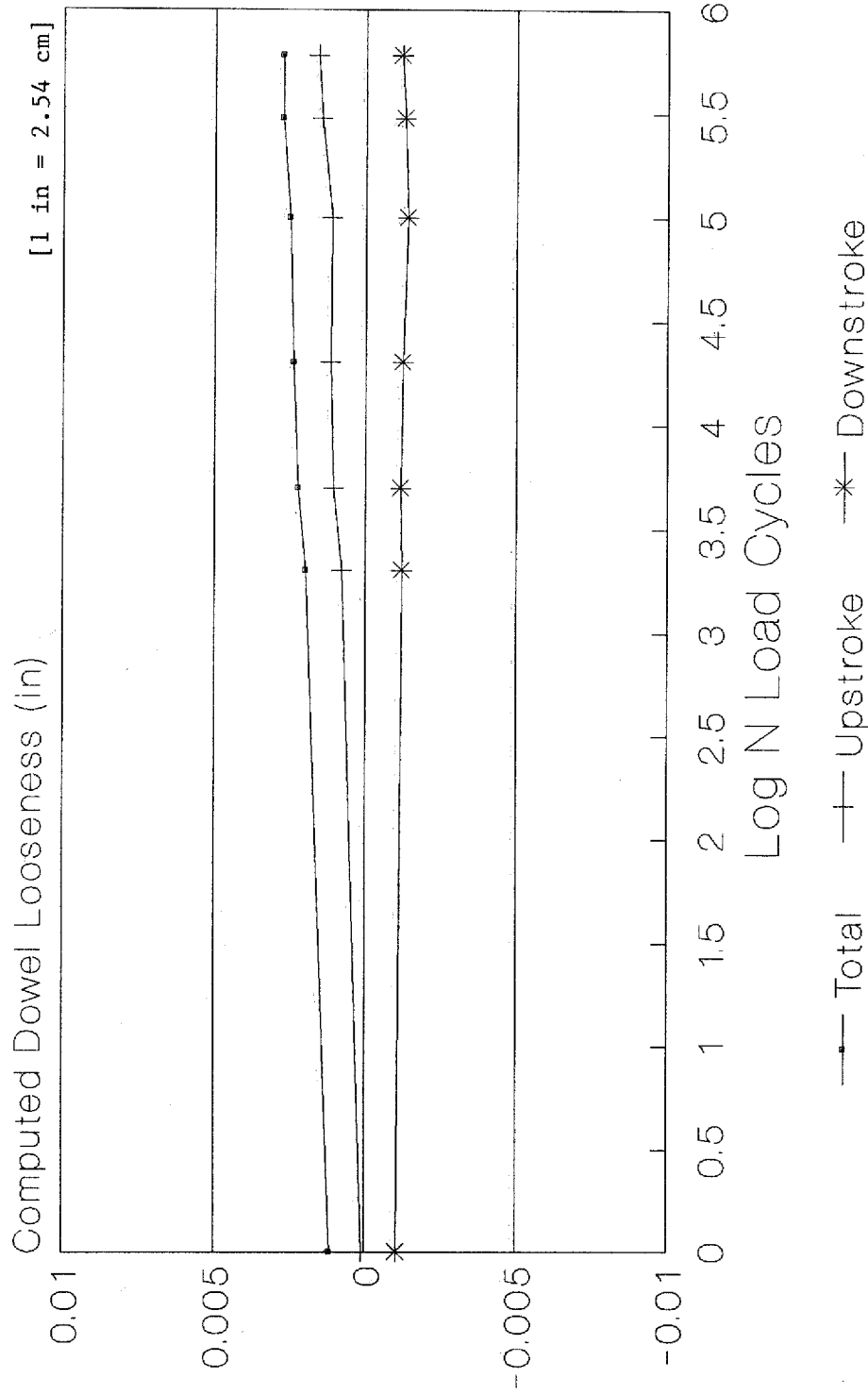


Figure 29. Computed dowel looseness vs. log load cycles for specimen D20 (1.5-in [3.8-cm] dowel, 1/8-in [0.3-cm] annual gap, 9-in [23-cm] embedment, high-energy drill, cement grout).

Dowel Looseness vs. Log N Specimen A10, 44, E7, Cement Grout

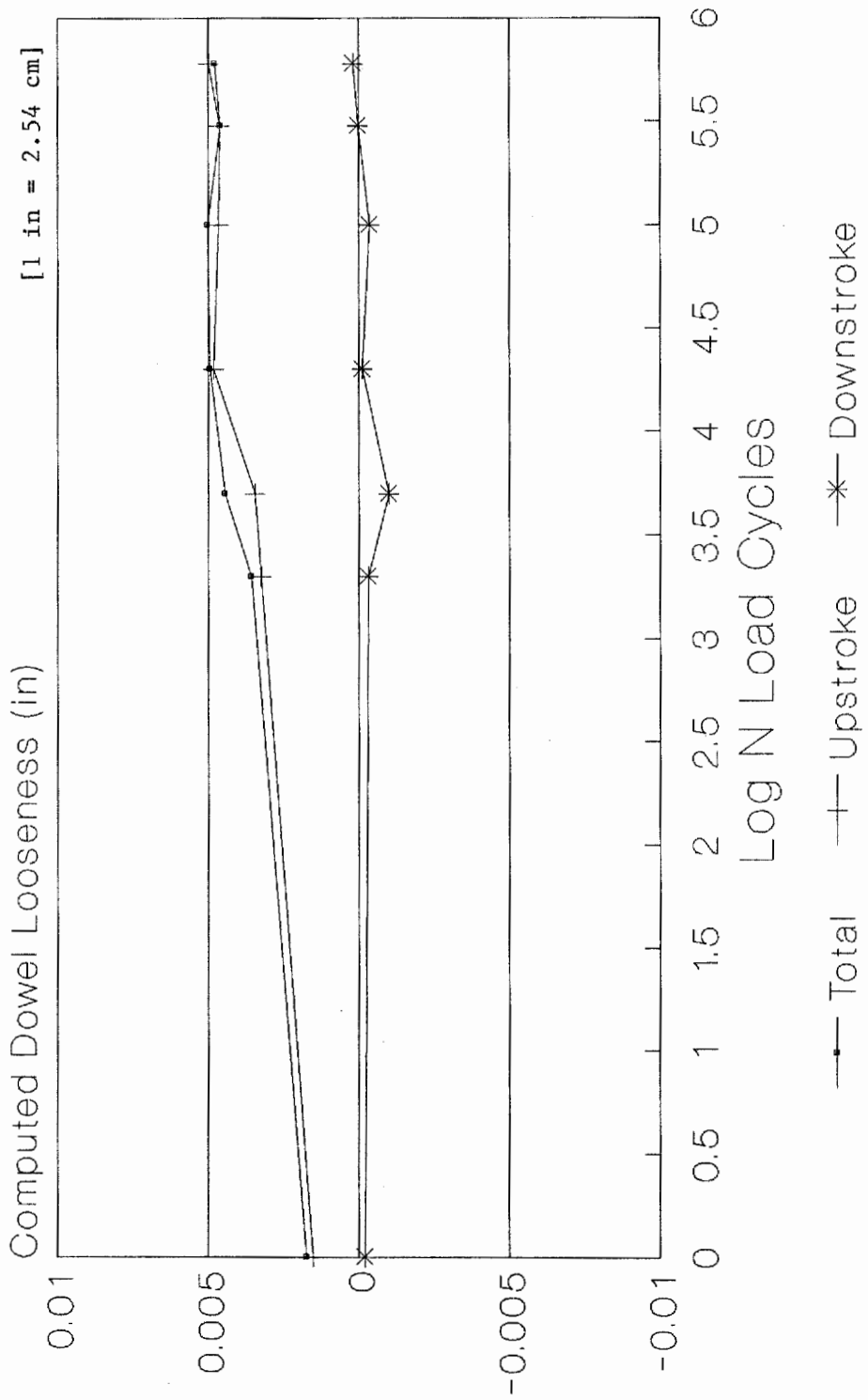


Figure 30. Computed dowel looseness vs. log load cycles for specimen A10 (1.5-in [3.8-cm] dowel, 1/8-in [0.3-cm] annual gap, 7-in [18-cm] embedment, low-energy drill, cement grout).

Specimen Lab1, 28 Days, 300000 Cycles Sensor Deflection vs. Load

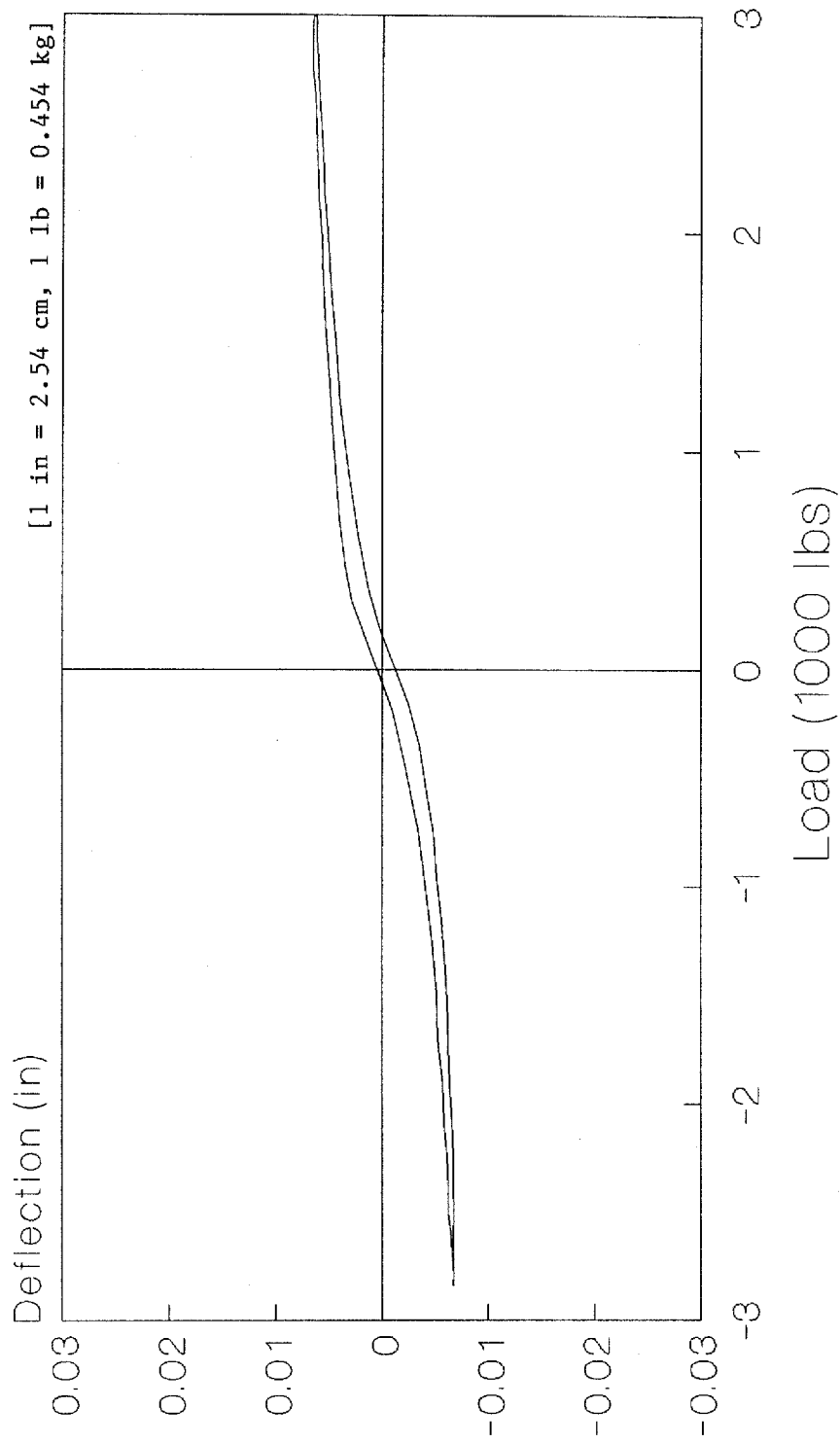


Figure 31. Measured load-deflection profile after 300,000 load cycles for cast-in-place specimen (1-in [2.5-cm] dowel, 9-in [23-cm] embedment).

Dowel Looseness vs. Log N

Specimen Lab1, 1" Dowel Cast-in-Place

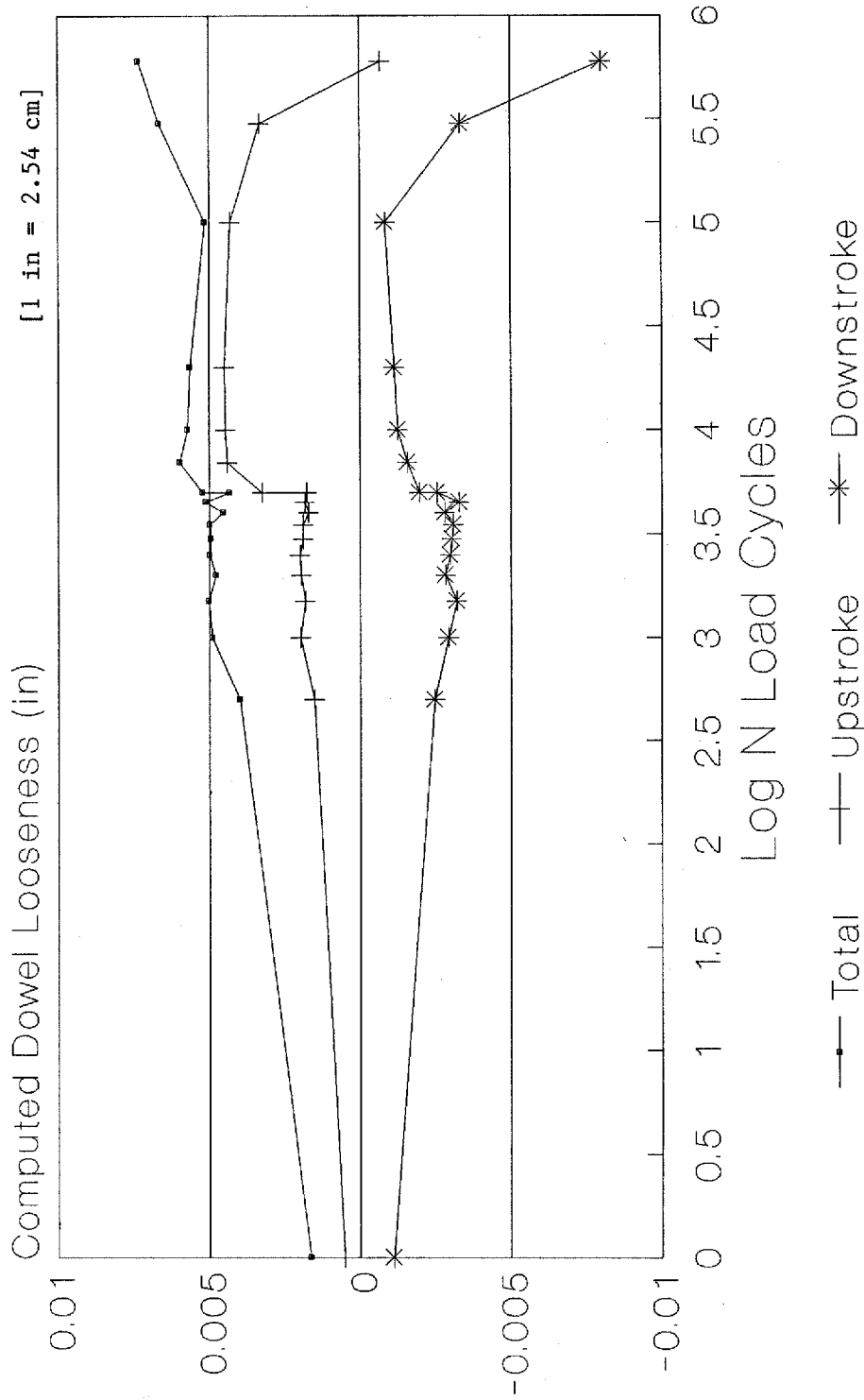


Figure 32. Computed dowel looseness vs. log load cycles for cast-in-place specimen (1-in [2.5-cm] dowel, 9-in [23-cm] embedment).

Specimen C9, 44 H7 C10, 300000 Cycles

Sensor Deflection vs. Load

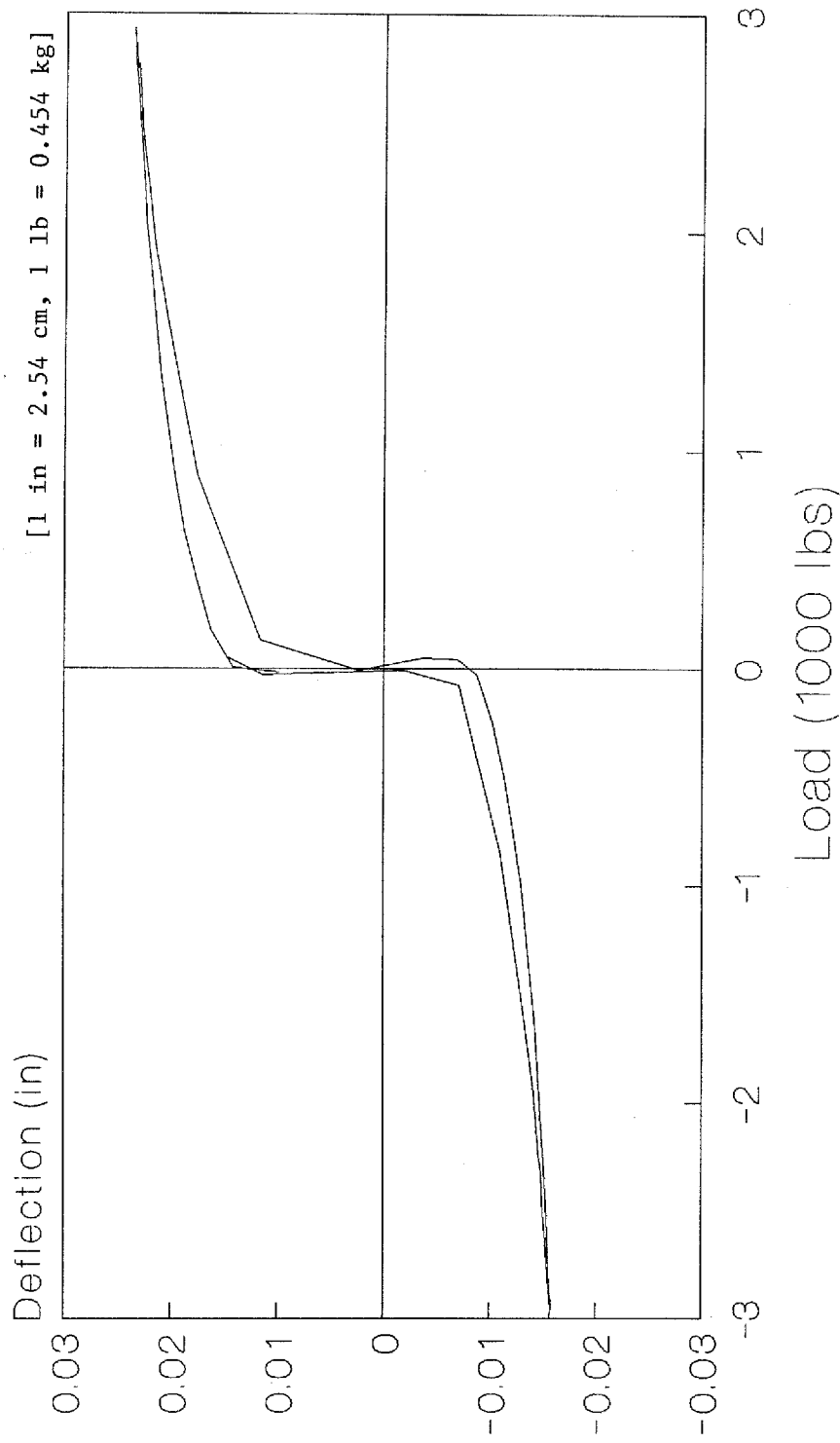


Figure 33. Measured load-deflection profile after 300,000 load cycles for stainless steel pipe (1.625-in [4.1-cm] by 1/8-in [0.3-cm] wall thickness pipe, 7-in [18-cm] embedment, medium-energy drill, epoxy mortar).

Dowel Looseness vs. Log N

Specimen C9, 44 H7 Epoxy, Hollow SS Bar

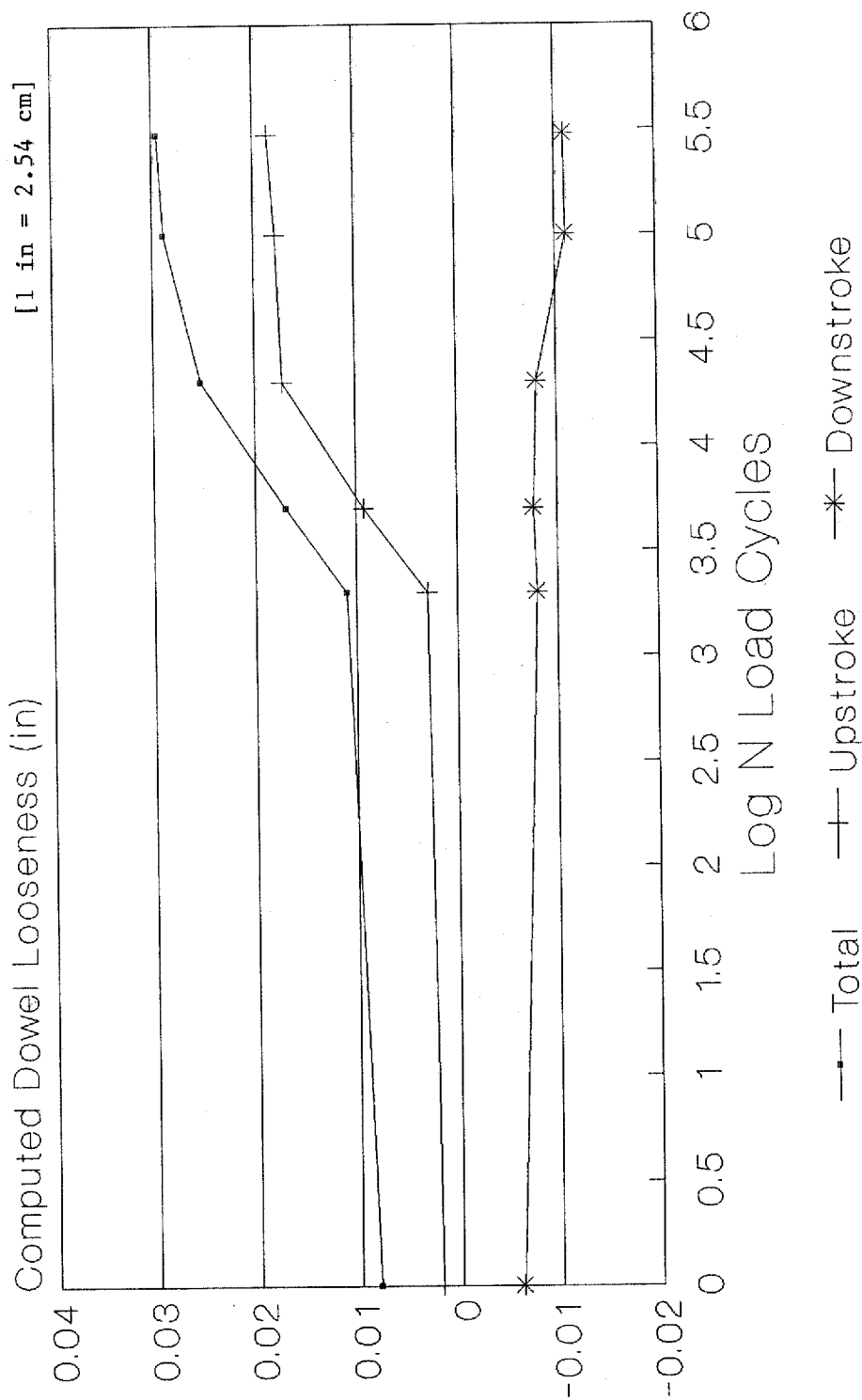


Figure 34. Computed dowel looseness vs. log load cycles for stainless steel pipe (1.625-in [4.1-cm] by 1/8-in [0.3-cm] wall thickness pipe, 7-in [18-cm] embedment, medium-energy drill, epoxy mortar).

REFERENCES
VOLUME IV -- APPENDIXES

1. Box, G. E. P., W. G. Hunter and J. S. Hunter, Statistics for Experimenters -- An Introduction to Design, Data Analysis, and Model Building, John Wiley and Sons, New York, N. Y., 1978.
2. Smith, K. D., M. B. Snyder, M. I. Darter, M. J. Reiter and K. T. Hall, "Pressure Relief and Other Joint Rehabilitation Techniques," Final Report, Federal Highway Administration, Washington, D.C., February, 1987.
3. Lippert, D. L., "Performance Evaluation of Jointed Concrete Pavement Rehabilitation Without Resurfacing," paper prepared for presentation at the 1987 Annual Meeting of the Transportation Research Board, Washington, D.C., 1987.
4. -, "Design and Control of Concrete Mixtures," Eleventh Edition, Portland Cement Association, Skokie, Illinois, July 1968.
5. Ioannides, A. M., "Analysis of Slabs-On-Grade For A Variety Of Loading and Support Conditions," Ph.D Thesis, University of Illinois, September, 1984.
6. Teller, L. W. and H. D. Cashell, "Performance of Doweled Joints Under Repetitive Loading," Bulletin 217, Highway Research Board, Washington, D.C., 1959.
7. Ciolko, A. T., P. J. Nussbaum and B. E. Colley, "Load Transfer of Dowel Bars and Star Lugs," Final Report, Construction Technology Laboratories, Skokie, IL, 1979.
8. PCLAB User Manual, University of Illinois, Urbana, 1986.
9. Nie, N. H., et. al., "Statistical Package for the Social Sciences," Second Edition, McGraw-Hill Book Company, New York, New York, 1975.
10. Lotus 1-2-3 Spreadsheet, User's Guide, Lotus Development Corporation.
11. Friberg, B. F., "Load and Deflection Characteristics of Dowels in Transverse Joints of Concrete Pavements," Proceedings, 18th Annual Meeting of the Highway Research Board, Washington, D.C., 1938.
12. Timoshenko, S., and J. M. Lessels, Applied Elasticity, Westinghouse Technical Night School Press, Pittsburgh, Pennsylvania, 1925.
13. Darter, M.I., Becker, J.M., Snyder, M.B. and Smith, R.E., "Concrete Pavement Evaluation System (COPES)," NCHRP Report No. 277, Transportation Research Board, 1985.
14. ERES Consultants, Inc., "Techniques For Pavement Rehabilitation," Participants Notebook, National Highway Institute/Federal Highway Administration, Third Revision, October, 1987.

